DEVELOPMENT OF A HIGH PRESSURE ABRASIVE WATER JET FOR CUTTING ~~SYSTEM~~ OPERATIONS

By

Mashhour M. Abudaka, B.Sc., M.Sc. (U.M.I.S.T.)

Thesis submitted for the degree of Doctor of Philosophy
in the Faculty of Engineering, University of London
and for
The Diploma of membership of the Imperial College

Department of Mechanical Engineering
Imperial College of Science, Technology and Medicine
London SW7 2BX

March 1989

If a man will begin with certainties, he shall end in doubts, but if he will be content to begin with doubts, he shall end in certainties

Robin Hyman

Acknowledgment

This research was mainly experimental in nature. Design and construction of equipment was involved, the greater part of the equipment having been fabricated and assembled in the Fatigue Laboratory in the Mechanical Engineering Department, Imperial College.

By definition, this type of experimental research requires team work and a great deal of informal discussion with many members of staff in the Mechanical Engineering Department and other departments of the college.

I owe much of my acquired interest in experimental research work to my supervisor and friend Dr. P. S. J. Crofton, whose hard work, informal guidance and encouragement has been an excellent driving force.

I am also grateful to Messrs Nick Tailor, Alex Noorbhai and Mike King from the Fatigue Laboratory for their fabrication work. Dr. C. Leach and Dr. P. Rogers of the Department of Metallurgy and Material Science for their technical assistance on ceramic materials. Mr. M. Applebaum of the Electrical and Electronic Engineering Department for the design and construction of the X-Y table control.

I gratefully acknowledge the financial support of UHDE, werk Hagen F.R.G. and The Arab-British Chamber Charitable Foundation.

I would like to thank my colleague Dr. S. John of the Mechanical Engineering Department for reading and correcting the thesis.

Finally, I am grateful to my parents, brothers and sisters for their support and encouragement.

Abstract

From a review of the literature, the disadvantages of existing abrasive water jet cutting systems have been identified. One of most important criterion in the cutting operation is the mass flow rate of the cutting medium, which influences the efficiency of the cutting operation.

This thesis reports a theoretical and experimental investigation into the high pressure-low flow abrasive water jets used in precision cutting operations. The advantages and disadvantages of similar existing higher flow systems are discussed. Small sapphire orifices (orifice diameters range from 0.05 to 0.25 mm) have been used to initially focus the water which is pumped at high pressure up to 3500 bar. The sapphire orifice minimises the jet dispersion because of its combined surface hardness and smoothness. A theoretical investigation of the jet spread as well as theoretical analysis of mixing abrasive particles with the water jet stream are presented. Existing theories on wear of ductile and brittle materials which are based on single particle erosion have been expanded for multi-particle erosion and the mathematical models are presented.

A high pressure water pump was installed and a test rig consists of X-Y table driven by two stepper motors, abrasive hopper, collection tanks, cutting heads and clamps were constructed.

Preliminary tests on cutting head designs revealed most critical components of the cutting head, the shape and length of the mixing chamber as well as the focusing tube length and operation life.

Cutting results using mainly mild steel and few brittle and ductile materials are reported and compared with the theoretical models to evaluate the cutting head efficiency. Focusing tube materials were tested and wear rate of such materials was measured and discussed.

Evaluation of the effect of several abrasive materials on the cutting speed and on the wear of the focusing tube is presented and discussed.

Contents

		Page
Nomenclature		VIII
List of figures		XI
List of tables		XIII
List of plates		XV
Chapter 1	**Introduction**	1
	1.1 Fluid mechanics	3
	1.2 Design of cutting head and mixing of abrasive particles with water jet	4
	1.3 The cutting process	6
	1.4 Cutting parameters	6
	1.5 Definitions	7
Chapter 2	**Literature review**	8
	2.1 Introduction	9
	2.2 Historical review of water jet nozzles	9
	2.3 Abrasive jet cutting nozzles	15
	2.4 Water jet related cutting parameters	18
	2.5 Material related cutting parameters	24
	2.6 Conclusions	34
Chapter 3	**Theoretical analysis**	36
	3.1 Introduction	37
	3.2 Water jet parameters	37
	3.3 Mixing of abrasive with water jet	43
	3.4 Approximate analytical solution for the velocity of the solid abrasive particles injected in a water jet	49
	3.5 The cutting mechanism of the abrasive water jet	54
	3.6 Erosion of ductile materials by particle impact	55

	3.7 Erosion of brittle materials	69
Chapter 4	**Construction of test rig**	71
	4.1 Description of testing unit requirements	72
	4.2 Pumping unit	72
	4.3 Rig layout	75
	4.4 Abrasive hopper	76
	4.5 Cutting tests	76
	4.6 Abrasive materials	77
	4.7 Constant parameters throughout the cutting tests	77
Chapter 5	**Cutting head**	80
	5.1 Introduction	81
	5.2 Cutting head design criteria	81
	5.3 The sapphire orifice	81
	5.4 Mixing chamber	83
	5.5 Tests on mixing chamber length	89
	5.6 Focusing tube	91
	5.7 Materials considered and tested for making the outlet tube	91
Chapter 6	**Results of cutting tests**	96
	6.1 Introduction	97
	6.2 Focusing tube	97
	6.3 Cutting tests	107
	6.4 Abrasive materials shapes and types	112
Chapter 7	**Discussion of results**	117
	7.1 Introduction	118
	7.2 Jet spread	119
	7.3 Mixing the abrasive with the water jet	120
	7.4 Cutting head design	127
	7.5 Abrasive particles	132
	7.6 Material removal process	134

Chapter 8 **Conclusions and proposals for future research** 136

8.1 Water jet expansion 137

8.2 Cutting head 138

8.3 Focusing tube 138

8.4 Abrasive materials 139

Appendix I Removal of brittle materials by impact 140

Appendix II 1 Sapphire orifice 147

2 X-Y table and control equipment 148

3 Parts of drive unit 151

4 Stepping motor drive board 151

5 Terminal connections 152

6 Nozzle clamp 155

7 Abrasive hopper 158

References 159

Appendix III back cover

1 Specimen material

2 Tests on cutting head

Nomenclature

h	abrasive water jet depth of cut
M	abrasive feed rate
Q	water volume flow rate
Q_A	air volume flow rate
P	operating pressure (or pressure difference)
d	orifice diameter (water nozzle)
m	mass flow rate of water
δ	boundary layer thickness
V_f	friction velocity
τ_o	wall shear stress
ρ_w	density of water jet
υ	dynamic viscosity of water
u	jet velocity in metre/second
u_x	traverse speed of cutting head
g	gravity constant
L_d	nozzle straight section length
u_0	mean jet core speed
u_1	inner jet streamwise velocity component
u_2	outer jet stream wise velocity component
$\bar{u}$	streamwise mean velocity component
u'	variations in streamwise velocity component
$\overline{u'}$	time average fluctuation of u'
$\bar{v}$	transverse mean velocity component
v'	variation in transverse velocity component
$\overline{v'}$	time average fluctuation of v'
L	mixing length of free jet
u_m	mean jet velocity
b	jet width on exit of nozzle
L_i	mixing length of free jet at section i, i = 1, 2, 3 .....
t	time
t^*	duration of cutting
P_s	abrasive chamber suction pressure
d_a	abrasive feed tube diameter
D	focusing tube (outlet tube) bore diameter
A	cross-section area of feed tube
Re	Reynolds number
ρ_I	air density
V_1	air velocity in abrasive feed tube

F_d	air drag force on particle
A_p	projected area of particle in the direction of motion
a	acceleration of particle
C_d	drag coefficient
V_m	velocity of particle before mixing with water jet
v_T	velocity of mixed jet
s	distance along the jet stream
R_x, R_y	horizontal and vertical component of cutting force
ϕ	$= R_y / R_x$, ratio of vertical to horizontal force
σ_p	horizontal plastic flow pressure
y_t	depth over which the particle contacts the material during cutting
l	depth of single particle cut
ψ	l / y_t
H	width of cut
x_t	x-direction cut
θ	particle rotation in the material during cutting
θ_0	initial rotation angle
V	speed of particle inside the water jet
v	speed of particle during cutting
α_0	critical angle of impingement
α	particle angle of attack, angle to the horizontal
α_1	initial angle of attack
T_f	rotational torque on particle during cutting
T_R	friction torque during cutting
δ(vol.)	volume removed
h_c	depth of cut due to cutting wear
F_x	hydrodynamic force in x-direction
F_y	hydrodynamic force in y-direction
c	ratio of portion of jet involved in the cutting to the diameter of the jet
d_j	jet diameter before cutting
$\delta(\text{vol.})_c$	volume removed due to material cutting
$\delta(\text{vol.})_d$	volume removed due to material deformation
h_d	depth of cut due to deformation wear
σ	$= \sigma_p / \alpha_1$
σ_y	yield stress
r'	imaginary and approximate radius
r	sphere radius with weight equal the particle weight
a	contact radius
a^*	effective contact radius
r^*	effective particle radius

x_m	maximum depth of indentation produced under brittle impact condition
$x_{el.}$	depth of cut due to elastic impact
$x_{pl.}$	depth of cut due to plastic deformation
m_a	mass of particle
F	contact force
ρ_p	particle mass density
U_d	total deformation energy
ν	poisson's ratio
E	Young's modulus
x	distance of approach
σ_a	maximum surface tensile stress
σ_b	pure bending stress
σ_R	radial stress
σ_f	failure stress
σ_u	the zero probability of failure stress
$\sigma_u`$	the maximum zero stress at R = a
s	probability of survival $s = e^{-B}$
B	risk of rupture
σ_o	scaling stress
m	parameter characterises the flaw distribution
h_s	distance of the maximum σ_a below the surface
α_f	angle between abrasive feed tube and the direction of water jet flow
τ_w	abrasive pipe wall shear stress
F_w	water jet drag force on particle
I	moment of inertia of single abrasive particle
A_c	area of contact during single particle cutting
ε	energy required to remove unit volume of material
V_b	the stressed volume in bending
W	brittle material volume removal rate

List of Figures

		Page
Fig. 2.1	*water jet nozzle*	*11*
Fig. 2.2	*sapphire orifice in steel holder*	*12*
Fig. 2.3	*schematic representation of material removal rate on attack angle*	*25*
Fig. 2.4	*predicted variation of volume removal with angle for a single abrasive grain*	*26*
Fig. 2.5	*wear rate of C60H steel V hardness of abrasive*	*28*
Fig. 2.6	*ductile erosion of annealed SAE 1020 steel as function of velocity*	*30*
Fig. 2.7	*overall contact surface in brittle erosion*	*31*
Fig. 2.8	*brittle erosion of glass by angular SiC grit, at $\alpha = 90^{o}$ as a function of velocity*	*33*
Fig. 2.9	*weight removal as a function of particle approach angle for plate of glass eroded by angular silicon carbide particles at V= 152 m/s.*	*35*
Fig. 3.1	*structure of jet*	*41*
Fig. 3.2	*water/abrasive mixing chamber*	*43*
Fig. 3.3	*control volume for flow in a constant - area duct with friction*	*45*
Fig. 3.4	*abrasive feed tube*	*46*
Fig. 3.5	*water/abrasive mixing*	*48*
Fig. 3.6	*presentation of the theoretical particle speed inside the jet*	*53*
Fig. 3.7	*particle cutting in a ductile material*	*56*
Fig. 3.8	*forces on single particle*	*57*
Fig. 3.9	*hydrodynamic forces on abrasive particle*	*60*
Fig. 3.10	*the drag coefficient variation with jet speed*	*62*
Fig. 3.11	*measured forces under jet*	*64*
Fig. 3.12	*abrasive jet cutting model*	*65*
Fig. 3.13	*deformation wear model*	*67*
Fig. 4.1	*pumping unit layout*	*73*
Fig. 4.2	*intensifier unit*	*74*

Fig. 4.3	*mild steel specimen*	79
Fig. 5.1	*sapphire orifice in the rubber seal*	84
Fig. 5.2	*cutting head without mixing chamber*	85
Fig. 5.3	*cutting head with a square section mixing chamber*	86
Fig. 5.4	*conical cutting head*	87
Fig. 5.5	*curved internal surface mixing chamber*	88
Fig. 5.6	*mixing chamber suction pressure variation with operation pressure*	90
Fig. 6.1	*wear of tungsten carbide outlet tube using garnet 80 abrasive*	103
Fig. 6.2	*worn out focusing tubes*	105
Fig. 6.3	*kerfing in 16 mm mild steel specimen related to focusing tube bore*	108
Fig. 6.4	*cutting time of specimen using different abrasive*	114
Fig. 6.5	*wear rate of tungsten carbide tube using several types of abrasives*	115
Fig. 7.1	*forces on two particles shape during jet penetration*	124
Fig. 7.2	*3 cavities (mixing chambers) cutting head*	131
Fig. 7.3	*particles sliding inside the focusing tube*	133
Fig. 7.4	*presentation of particles on impact with the specimen*	133

List of Tables

		Page
Table 2.1	*comparison of abrasive water jet cutting approaches*	*22*
Table 5.1	*mechanical properties of materials used for making focusing tube*	*92*
Table 6.1	*wear results of T.C. tubes using flint as abrasive*	*98*
Table 6.2	*wear results of T.C. tubes using white alumina abrasive*	*99*
Table 6.3	*wear result of zirconia tubes using white alumina abrasive*	*100*
Table 6.4	*speed of cut using flint and alumina abrasive and test of several lengths of focusing tubes*	*101*
Table 6.5	*cutting speed using garnet as abrasive*	*102*

List of Plates

		page
Plate 4.1	*abrasive hopper, cutting head, clamp and table*	*78*
Plate 5.1	*unused sapphire orifice x200*	*82*
Plate 5.2	*used sapphire orifice x 500*	*82*
Plate 5.3	*tungsten carbide focusing tubes*	*92*
Plate 5.4	*zirconia focusing tube*	*93*
Plate 6.1	*no air flow through to the chamber*	*106*
Plate 6.2	*open abrasive pipe*	*106*
Plate 6.3	*cut through silceram*	*110*
Plate 6.4	*cut through mild steel*	*111*
Plate 6.5	*flint particles x 100*	*113*
Plate 6.6	*white alumina particles x 100*	*115*
Plate 6.7	*S type alumina particles x 50*	*116*
Plate 6.8	*garnet particles x 100*	*116*
Plate 7.1	*worn out tungsten carbide focusing tube*	*121*
Plate 7.2	*kerfing in thick mild steel*	*125*
Plate 7.3	*16 mm thick mild steel δ = 0.2 mm*	*126*
Plate 7.4	*surface of cut shows ductile cutting x 1000*	*128*

Chapter 1

Introduction

The cutting power of water has been known since the beginning of civilisation, rivers cut valleys destroy houses and bridges. As the water speed and mass flow rate increases the cutting power of water is more effective. Recently this ancient knowledge has been utilised as a result of the evolution of the new technology especially high pressure pumps and intensifiers and wear resistant materials.

Sand blasting has been used for metals surface treatments and surface cleaning, sand particles are entrained in an air jet, the air in this case is used to accelerate the abrasive particles which are fed before the jet nozzle, the nozzle is usually made of tungsten carbide or boron carbide to resist wear.

The need for the cutting power of water stems from the fact that water jets are safe to use in cutting operations in hazardous environment where fire risks exist such as coal mines and oil fields in which fires are a frequent occurrence. Water is denser than air hence more mechanical power is available to be transferred to the abrasive particles.

Using the appropriate nozzle type and sizes has successfully enabled water jets to be used in cutting operation which would otherwise be carried out by conventional cutting methods. The development of new materials in engineering, such as polymers and polymer composites necessitate the use of new cutting methods other than the conventional ones. Very hard materials such as titanium alloys are also difficult to cut, whereas they are relatively more economic and easily cut by abrasive entrained water jets. Alloy materials of this type can be cut without any significant increase in temperature because the water acts as an instant cooling medium and thus avoids any metallurgical change.

The wide availability of water and abrasive (sand) and the advance of pump technology made the idea of using water and abrasive as cutting tool an attractive reality which is still in its preliminarily development stages.

More technologically advanced uses for water jets and abrasive water jets are precision cutting and cold cutting of hard metal, alloys and glass. The use of abrasive water jets in the remotely controlled cutting operations inside radioactive nuclear reactors require them to consume minimum water and abrasive flow rates, since the products of the cut and the water and abrasive have to be collected and processed or safely stored. However, in the most advanced cutting system available now, water and abrasive flow rates are considered to be high (7 to 8 kg/min). of abrasive and water. This work is concerned with cutting systems with lower water flow rates and abrasive mass flow rates of not more than 4.5 kg/min.

In this thesis, the research is divided into three areas which are considered to be the most important parts of the abrasive water jet cutting; water jet spread, cutting head design and wear of materials.

1.1- Fluid mechanics

Little is known about supersonic water jets. In a low pressure water jet, water is considered to be an incompressible fluid therefore studying the jet flow is a comparatively straight forward fluid mechanics problem. However, at a high pressure (>1000 bar), it is known that the water is compressible and the occurrence of water shock waves along the jet is indicative of density change. Air entrainment and water/air friction are additional factors which influence jet spread which is undesirable for precision cutting.

Mechanical friction between the water stream and orifice materials (and the development of boundary layer on the jet surface) have been shown to stimulate jet spread. Hard but smooth surface orifice materials result in less dispersed jets, consequentially materials such as sapphire are used in making jet orifices. In this work, orifices of hole sizes 0.1, 0.15, 0.18, 0.2 and 0.25 mm are tested in cutting polymer materials using water without abrasive material. Then the water pressure was steadily increased, jet spread or jet coherence were observed. Observations indicates,

as expected, that small size orifices give shorter jet core length . The core length becomes even shorter if the water pressure is increased. A long and coherent jet core is required to cut hard and tough materials, optimum water mass flow rate is also needed to carry the maximum kinetic energy available from the pump and transfer it to the abrasive particles.

Cutting hard material differ from cutting soft materials which can be cut with water alone in that the pressure and the size of the orifice are more critical. High pressure can cause relatively more jet spread than lower pressure which might be just sufficient to penetrate the material. Large orifice size with lower operating pressure might result in improved cut quality because of the decrease in jet spread.

Two types of standard sapphire orifices are manufactured for this propose (*Seitz of Switzerland*), the two types differ in the external geometry of the jewel steel mounting, especially the stabiliser length.

1.2- Design of cutting head and mixing of abrasive particles with the water jet

The addition of abrasive materials to the water jet speeds up the wear process of the jet on the surface of the cut material and hence increases the material removal rate. The methods by which the the abrasive particles are introduced to the jet have been and are still open to debate and large scope of developments and discussion. Down stream abrasive addition or so called 'cutting head mixing' is preferred to perform precision cutting as opposed to up stream mixing or a direct jet in which water and abrasive are mixed and pumped before the cutting head. The advantages and disadvantages of the two systems are fully discussed in Chapter 2. This thesis focuses on the system in which the abrasive particles are added and mixed with the jet in the cutting head by this avoiding any internal pump wear.

It is evident that a water jet alone has relatively insignificant cutting capabilities for hard and tough materials such as metals. However, the addition of abrasive particles to

the water jet results in a rapid increase in the speed of cut. Also, the speed of cut would be greatly increased if the abrasive particle speed is as high as the speed of the core of water jet. For this reason, a good water/abrasive mixing is a prime requirement for an efficient cutting process.

There is little theoretical analysis of the mixing of abrasive particles with a high speed water jet. Applying the drag law on particles inside the water stream to simulate the increase in particles speed oversimplify the real problem. It is believed that the particles tend to bounce on the surface of the jet and the speed acquired by the particles is probably gained on impact along the surface of the jet. Due to air entrainment, the density of the jet decrease upstream to reach a lower density than the water density inside the nozzle or in a short length from the water sapphire exit. This change in density reduces pressure in the mixing chamber, the reduction in pressure is called the Venturi effect which is used to draw the abrasive particles into the chamber.

The mixing of abrasive materials with the high speed jet can be enhanced by designing particular cutting head internal geometry, the incorporation of a mixing chamber in the cutting head is essential to draw the abrasive towards the jet stream. The shape of the chamber's internal surface must encourage the mixing process and at the same time minimise the cutting head wear.

The wear of some parts of the cutting head is one of the major obstacles facing the development of abrasive water jet cutting technology especially precision cutting. The wear of the focusing tube in the cutting head is a common problem. It is hoped that this wear can be minimised by suitable cutting head design and in the general context of a cutting optimisation procedure, for example, avoiding the use of unnecessary high operating pressure or high abrasive flow rate and high water mass flow rate. Alternative hard and cheap materials such as ceramics to make the outlet tube are widely available and can replace tungsten carbide or boron carbide which are expensive and difficult to machine or form to the required shapes.

1.3- The cutting process

The cutting process is essentially carried out on particle impact; Particle abrasion of material, material fracture on impact and material wear by repeated impacts probably are all involved in the cutting process. The different wear modes occur depending on the mechanical properties of the cut material as well as type and shape of the abrasive particle. Consequently, the operational parameters must be altered and optimised for materials with different mechanical properties. Quality of cut surface, speed of cut and depth of cut are material related hence can be described by studying failure mode.

Theoretical analysis of cutting by single particle impact are widely available, this analysis, after some assumptions, are generalised to multi-particle impact. The effect of water stream on the actual cutting operation is considered as redundant , since all cutting is considered to be carried out by the abrasive particles.

1.4 - Cutting parameters

From the above descriptions, the parameters of abrasive water jet cutting can be identified as follows;

1- abrasive mass flow rate

2- water mass flow rate

3- stand off distance of cutting head from work piece

4- pump operating pressure

5- speed of cut

6- number of passes

7- angle of abrasive attack to the work piece

8- type and size of abrasive material

9- focusing tube length

10- focusing tube diameter

Mixing abrasive materials with the water jet 'or the degree of mixing of abrasive with jet' can be considered as dependent on the cutting head design.

1.5 - Definitions

Cutting by abrasive water jets is known as a gradual wear of material surface. There are many different forms of material wear, the wear forms which are believed to be involved in the abrasive water jet cutting process are:-

1- **Particle abrasion**; can be described as ploughing in the material occuring in ductile materials and at shallow angle of attack.

2- **Particle erosion**; material removal by interaction of particle(solid of liquid) and surface of the material.

3- **Impact wear**; material surface fractures, as result of particle impact, which intersect and cause material removal, occurs mainly in brittle material wear.

4- **Water (liquid) cavitation**; liquid interaction with surface of material, described by formation and bursting of bubbles on the material surface which results in a material removal.

Chapter 2

Literature Review

2.1. Introduction

A water jet can be used as a "non-wearing cutter " for destroying or cutting rocks and cutting metals. High pressure equipment such as pumps, intensifiers, pipes and nozzles are required.

In this survey, particular attention will be given to the development of the cutting nozzle. To increase the cutting speed for soft materials, and to cut hard materials like steels. Abrasive materials have been added to the water, adding abrasive to the water has created new problems, such as refocussing the mixed jet and increasing the wear rate of the cutting head. This are just two examples of those problems. The nozzle design, and the range of water pressure are being considered in the light of possible improvements in the cutting process. The way abrasive is added is important, to minimise wear in the cutting head and hence increase the efficiency of the cutting process.

Attention also will be paid to the wear mechanism of materials, since abrasive water jet cutting operation can be considered as a combination of fluid mechanics (formation of coherent jet) as well as wear of materials.

2.2.- Historical review of water jet nozzles

First attempts to use water jets in cutting were to cut coal and rocks under ground. Cutting rocks and coal by steel picks causes ignition of methane, hence high speed water jets were considered to provide a method of cutting which is free from this hazard. It is envisaged that rock cutting would be carried out by much higher pressures (compared with coal cutting) and much smaller flow rates, which would be obtained by using small nozzles; no attempt would be made to use the water to transport the rocks away.

Voitseckhovskii, Nikolaev, Ludin, Maier and Chermenskii 1963 (Ref. 1) showed that rocks could be rapidly cut by water jets. In the same year Farmer and Attewell (Ref. 2) studied the penetration of rocks by water jets at up to 1700 bar water pressure. Meanwhile Bryan (Ref. 3) suggested cutting wood, metals, concrete and brick with

water jets.

Precision cutting requires small nozzles to produce fine jets, which precludes the achievement of the good surface finish required for a coherent, continuous and low turbulence jet.

Leach and Walker in 1966 (Ref. 4) described nozzle designs to minimise liquid dispersion. They tested a number of the nozzles and concluded that a 13^{o} cone followed by a parallel portion about 2.5 nozzle diameters long, was optimum. Using X-ray photographs of the water jet from a 1 mm nozzle at pressures 130 and 600 atmosphere, Leach and Walker found that there is a central core which contains most of the mass of the water, but this core is not continuous, except close to the nozzle. Also surrounding the core, is a fine spray of little mass, which is responsible for the visual indication of rapid breakup. When the pressure behind the nozzle is lower there is less fine spray, but there is little mass in the core. Also in this paper, Leach and Walker have reported tests for 14 nozzle shapes, all of which were in the form of a contraction followed by 3 mm long section of 1 mm diameter (Fig. 2.1), the contraction angles varied from 3^{o} to 45^{o} with and without the internal corners of the nozzle rounded. The results show that several nozzle shapes give good results, poor results are obtained for large contraction angles ($> 20^{o}$), and nozzles with sharp internal corners are slightly better than those with rounded corners .
Though Leach and Walker were only concerned with the design of the nozzle rather than the surface finish of the nozzle, their results were the first to explore a potential nozzle design for the cutting process. However, Leach & Walker used additives to reduce turbulence.

For submerged water jets Voitsekhovskii and others in 1972 (Ref. 5) found that rocks and metals (steel) can be effectively cut with a nozzle with a final approach angle leading to the parallel bore of 3^{o} and water pressure of up to 2000 bar. However, the material removal rate was very small compared with the recently developed abrasive water jet.

In recent years attention has been given to the surface finish of the nozzle to reduce the jet spread. Synthetic sapphire orifices still being most widely used because of its combined smoothness of the surface and high hardness to resist wear. The jewel usually has a conical entry on one side and a flat (180^{o}) entry on the other (Fig. 2.2). Since it is easier to produce a good finish of the edge on the flat surface, this side is used as the upstream edge, (Ref. 6, 7, and 8).

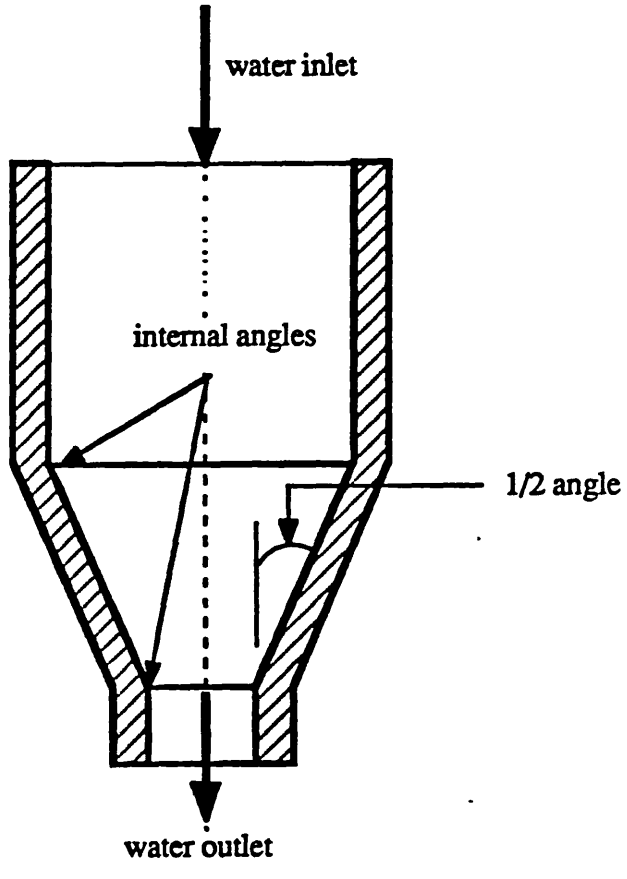


Fig. 2.1 Water jet nozzle

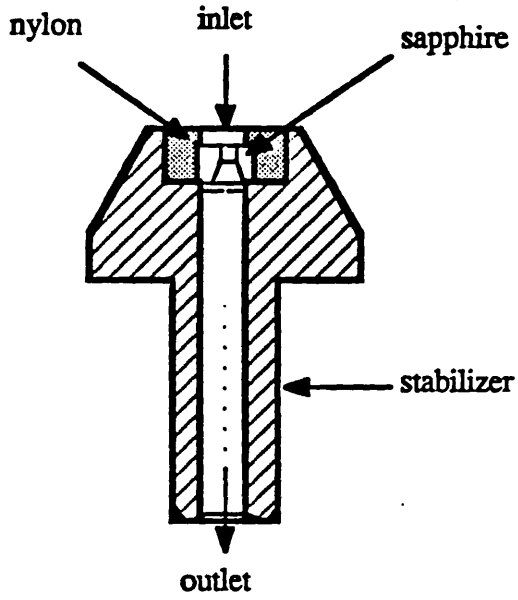


Fig. 2.2 Sapphire orifice mounted in steel holder

A great deal of literature describing the jet stability problem exists, unfortunately virtually all jet stability work has dealt with velocities significantly lower than those used for cutting purposes. An excellent review of this work is given in 1973 by McCarthy and Malloy (Ref. 9).

In 1972 Harris and Brierley (Ref. 8) tried tungsten carbide and diamond orifices with conical or rounded entries, but these did not perform as well as sapphire orifices, largely because it was difficult to produce sufficiently good finish on the hard materials. The authors also investigated the effect of other parameters such as nozzle size and water pressure in cutting newsprint, box board, plastics, leather, hardwood pulp sheets and asbestos cement board.

A theoretical analysis of nozzle designs was carried out by Lohn and Brent in 1976 (Ref. 10). They developed a computer program to design nozzles by determination of the fluid flow within the nozzle, and to estimate the effect on the jet flow after exit from the nozzle. As a result of their analysis, Lohn and Brent recommended that the nozzle length should be shortened and the nozzle made with a large converging angles, but these recommendations are limited by cavitation and separation considerations. Such considerations require that half angles be on the order of 20^{o} to 30^{o} with lengths from 5.1 to 10.2 cm with the exact values varying for each internal shape and flow condition. However, it should be noted that the analysis was limited to pressures under 350 bar and flow rate between 0.25 and 25.20 litre/sec. (15 and 1500 kg/min.)

Yanaida and Ohashi in 1980 (Ref. 11) have developed a mathematical expression for the axial dynamic pressure of all the regions of the water jets in air i .e . , in the continuous flow region, droplet flow region and diffused flow region. Yanaida and Ohashi used experimental results to evaluate empirical constants in the theoretical analysis.

A further theoretical and experimental study was made by Amono and Neusen in 1982 (Ref. 12). The purpose of the study was to examine the behaviour of high velocity

jets used in jet cutting . In this paper, a numerical procedure is described which allows solution of the Navier-Stokes equations in conjunction with a two equation turbulence model. The procedure is then applied to jets with nozzle exit velocities up to 900 m/s. The pressure distributions over a flat plate target were obtained from the calculations. One of the authors main conclusions was that the influence of the nozzle exit velocity is much larger than that of the turbulence intensity level in the nozzle. However, the paper is concerned largely with the choice of turbulence model for a free jet rather than the inlet condition of the jet .

Konig and Wulf, 1984 (Ref. 13) discussed the quality of the cut for three different nozzle designs. The orifices in the three nozzles were made of sapphire mounted on metal holders. The designs of the inlet and outlet of the nozzles were also varied. The authors found that the quality of the cut was influenced by other parameters, among them the standoff distance and the feed rate of the work piece .

A numerical study by Amano and Kodali, 1984 (Ref. 14) has been reported on the turbulent flow in a closed passage, to simulate a slot in a cutting operation, the effect of parameters such as passage width, slot width and passage depth on the cutting operation were discussed.

Another numeric-mathematical simulation of the cutting process was carried out in 1986 by Przyklenk and Schlatter (Ref. 15). The resulted computer package can be used to optimise the layout of pipe work before setting up an installation as well as the simulation of the stock removal by the water jet.

The effect of an air mantle around a submerged jet is explained in two papers by Gelfort and other in 1984-1986 (Ref. 16) and (Ref. 17). In these papers, it is shown that the spread of the submerged water jet in water tank can be decreased by an air mantle around the jet.

2.3- Abrasive jet cutting nozzles

Water jets alone are not suitable for all cutting applications and when materials are hard, very high pressure is needed for the jet to be an efficient cutting mechanism. But increasing the pressure is limited by substantial jet-wall interaction which has a detrimental effect on performance of the cutting process as reported in 1976 by Labus (Ref . 18), 1978 by Mazurkiewicz, Sebastian and Galecki (Ref .19) and in 1982 by Amano and Neusen (Ref. 12).

The idea of employing abrasive streams for removal of material has been in use for many years. Sandblasting(abrasive-air jet) techniques used for cleaning and surface finishing applications (Refs. 20, 21, 22). Nozzles were developed for high air or water pressures and high abrasive flow rates. The patented nozzles (Refs. 23, 24, 25, 26) are widely used in the sandblasting industry today. A detailed comparison between these nozzles was carried out by Hashish in 1982 (Ref. 27). The use of water with abrasive for surface cleaning has one advantage over dry abrasive techniques. Any dust generated is effectively damped down by the water, also abrasive water jet cleaning is well suited to cleaning underwater structures such as drilling platforms (Ref. 22, 28, 29, 30, 31). Increasing the water pressure will increase the abrasives speed and for cutting application, this high speed abrasives is focused at small area to give an efficient narrow cut. However, any further increase in pressure or decrease in water nozzle diameter resulted in dispersion of jet, hence increase in cut width.

The abrasive is either entrained into the high velocity water jet after it has left the nozzle or mixed with water then pumped through a single nozzle. The advantages and disadvantages of mixing the abrasive by the two ways namely down stream and up stream mixing are open to debate.

Hashish 1982 (Ref. 27) discussed the general advantages of downstream mixing, which are;

(1) Wear by abrasives is restricted to the mixing area and can be minimised.

(2) The system easily adapts to state of the art high-pressure pumps.

The advantages of upstream mixing lie in its more effective cutting capabilities and the compactness of the nozzle head.

For downstream mixing the abrasive is entrained in the high velocity water jet after it has left the nozzle. Hashish (Refs. 27, 32, 33, 34) preferred this method because the abrasive does not pass through the pump or the nozzle and therefore the problems of wear in these components are avoided. In many instances the equipment acts similarly in principle to a jet pump with the abrasive being drawn into a region of low pressure. Several downstream-mixing approaches were discussed by Hashish (Ref. 27), some of these abrasive jet cutting approaches are :

a - Single jet side abrasive feed.

b - Multiple jet central abrasive feed.

c - Annular jet central abrasive feed.

d - Single jet external feed or taped abrasive.

The advantages and disadvantages of these approaches are discussed in Hashish's paper.

In most of the above cases, abrasive and water flow rates were not used as important factor in the cutting systems. Water flow rate was increased and focusing tube diameter was also increased to overcome the jet spread. Single jet side abrasive feed consumed minimum abrasive and water flow rates of at least 8 kg/min.

Trials on two different abrasive jet cutting heads are reported in a paper by Saunders 1982 (Ref. 35) both of these abrasive heads operate on the principal of a "jet pump" by using a high velocity water jet to generate a region of low pressure in a mixing chamber into which an abrasive laden fluid is drawn. For most the trials described in Saunders paper, air was used as the transporting fluid. Saunders tested nozzles to cut concrete and steel at operating pressures of up to about 1000 bar and water nozzle sizes used were 1.5 mm, 1.8 mm and 2.2 mm(not less than 10 kg/min of mixed abrasive and water flow rates). Saunders reported the performance of the cutting head under different parameters and operating conditions such as; stand off distance, abrasive feed rate, angle of attack, type and size of abrasive, operating pressure, water nozzle size

and depth of cut. There are several papers for Saunders and others from the BHRA on abrasive cutting with downstream mixing (Ref. 36, 37, and 38).

In 1984, Yie (Ref. 39) used multiple-water jet nozzle, the nozzles have several water jets arranged in a circular pattern and converge axially to form a single jet stream. The abrasive is fed from the centre of the converging jets. The advantages of such design is that the mixing efficiency is improved, but as a result of using several jets which must meet at a single point, water flow rate was greatly increased to 10 kg/min. The width of cut was large about 10mm in concrete as reported by Yie. Moreover, the fabrication of the head is laborious job since accuracy is required in making the jets, often 5-6 or more, must meet at one point. Increasing the operating pressure results in changing the position of this meeting point. Yie used the head to cut metals, concrete, rocks, glass, ceramics, plastics and composites; data of the head performance in cutting these materials is reported in this paper.

In 1986, the BHRA devised a new abrasive cutting technique by a direct injection abrasive jetting "DIAJET" (Ref. 40). By this method the abrasive particles are accelerated along the water through a single nozzle. Pumping the slurry (water/abrasive mixture) is achieved by pressurising a vessel using the conventional high pressure plain water jetting pump. The vessel incorporate abrasive storage and metering and allows the water to pick up a controlled concentration of abrasive prior to passing this through along flexible hose to the "DIAJET" nozzle at the cutting station. According to the paper, the details design of the nozzle avoids unacceptable rates of wear. However what is known is the system consumes a large flow rate of abrasive and water (15 kg/min) which is unacceptable in any controlled precision cutting. However, wear rate of the nozzle is not discussed.

The optimisation of the cutting parameters of down stream mixing is discussed by Hashish in 1982 and 1986 (Refs. 27 & 34), and by Saunders in 1982 (Ref. 35). The main parameters involved in the cutting operation are discussed. From the above studies, parameter can be divided into two types:-

water jet related parameter such as:

stand off distance, abrasive feed rate, water flow rate, traverse speed number of passes and operating pressure.

And the cut material related parameters such as:

angle of attack and type and size of abrasive.

2.4- Water jet related cutting parameters

2.4.1- Stand off distance

The stand off distance is considered as the gap between the end of the outlet tube and the test sample. There is a general a agreement that the shorter the stand off distance the deeper the cut. However, Saunders (Ref. 35) found that, when using a certain stand off distance, abrasive particles are deflected back from the work piece surface and cause severe erosion of the external surface of the cutting head.

Hashish (Ref. 27) noted that the effect of increase of stand off distance, as a result kerfing in the material is compensated by the development of the kerf which keeps the jet intact.

2.4.2- Abrasive feed rate

For different abrasive and at fixed pressure, Saunders (Ref. 35) derived a relationship between the depth of cut (h) and abrasive feed rate (M) which is approximately $h \propto (M)^{0.8}$, the upper limit of this relationship as Saunders noted is determined by capacity of the cutting head, increasing the feed rate over this limit causes a blockage in the abrasive feed pipe. Hashish (Refs. 33, 34, 41) suggested the approximate relationship:-

$$h \propto \frac{\frac{M}{m} QP}{\left(1+\frac{M}{m}\right)^2}$$

Although, Hashish developed the above relationship between depth of cut and the abrasive flow rate, he listed a large number of parameters which have effect on this

global relationship. However, there is a general agreement on the existence of a critical abrasive flow rate. Studying the abrasive flow rate, the researcher's main concerns were the effect of abrasive flow rate on speed of cut and depth cut.

Generally, abrasive feed rate is deliberately increased for faster cutting operation without and consideration to excessive flow rate or to wear of the cutting head outlet tube.

2.4.3- Operating pressure

Speed of jet and hence the speed of abrasive particles depends upon the operating pressure. Both Hashish and Saunders in 1982 (Ref. 27) and (Ref. 35) studied the effect of pressure on depth of cut of steel and concrete, the results show an initial linear relation between pressure and depth of cut, Hashish's results show the initial linear relation followed by a declining deviation from linearity, while Saunders results show the linear relation followed by a remarkable increase in depth of cut by increasing the pressure. This difference may be explained by the nozzle designs which plays a big part in mixing of abrasive and the momentum change of the pressurised water. Hashish explained the declining deviation from linearity by the decrease in efficiencies of the water jet orifice and the other hydraulic components as pressure increases.

In 1982, Hashish (Ref. 27) discussed the relationship between power of water pump, pressure and depth of cut and concluded that doubling the power does not double the depth of cut, hence an optimum operating pressure should be determined as a compromise between the rate of cutting and power requirements. In 1986 Hashish (Ref. 34) reported that the most efficient utilisation of the hydraulic power will occur at a pressure equal to 3 times the threshold pressure (threshold pressure is the optimum pressure required to cut a given thickness of material). However, Hashish discussed factors influencing the choice of an optimum working pressure such as wear rate of nozzle, pump maintenance, coefficients of discharge, mixing and flow of abrasive and finally, the limitation of pressure at which the equipment can be used (i.e flexible hoses).

2.4.4- Water flow rate

The rate of momentum carried by the water jet depends upon two parameters; pressure (P) and mass flow rate of water (m). m, changes by either changing the pressure, P ($m \propto P^{0.5}$) or by changing the water jet orifice size (d) ($m \propto d^2$). The relationship between water pressure, mass flow rate, nozzle orifice diameter and hydraulic power are given in the pump manufacturer manual.

Hashish 1986 (Ref. 34) tested two water jet orifices 0.25 mm and 0.38 mm, He argued that increasing the size of orifice from 0.25 mm to 0.38 mm will increase the water flow rate, at any pressure, by a factor of 2.25, while the depth of cut at the same pressure is only increased by a factor of about 2. He concluded that the the percentage increase in depth of cut is always lower than the percentage increase in water flow rate. Hashish discussed the disadvantages of increasing the water flow rate beyond a certain limit which he did not quantify. In this paper and following papers Hashish continued to use large water flow rate, over 7 kg/min., to reduce jet spread and increase speed of cut.

2.4.5- Traverse speed

Hashish (Refs. 27, 34 and 41) studied the effect of traverse speed on depth of cut and the rate of the kerf area generation. It was found that an optimum traverse speed exists for maximum kerf area generation. This should not be generalised since for concrete cutting the kerf area generation increases with increasing traverse speed for a given number of passes. However, Hashish pointed out that the optimum traverse speed is a function of all the other cutting parameters.

There are other factors which will be affected by the traverse speed, Hashish (Ref. 34) discussed these factors which include:- quality of cut, surface finish and manipulation of work piece.

2.4.6- Number of passes

Hashish (Refs. 27, 24), Yie (Ref. 39) and Nakaya (Ref. 42) have studied the effect of number of passes on depth of cut. There is general agreement that the increase of number of passes results in a linear increase in depth of cut to a certain limit. This limit is controlled by the stand off distance which increases as the cumulative depth of cut is increased. The limit is dependent on other parameters such as; operating pressure and water mass flow rate. Hashish observed that low cutting speed (more number of passes) will result in smoother cut surface.

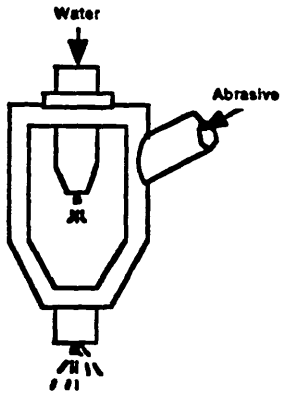
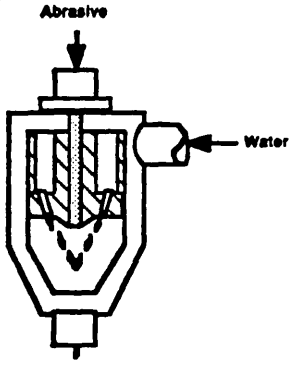
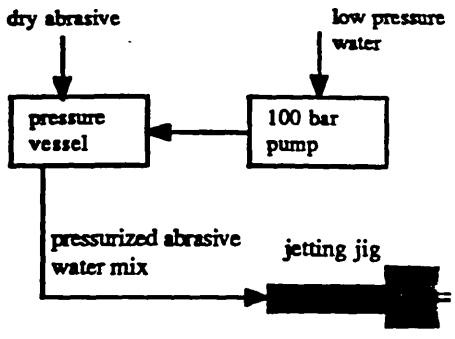
	Single jet side feed Hashish Refs. 27, 32-34 BHRA Refs. 35-38	Multi- jet central feed Yie Ref. 39	DIAJET BHRA Ref.40
nozzle type			
Max. operating pressure	4000 bar	1380 bar	340 bar
Abrasive feed rate	Garnet 1 kg/min. Abrasive 7 kg/min. Water	Garnet 0.5 kg/min. Abrasive 10 kg/min. Water	Mansfield 20 sand 13 kg/min. Abarsive and Water (slurry)
Speed of cut	Mild steel 15mm thick 150mm/min. removal rate = 6.75 cc/min.	Stainless steel 3mm thick 130 mm/min removal rate = 3.9 cc/min.	Mild steel 13mm thick 300mm/min. removal rate = 9.75 cc/min.
Nozzle outlet diameter	3mm	Width of cut 5-10mm	2.8 mm
Pump power	45KW	45KW	5.5KW

Table 2.1 *Comparison of abrasive water jet cutting approaches*

A mathematical model of abrasive water jet cutting was investigated in 1984 by Hashish (Refs. 33, 43). The investigation involved visualisation of the cutting interface and analysis of the erosion process by abrasive water jets. The model uses existing theories on the erosion of ductile metals by solid particle impact, namely the two modes of wear; a cutting wear mode, which occurs at the top of the kerf primarily due to particle impact at shallow angles, and a deformation wear mode, which occurs deeper in the kerf and is associated with large angles of impact. In these papers, Hashish presented a global cutting equation to predict the depth of cut as a function of the different abrasive water jet parameters.

He also compared modelled and experimental results. Although Hashish found good agreement between modelled and experimental results, the model fails to predict :

- The effect of particle size which is related to the cut material.
- The effect of traverse rate on the cutting process.
- The mechanism of particle water jet mixing.

However, one of Hashish's conclusions was the role of water is primarily to accelerate the particles to high velocities. Hence, water interaction effects on the micro-cutting process can be neglected. *This model will be discussed fully and modified in chapter 3 as part of the theoretical analysis.*

Another mathematical model by Tan 1986 (Ref. 44), was programmed to examine the effect of using abrasive water jet cutting on surface finish of the cut. In his model, Tan made use of the physical principles first adopted by Mellor (Ref. 45). These principles relate the jet kinematics to the cut material properties. Tan used Hashish's (Refs. 33, 46) hypothesis of the cutting process. This hypothesis divide the process into three stages:

(i) An entry stage.

(ii) A cyclic cutting stage.

(iii) An exit stage.

Tan compared the model results with experimental results and showed them to be in good agreement for a work piece of mild steel. Both model and experimental results were taken for variations in water supply pressure, jet traverse speed and abrasive grit

size.

Tan suggested using the model to study any striated surface finish which is common to most single stream cutting techniques, such as laser or flame cutting.

2.5- Material related parameters

Wear of materials varies according to their mechanical properties. The parameters of the any cutting process change accordingly.

2.5.1 Ductile materials

(a) Angle of attack

Since cutting is carried out by means of wear of material by abrasive impact, Wellinger 1949 (Ref. 47) determined the wear as a function of impact angle. Testing low carbon steel, which is soft and ductile, and a hardened high-carbon steel, which is brittle. It was found that the hard and brittle steel appears to be more erosion resistant at low impact angles than the soft steel, while at high impact angles the reverse is true (Fig. 2.3).

Finnie 1958 (Ref. 48), 1960 (Ref. 49), and 1962 (Ref. 50) has discussed the wear mechanism of brittle and ductile materials.

Bitter 1963 (Ref. 51) derived a formulae to express wear ı as function of mass and velocity of the impinging particles, impingement angle and mechanical and physical properties both of erosive particles and eroded body.

A great deal of literature has been published on wear mechanism (Refs. 52 to 73). Ives and Rulf 1979 (Ref. 58) obtained some experimental results on wear rate of brittle and ductile materials, the results show the variant responses of wear to the abrasive angle of attack .

The predicted volume removal rate, the cutting and deformation wear varies with angle of attack (α) as shown in (Fig. 2.4). Finnie (Ref. 48) showed that the predicted variation of material removal with the angle of attack for a single grain has the same

general form as the experimental data for erosion by many grains. In particular, for maximum wear , they are closely in agreement, at $\alpha = 90°$ the predicted result is zero volume removal rate while the experimental results indicate the occurrence of wear . The reason for the variation between prediction and experiment is that the analysis assumes that the particle strikes a smooth surface and the surface remains smooth after impact. In practice, after the first strike the surface is roughened and subsequent particle strikes the eroded surface at a wide variety of true angles created by impressions on the previously smooth surface.

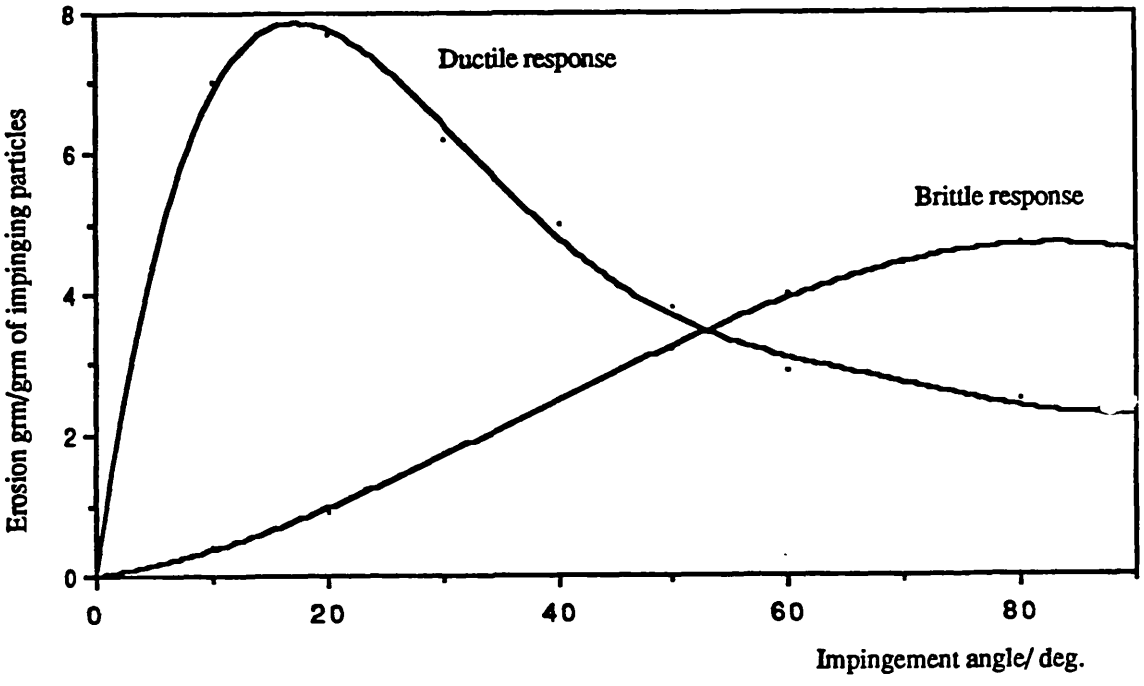


Fig. 2.3 Schematic representation of material removal rate on attack angle

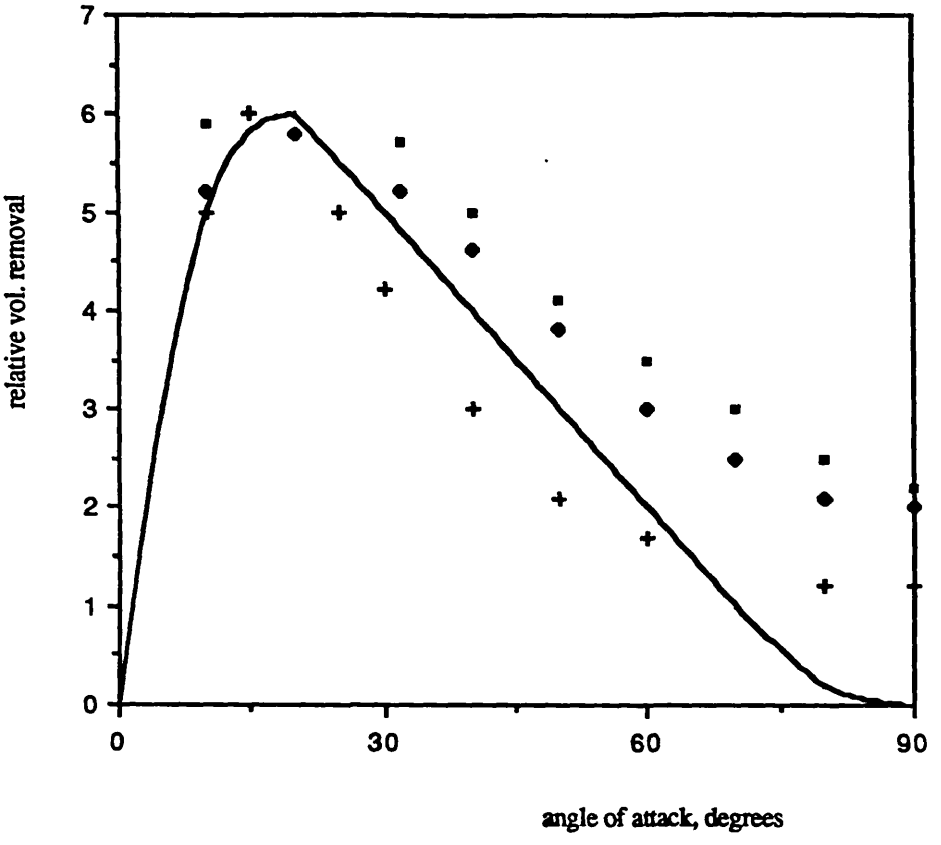


***Fig. 2.4** Predicted variation of volume removal with angle for a single abrasive grain. Experimental points for erosion by many grains (+ aluminium, ♦ copper, ▪ SAE steel) are plotted so that the maximum erosion is the same in all cases (Ref 48)*

In 1982 Saunders (Ref. 35) studied both stationary and moving cutting head in cutting mild steel, and found the angled head to perform better in both situation. For a moving head it was found that the direction of deviation relative to the direction of motion is important. A jet angled backwards from the direction of traverse is found to improve performance.

(b) Type and size of abrasive

Wellinger and Uetz 1958 (Ref. 73) found strong dependence of the erosion upon the hardness of the attacked surface, in relation to the hardness of the abrasive particles (Fig. 2.5).

It has been shown that for cutting erosion to take place, the hardness of abrasive particles must be greater than the hardness of the eroded material. Variation of the abrasive hardness above the material hardness is not important. Accordingly, the relative wear resistance of the materials should show little change as the abrasive hardness increase over the material hardness.

Sharp angular particles will produce more material wear than spherical particles of the same abrasive material. In the analysis, the parameter ϕ ($\phi = R_y/R_x$, Ratio of vertical to horizontal force of particle on material) will change with changing the particle shape, ϕ increases as the particles become less angular and more spherical. Finnie found that an increase in ϕ increases the angle of maximum erosion, and decreases the surface weight loss at this angle. The predicted angle of maximum erosion is insensitive to particle shape.

Strong abrasive cuts as a single unit or fracture internally. While fragile abrasive increases secondary erosion (Refs. 56, 74). However, a generally strong abrasive increases the wear process.

Size of abrasive also influence the wear process, the optimum size to achieve maximum wear rate is a function of the material's mechanical properties. Hashish (Ref. 34) reported that 250 μm (mesh 60) abrasive are more effective in steel cutting than finer size 150 μm (mesh 100) and coarser sizes 500 μm (mesh 36).

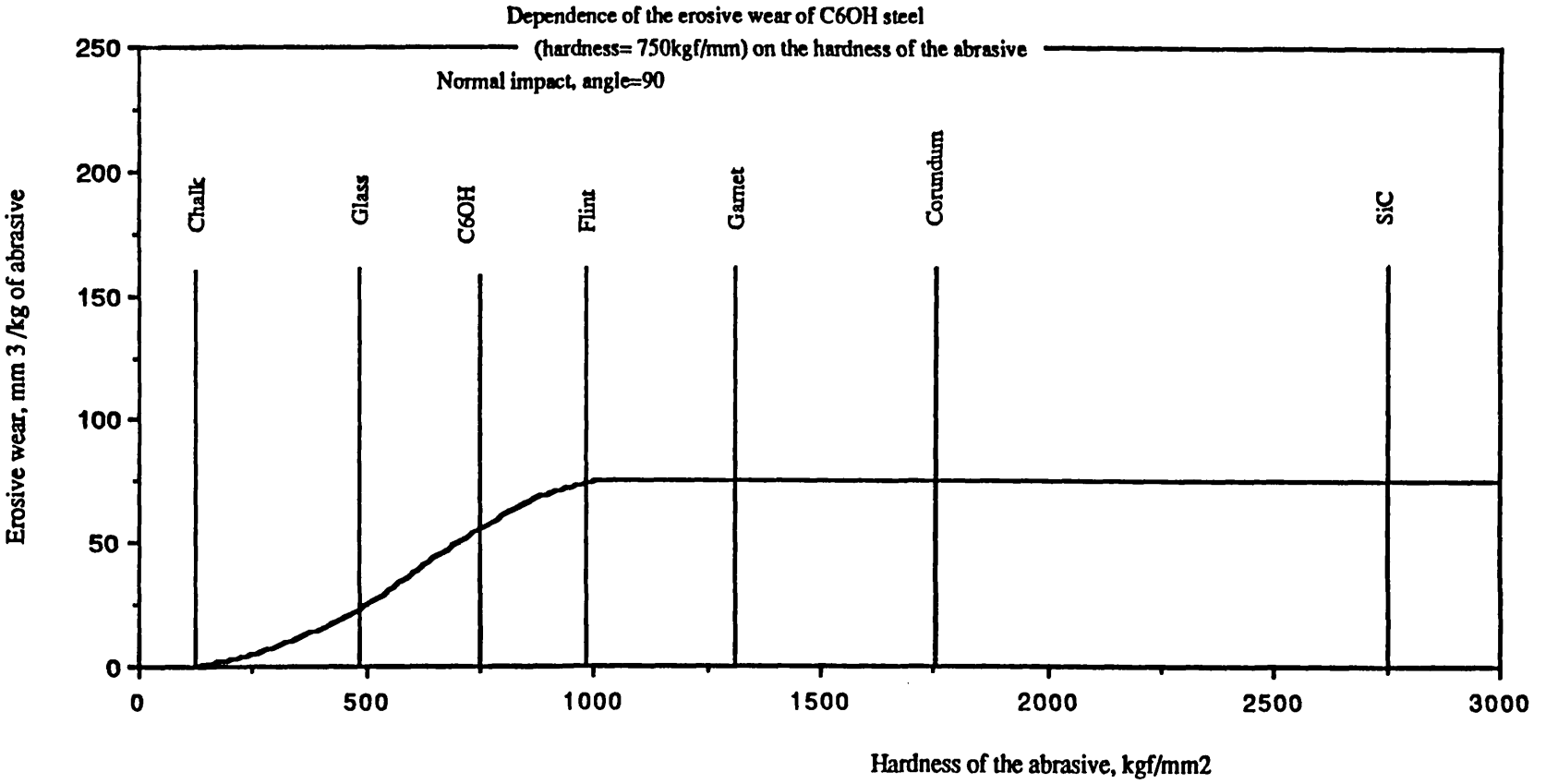


Fig. 2.5 Wear rate of C60H steel V Hardness of abrasives (Ref. 73)

Saunders (Ref. 35) tried several abrasives at maximum feed rate, the abrasives are listed according to performance.

- Silicon Carbide, gave best results
- Copper slag
- Aluminium Oxide (Garnet)
- Olivine
- Mansel Sand.

Also, Saunders found that the abrasive particle size is important. Fine silicon carbide grade 80 (180 Microns) gives the best performance.

(c) Influence of the particle velocity

From experimental work on several metals, Finnie found the relation between weight loss (W) and the velocity of particles (V) (Fig. 2.6).

The line $W \sim V^2$ gives a good fit to the data of weight loss of annealed SAE 1020 steel impacted by 46 mesh silicon carbide grains at angle $\alpha = 20^\circ$, at low velocities the particles produce only elastic stresses at the surface and hence the weight loss at low velocities will decrease more rapidly than predicted by the expression $W \sim V^2$. This decrease is also a function of particle shape (Ref. 48). It is found that hardened spherical steel shots impacting an annealed steel produce much less wear than predicted at low velocities for silicon carbide grains, this is because the fact that spherical shots do not have sharp edges for cutting to takeplace. However, both spherical and angular abrasives, the maximum wear angle of attack is not influenced by particle velocity.

2.5.2- Brittle materials

Ideally brittle materials cannot deform plastically, but instead, they crack and fracture when they are subjected to large impact stresses.

The complexity of the wear process of brittle materials has predictably resulted in more than one theory describing mechanism of brittle materials wear.

Sheldon and Finnie (Refs. 71, 75) have predicted the volume removal rate by studying the interaction of the eroding particle and the surface (Fig. 2.7) *See appendix I.*, For failure to occur, a critical tensile stress must be achieved.

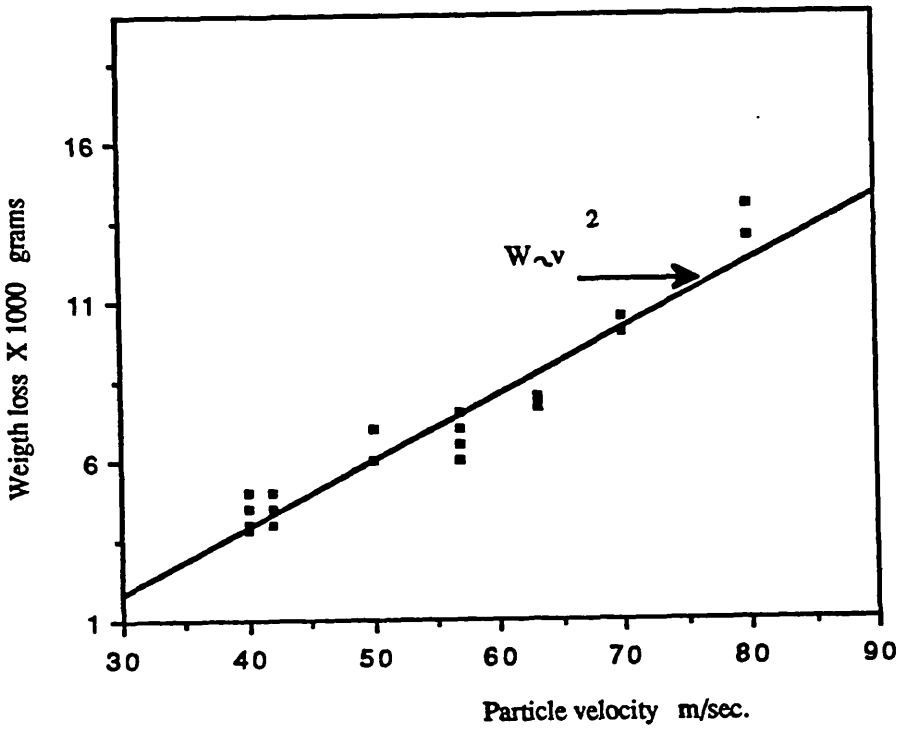


Fig. 2.6 Ductile wear *of annealed SAE 1020 steel as a function of velocity*

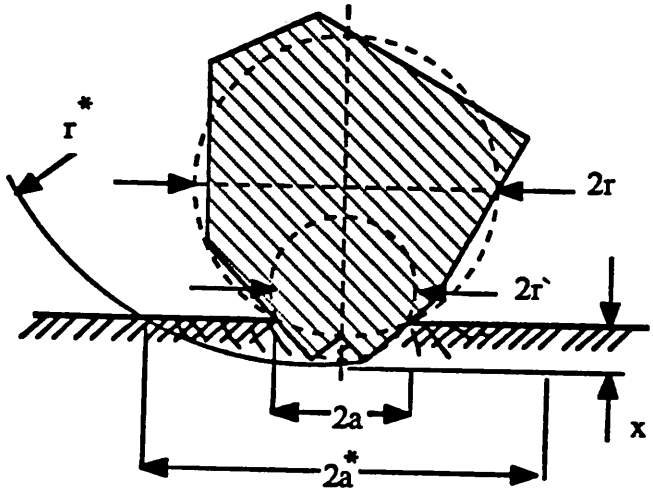


Fig 2.7 Overall contact surface in brittle wear

The classical Hertz equations predict the relationships between force, stress and indentation depth for a static loading of a continuous plane surface by a sphere have been extended by impact conditions (Ref. 76).

The cone and ring cracks which form in a Hertzian are assumed to intersect and cause mass loss by breakout of chunks of materials. The accuracy of the analysis is questionable at moderate impact velocities at which the assumed quasistatic stress distributions become inaccurate. However, the analysis is useful in predicting the relative volume removal rate of metals.

An alternative theory to the Hertzian analysis is based upon dynamics plastic indentation (Ref. 77). In this paper, it is assumed that the propagation of radial cracks outward from the contact zone and propagate between the radial cracks on planes nearly parallel to the surface. The model predicts a wear rate dependence of velocity . The analysis proved to be limited to certain brittle material and particular abrasive types such as silicon carbide (Ref. 78).

(a) Angle of attack

It is shown (Ref. 75) that cracks initiated when critical tensile stress is reached. The intensity of tensile stress is governed by the normal component (V sinα) of the impact velocity. In ductile wear , cutting wear takes place, which make ductile materials more sensitive to angle of attack, while in brittle wear n, maximum volume removal rate is achieved at near normal angle of attack for angular shaped particles and at 90° for spherical particles.

(b) Particle velocity

The dependence of volume removal rate of brittle materials is very different from the ductile materials. The velocity relation d(vol.) $\sim V^n$ is found near linear as ductile wear but n (constant) ranges from 3 to 6 (Fig. 2.8).

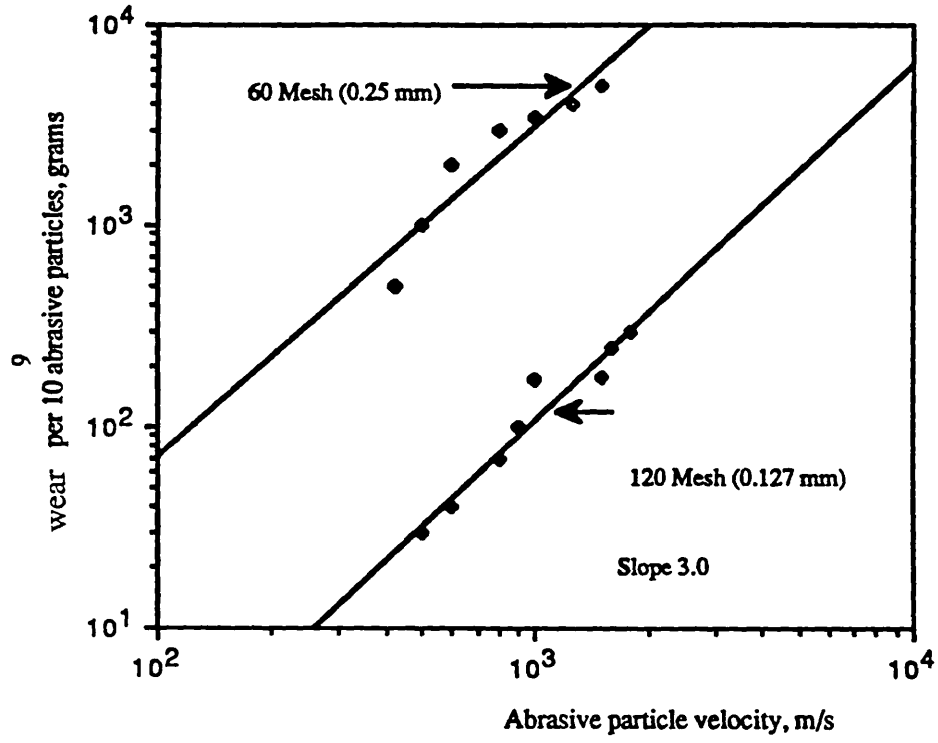


***Fig. 2.8** Brittle* wear *of glass by angular SiC grit, at $\alpha = 90^o$ as a function of velocity (Ref. 71)*

(c) Type and size of abrasive

Shape, size and density of abrasive particles are important factors which influence the wear process of ductile materials. This is not the case for brittle materials, since no ductile cutting occurs in brittle materials wear , the shape of the particle has little importance except in that spherical shape particles is relatively dense hence have larger kinetic energy on impact and therefore cause larger and deeper craters in the surface.

It is shown (Ref. 71), that small particles can produce the effect of ductile erosive cutting in nominally brittle materials. (Fig. 2.9) show that weight removal against α relation for three sizes of angular SiC grit (127, 21 and 9 μm 120, 500 and 1000 mesh respectively), eroding a plate of glass, a nominally brittle material. Small size grit (9 μm) produces a typical ductile wear , while the other sizes produce a brittle wear characteristic. This is explained by the distribution of flaws throughout the material. The flaws produce stress concentrations upon contact loading and the probability of encountering these, decrease with decreasing dimensions of the contact region. Thus, the fracture strength effectively increases for small size particles, and the material tend to flow instead of fracturing.

2.6-Conclusions

From the literature search, performance of cutting heads, such as mass flow of water and abrasive and speed of cut are extensively reported. However, for commercial reasons, the cutting head design description was never disclosed or discussed. The focusing tube length and its operational life were not considered to have influence in the cutting operation. In many cases, the general belief is that the mixed jet focusing and cutting head wear are minimised by increasing abrasive and water flow rates. The internal shapes of cutting head or mixing chamber shape have not been discussed or tested. alternative new and cheap hard materials such as ceramics to replace tungsten carbide and boron carbide (which virtually selected by all researchers) are not examined.

In many of the above cases, tests on single particle wear are considered as indicative to the general trend of material wear for a stream of particles impact.

Mixing abrasive with the water jet was considered as important factor which influence the cutting operation. Yet, there is no theoretical or experimental research work on this topic.

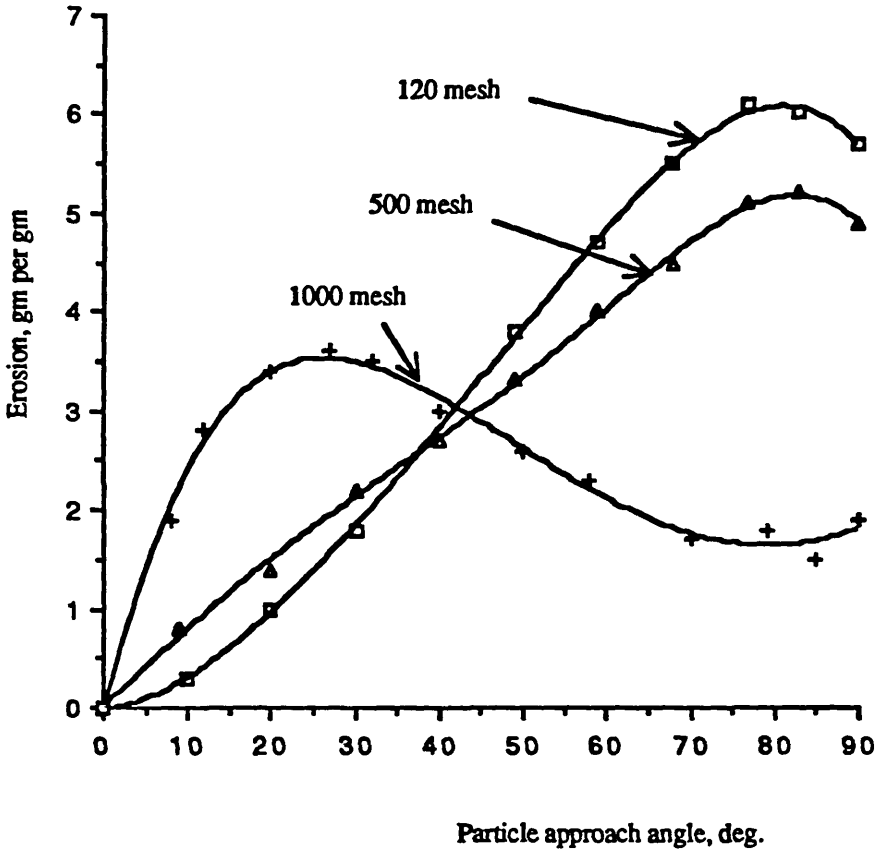


Fig. 2.9 Weight removal as a function of particle approach angle for plate of glass eroded by angular silicon carbide particles at V *=152 m/s, (Ref. 71)*

Chapter 3

Theoretical Analysis

3.1-Introduction

Many researchers have attempted to define universal qualitative and quantitative correlations between the many parameters involved in material wear by single or multiple particles. The basic objective of their research was to reduce material wear. However, the objective of this thesis is the opposite. Cutting heads are designed to create continuous abrasive and water mixed jet to further this aim.

A stable continuous water jet is essential for the cutting operation. All the parameters which may have an effect on the stability of the jet are thoroughly investigated.
In the light of previous work on abrasive water jet cutting and material wear, a critical approach will be adopted to the jet spread and actual cutting operation. Particular attention is given to parameters such as water jet spread, nozzle surface roughness, water pressure and jet velocity, mixing chamber design, mixing of abrasive with the continuous jet and finally the cutting mechanism of the abrasive-water mixed.

Some of the existing hypothesis on materials wear are adopted and in some instances are modified to simulate a continuous cutting operation.
The use of preliminary tests and observations of the jet will be in such help for theoretical analyses.

3.2-Water jet parameters

Since the major requirement of a water cutting jet nozzle is the efficient conversion of potential energy to kinetic energy, a great deal of attention has been paid to the geometry and surface finish of the nozzle's internal surfaces. In this thesis, disregarding the water nozzle's internal angles might be justified because of the high water pressure and low water mass flow rate. The internal volume of the pipe, up stream the sapphire orifice, can be considered as a large reservoir of low turbulence water, thus the wall induced eddies do not disturb the centre line stream of the flow. The level of turbulence at the outlet will be affected by the sapphire wall roughness. To obtain a value of this roughness height, the thickness of the laminar sublayer must be calculated, since roughness within the layer will not disturb the inner flow.

The thickness of the layer is given by:- (Ref. 4)

$$\delta = \frac{5\upsilon}{V_f}$$

Where V_f is the friction velocity

$$V_f = \sqrt{\frac{\tau_o}{\rho_w}}$$

and τ_0 is the shearing stress at the wall.

The mean velocity through 0.25mm sapphire hole can be calculated using Bernoulli's equation

$$u^2 = \frac{2gp}{\rho_w}$$

$$u = 14\sqrt{p}$$

where P is the operating pressure in bars, the actual driving pressure is the operating pressure minus the pressure loss within the nozzle friction and contraction, which usually evaluated experimentally for the nozzle in use (sapphire surface smoothness = 0.015×10^{-6} m).

The thickness of the boundary sublayer is very small and its the effect on the jet stability is considered to be of minor importance especially that of high speed jets. It has been established that δ decreases rapidly as Re increases (Ref. 79).

The nozzle aspect ratio L_d/d was investigated (Ref. 4), it is found that a hole followed by a straight section of length L_d = 3xd is best, increasing L_d will increase the nozzle pressure loss without any improvement in jet stability. Since sapphire nozzles have very smooth and hard surface, it is assumed that L_d /d ratio is less significant as far as high speed jet is concerned. However, the sapphire hole followed by a straight length will make the jet more stable than a hole with no straight section following.

The structure of submerged turbulent jets is well known (Ref. 80), the jet can be divided into 3 distinguishable flow regions (Fig. 3.1); The initial, transitional and main region.

Assuming that the velocity field at the initial cross section of the jet is uniform, the boundaries of the mixing layers form diverging surfaces, which intersect at the edge of the exit hole. On the other side, the boundary layer comes into contact with the stationary air, and at all points on the outside boundary the velocity component in x-directiion are equal to zero (u_2=0). On the inside, the boundary layer changes to a constant velocity core u_1 which is equal to u_0. Considering these assumptions, it is possible to evaluate the spread of a turbulent jet in air.

In a turbulent jet the velocity components at any point are described by time averaged values and the randomly varying perturbation.

$$u = \bar{u} + u' \qquad\qquad \omega = \bar{v} + v'$$

the average fluctuation over a finite time interval is zero.

$$\overline{u'} = \overline{v'} = 0$$

If the mean free path of a fluid particle (mixing length) in a turbulent stream is equal to L, when moved in a transverse direction, the fluid particle reaches a layer in which the mean velocity differs from what it was in the layer which the particle separated by the following value:-

$$\Delta\bar{u} = L\frac{\partial\bar{u}}{\partial y}$$

the fluid particle merges with the mass of the new layer which will be accompanied by a discontinuous variations in velocity of:-

$$u' = \Delta\bar{u}$$

these variations of the streamwise velocity component are of the order

$$u' \sim L\frac{\partial\bar{u}}{\partial y}$$

Also, it is assumed that that the transverse variations in velocity v' are proportional to streamwise variations u' but with the opposite sign $-v' \sim u'$ therefore;

$$-v' \sim L\frac{\partial\bar{u}}{\partial y}$$

In free stream, Prandtl (Ref. 81) assumed that the mixing length at any cross section of the stream was constant. $L(y) = \text{constant}$

By the similarity of boundary layers in different cross sections of free stream, it has been established by a large number of experiments in which the velocity profiles proved to be universal when plotted with dimensionless coordinates.

$$\frac{u}{u_m} = f\left(\frac{y}{b}\right) \tag{3.1}$$

also the variation in the mixing length along the x-axes L = L(x) may be established by means of available experimental data.

The similarity of boundary layers in the sections of the given free stream implies, among other things, the similarity of geometric dimensions. Therefore, equality may be expected between the dimensionless mixing lengths for the sections of the stream:-

$$\frac{L_1}{b_1} = \frac{L_2}{b_2} = \text{----------} = \text{constant} \tag{3.2}$$

to define the law in which the mixing length increases, Prandtl (Ref. 81) assumes that the growth of the jet is controlled by the transverse perturbation velocity.

$$\frac{db}{dt} \sim v' \sim -L\frac{\partial \bar{u}}{\partial y} \tag{3.3}$$

from the similarity of velocity profiles in different cross sections of the jet, it is possible to write:-

$$\frac{\partial \bar{u}}{\partial y} \sim \frac{u_m}{b} \tag{3.4}$$

hence,

$$\frac{db}{dt} \sim \frac{L}{b} u_m \sim u_m \tag{3.5}$$

The rate of growth of the jet can be written as:-

$$\frac{db}{dt} = \frac{db}{dx} \cdot \frac{dx}{dt} \sim \frac{db}{dx} \cdot u_m \tag{3.6}$$

from equations (3.5) and (3.6)

$$\frac{db}{dx} = \text{constant}, \quad \text{which gives} \quad b = x \cdot \text{constant}$$

and from eq. (3.2), $L = \text{const.} \cdot x$

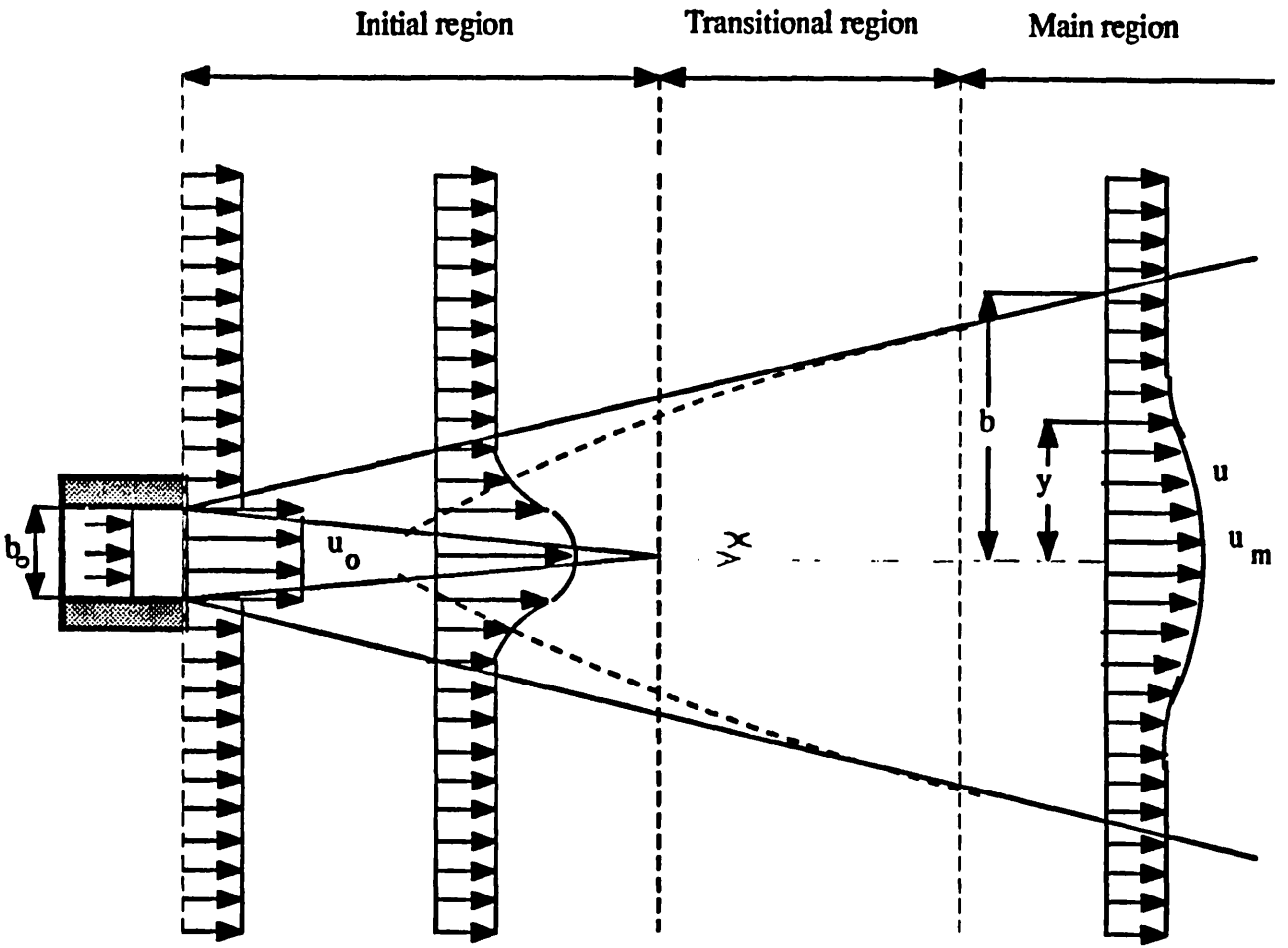


Fig. 3.1 Structure of jet

These analysis establish a law describing the increase of thickness and mixing length of submerged jet in the direction of flow. The above analysis is also valid for a jet spreading through coflowing or counterflowing external stream. However, the value of the constant will change according to the state of the external stream.
Experimental results by Yanaida (Ref. 82) show the spread in the initial region of the flow is different from that of spread in the main region. Yanaida found a relationship between x and b in the main region which is:-

$$b = k_1\sqrt{x} \qquad k_1 \text{ is a constant} = 0.237$$

This non-linear relationship differs from the previous analysis which predicts a linear jet spread. It is reasonable to assume that the analysis perfectly correct for turbulent flow but only at low Reynolds numbers. It is considered that in turbulent flow region Re > 2000.

Yanaida's experimental results were conducted at Reynolds numbers ranged from 170,000 to 650,000. The difference in the final equations can be related to factors not considered in the analytical approach, such as nozzle hole skin friction and air friction after exit from nozzle.These factors are important and apparent at large Re, this may have produced the non-linear relationship of the jet spread. It is universally acceptable, that the smooth exit hole reduces the thickness of boundary layer of the emerging jet and hence the spread of the jet. Because of the smoothness and hardness of surface, sapphire orifices are used. The spread of jet, emerging at ultra-high speed (2 to 3 times the speed of sound in this case) is largely affected by air friction, air is also entrained in the jet, the entrainment is increased in the main region of the jet where the spread is substantial. Observations of jets when air flow is restricted around it confirm these suggestions.

3.3- Mixing of abrasive with water jet

There are restricted experimental results on the problem of mixing of abrasive (dry or wet) with high speed jet, (Refs. 83, 84) are examples of such reported research. Abrasive is added to the high speed water jet solely to cut very hard materials, and also to increase the cutting speed of the water jet, it is essential that the kinetic energy is transferred from the water to the abrasive particles. The method adopted here is to freely introduce the abrasive to the high speed water jet (Fig. 3.2), the abrasive is sucked into the mixing chamber of the nozzle. The suction pressure, which is generated by the Venturi effect, is dependent on focusing tube bore diameter (D), sapphire orifice diameter (d) or water mass flow rate (m) and the mixing chamber design, which includes the shape of mixing chamber. In developing a theory to predict the mixing of abrasive particles with a water jet, the following analysis has been adopted.

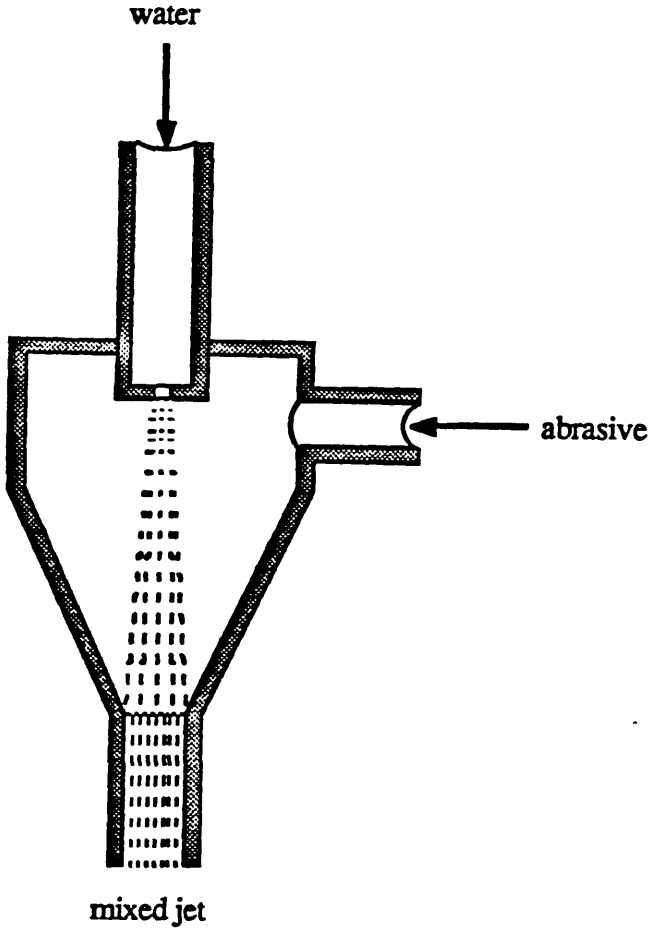


Fig. 3.2 Water/abrasive mixing chamber

Assuming the abrasive suction pressure is P_s and abrasive feed tube bore d_a. The abrasive is sucked in entrained by air, which assists the flow of abrasive, as it has been observed that in restricting air flow, a blockage occurs through the abrasive feed pipe. It is apparent that abrasive is dragged by air flow into the mixing chamber.

From compressible flow theories, the speed of air flow can be calculated (Ref. 85), by assuming the following;

1- steady one-dimensional adiabatic flow

2- constant area straight tube

3- negligible potential energy changes

4- wall shear stress is small at large Re, therefore will be neglected.

From continuity of flow (Fig. 3.3),

$$Q = A\,V \tag{3.8}$$

From the x- momentum eq.,

$$P\,A - (P + dP)\,A - \tau_w\,\pi\,d_a\,dx = Q_A\,\rho_I\,(V + dV - V) \tag{3.9}$$

$$\tau_w\,\pi\,d_a\,dx = 0$$

τ_w is abrasive feed pipe wall shear stress

substituting eq. 3.8 in eq. 3.9,

$$-dP = \rho_I\,V\,dV$$

$$-\int_{P_s}^{0} dP = \int_{0}^{V_I} \rho_I V d$$

therefore,

$$P_s = \frac{1}{2}\,\rho_I\,V_I^2 \tag{3.10}$$

knowing the suction pressure and density of air V_I the speed of air can be calculated from equation (3.10).

To calculate the speed at which abrasive is travelling, it will be assumed that abrasive initially is at rest and the air drag force exerted on abrasive particle inside the feed tube (Fig. 3.4) can be estimated. All internal friction and impact between abrasive particles are ignored.

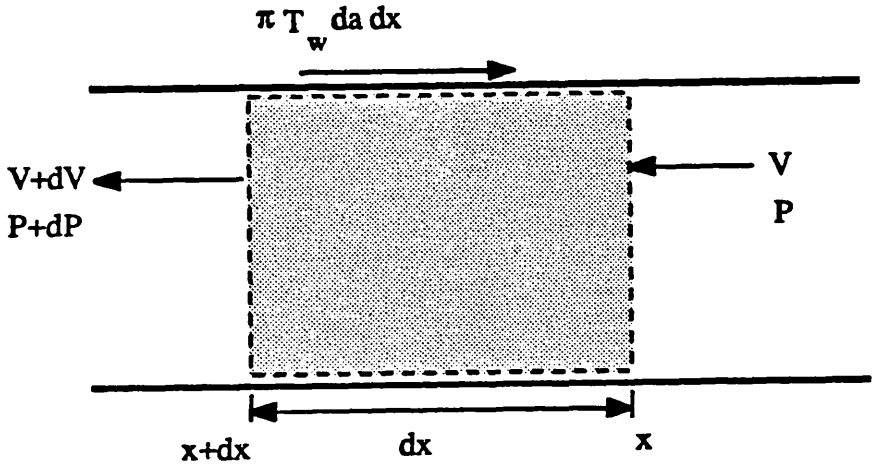


Fig. 3.3 Control volume for flow in a constant-area duct with friction

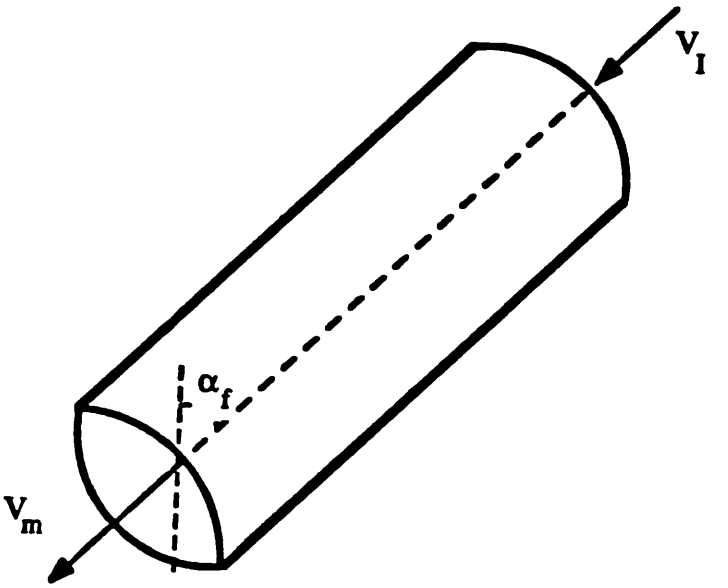


Fig. 3.4 Abrasive feed tube

$$F_d = \frac{1}{2} C_d A_p \rho_I V_I \tag{3.11}$$

where,

F_d - the drag force exerted on the abrasive particle

A_p - projected area of the particle in the direction of motion

and $F_d = m_a \mathbf{a}$

m_a - mass of particle

a - acceleration of particle

Using linear motion laws and substituting for,

$$\mathbf{a} = \frac{F_d}{m_a}$$

then,

$$V_m^2 = 2 \frac{F_d}{m_a} x \tag{3.12}$$

Where,

x is the distance between outlet of abrasive feed tube and jet of water.

V_m is the velocity of abrasive particle before impact with jet.

If the abrasive feed tube is at α_f degrees to the water jet, the water jet velocity is u.

The conservation of energy law can be applied to calculate the total energy of water and abrasive in the direction of the jet flow (Fig. 3.5).

Energy is conserved, i.e.,

$$\frac{1}{2} \dot{m} u^2 + \frac{1}{2} \sum m_a (V_m \cos\alpha_f)^2 = \frac{1}{2} (\dot{m} + \sum m_a) v_T \tag{3.13}$$

if,

1- jet air entrainment is ignored.

2- no impact between abrasive particles.

3- complete mixing of abrasive and water.

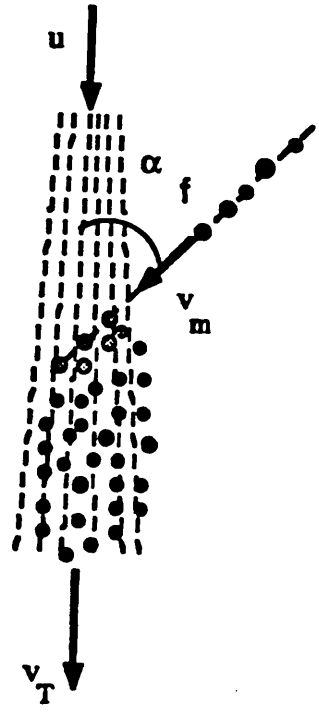


Fig. 3.5 Water/abrasive mixing

3.4- Approximate analytical solution for the velocity of the solid abrasive particles injected in a water jet.

If the effect of gravitational forces on the motion of the water jet and on injected abrasive particles is negligible and if the flow parameters (including the velocity) are constant across any cross-section of the flow, then the force on any abrasive particle in the jet is:-

$$F_w = \frac{1}{2} C_d(s)\, \rho_w(s) \left(u(s) - V_m(s) \cos\alpha_f \right)^n \qquad (3.14)$$

Where C_d, ρ_w, u and V_m are functions of s, the distance along the jet flow, $C_d = C_d(s)$, $\rho_w = \rho_w(s)$, $u = u(s)$ and $V_m = V_m(s)$ and n is a real number. Assuming C_d and ρ_w are constants along the jet

Eq. 3.14 reduces to

$$F_w = K (u - V_m)^n \qquad \text{where K is a constant, hence}$$

$$m_a \cdot \frac{ds^2}{dt^2} = K (u - V_m)^n \qquad (3.15)$$

In general, u is a function of time or, alternatively, of distance from the point of injection, since the jet slows down due to air friction and air entrainment. Thus, to solve for the velocity of an abrasive particle another relationship is needed to describe the variations of u with time of distance, s. If, however, u can be assumed roughly constant (i.e. the same average values are used) then such an additional relationship becomes unnecessary and the abrasive velocity can be found by solving the equation:-

$$\frac{d^2s}{dt^2} = \frac{K}{m_a} \left(u - \frac{ds}{dt} \right)^n \qquad (3.16)$$

(assuming u is constant)

This non-linear ordinary differential equation has no general analytic solution for any n. However, by making the substitution V = ds/dt, the equation can be rewritten as,

$$\frac{d}{dt}(V) = \frac{dV}{ds} \cdot \frac{ds}{dt} = V \cdot \frac{dV}{ds} = \frac{K}{m_a} (u - V)^n \qquad (3.17)$$

from which it is possible to find (in implicit form) an analytical solution for V for any

value of n. This can be conveniently done by introducing the substitution (u-V) = z from which -dV/ds = dz/ds. This equation (3.17) becomes,

$$-(u - z)\frac{dz}{ds} = \frac{K}{m_a} . z^n \tag{3.18}$$

hence,

$$\frac{z - u}{z^n} . \frac{dz}{ds} = \frac{K}{m_a} \tag{3.19}$$

Integrating (3.19) yields,

$$\int z^{1-n} . dz - u \int z^{-n} . dz = \frac{K}{m_a} . s + C \tag{3.20}$$

The integration is standard but n = 2 and n = 1 are special cases :

1 <u>n = 1 ;</u> Equation (3.20) yields

$$z - u \ln z = \frac{K}{m_a} . s + C$$

but when s = 0 , i.e. at the point of injection of the abrasive

$$(u - V_m) - u \ln (u - V_m) = C$$

hence,

$$z - u \ln z = \frac{K}{m_a} . s + (u - V_m) - u \ln(u - V_m) \tag{3.21}$$

2 <u>n = 2 ;</u> Equation (3.20) yields

$$\ln z + \frac{u}{z} = \frac{K}{m_a} . s + C$$

when s = 0,

$$\ln (u - V_m) + \frac{u}{(u - V_m)} = C$$

hence,

$$\ln z + \frac{u}{z} = \frac{K}{m_a} . s + \ln (u - V_m) + \frac{u}{(u - V_m)} \tag{3.22}$$

3 <u>n > 2</u> This includes any real value of n > 2, e.g. 2.1, 2.8 and so on . The equation (3.20) yields:-

$$\frac{z^{2-n}}{(2-n)} - u . \frac{z^{1-n}}{(1-n)} = \frac{K}{m_a} . s + C$$

or

$$\frac{z^{1-n}\left[\, z\,(1-n) - u\,(2-n)\,\right]}{(2-n)(1-n)} = \frac{K}{m_a}.\, s + C$$

when $s = 0$,

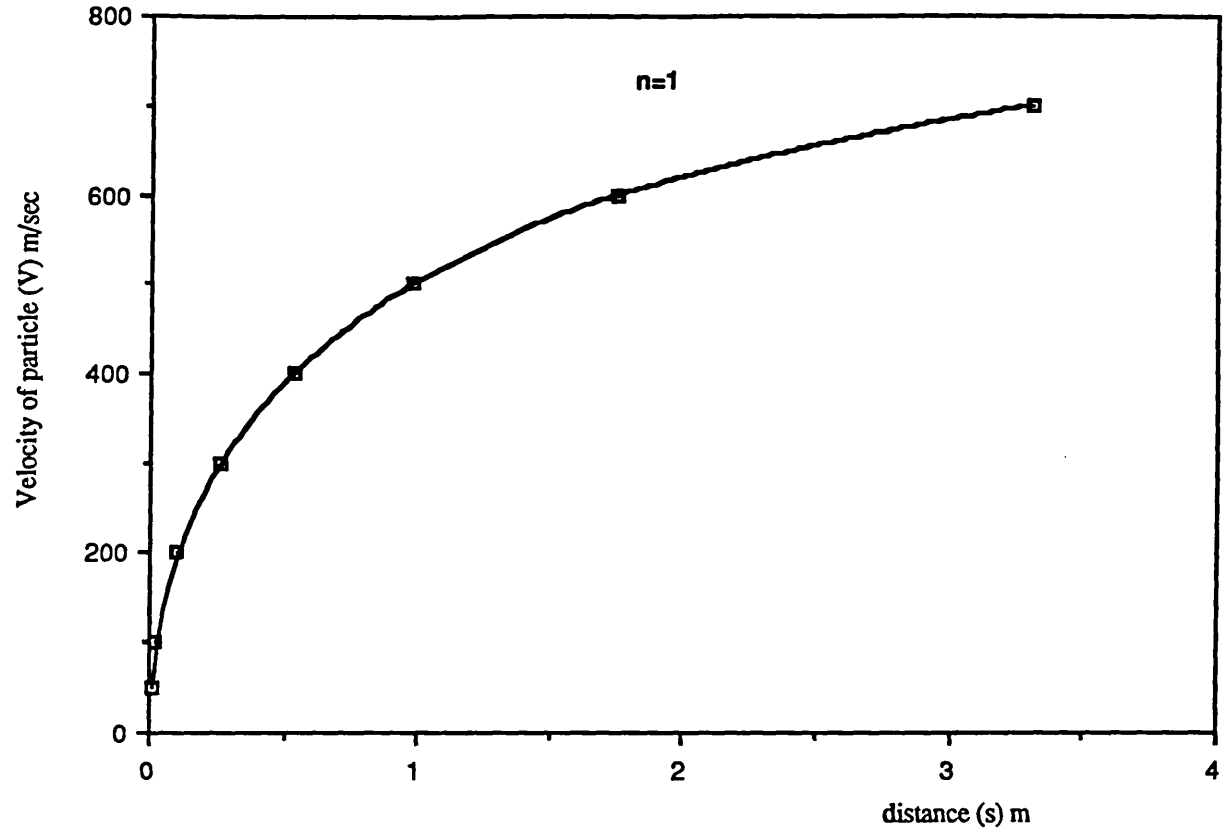
$$\frac{(u - V_m)^{1-n}\left[(u - V_m)(1 - n) - u\,(2 - n)\right]}{(2 - n)(1-n)} = \frac{(u - V_m)^{1-n}\left(-V_m(1 - n) - u\right)}{(2 - n)(1 - n)} = C$$

hence,

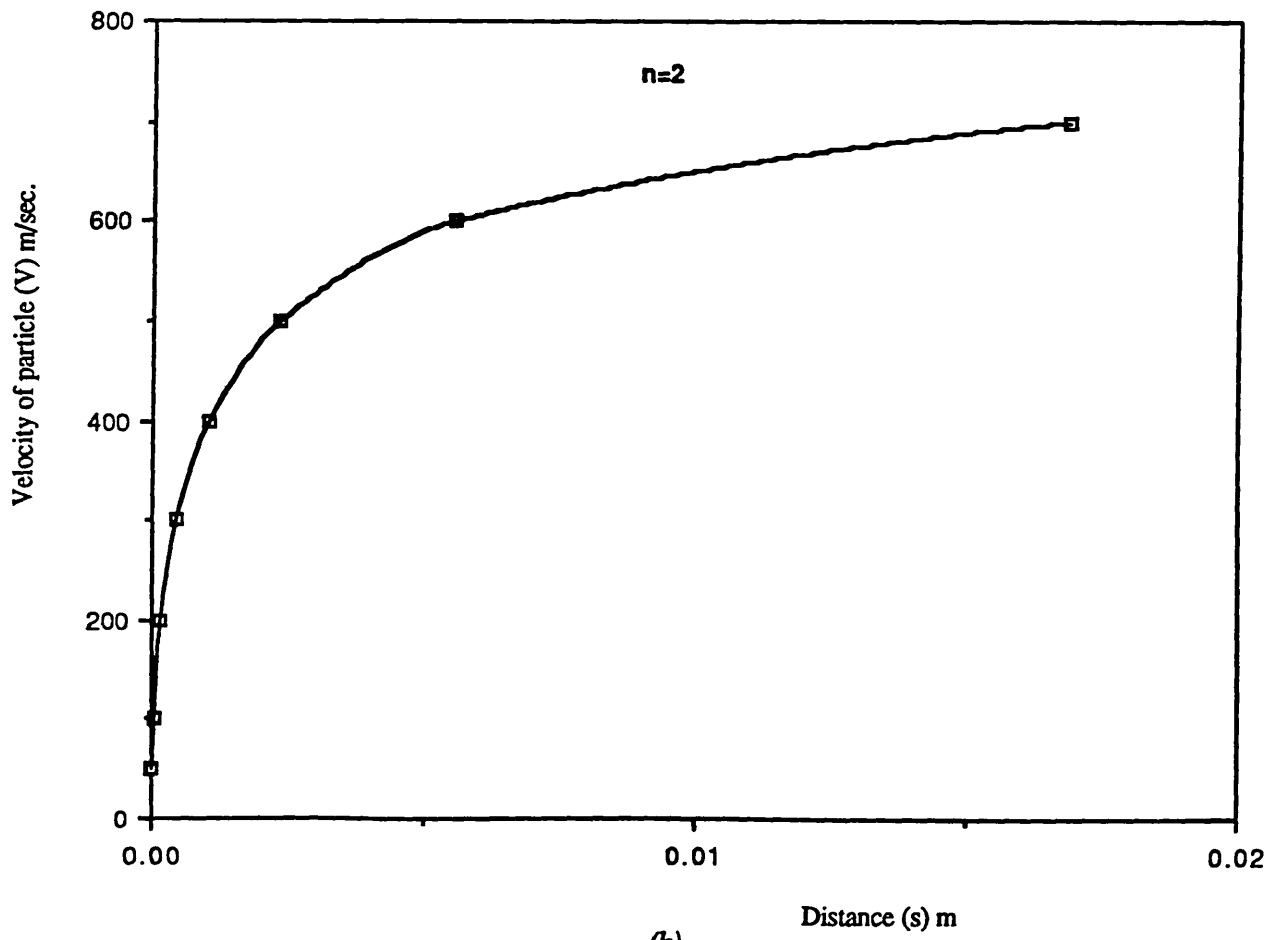
$$\frac{z^{(1-n)}\left[\, z\,(1-n) - u\,(2 - n)\,\right]}{(2-n)(1-n)} = \frac{K}{m_a}.\, s + \frac{(u - V_m)^{1-n}\left(-V_m(1 - n) - u\,\right)}{(2 - n)\,(1 - n)} \qquad (3.22)$$

For each of the above three cases the value of V at any distance (tube length) s, may be found or more appropriate 's' can be found at which the particle achieves the same speed as the jet medium. The variations of 's' against the v are shown (Fig. 3.6 a,b,c and d).

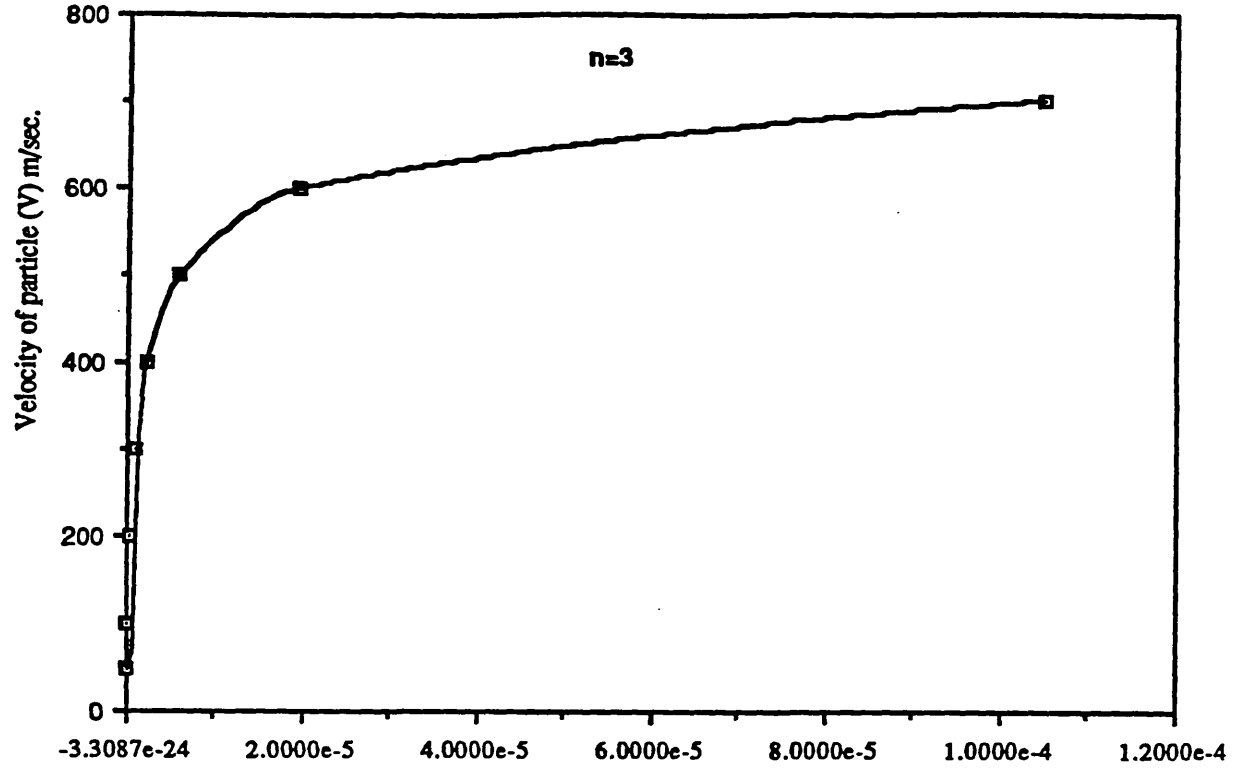
As the speed of the water jet increases the water density ρ_w and the drag coefficient C_d are decreased, *as it will be shown later in (Fig. 3.10)*, at large Re (turbulent flow) the coefficient becomes very small (C_d= 0.01 at Re= 10^7) and with a random variation in magnitude.


n=1
Velocity of particle (V) m/sec
800
600
400
200
0
0
1
2
3
4
distance (s) m

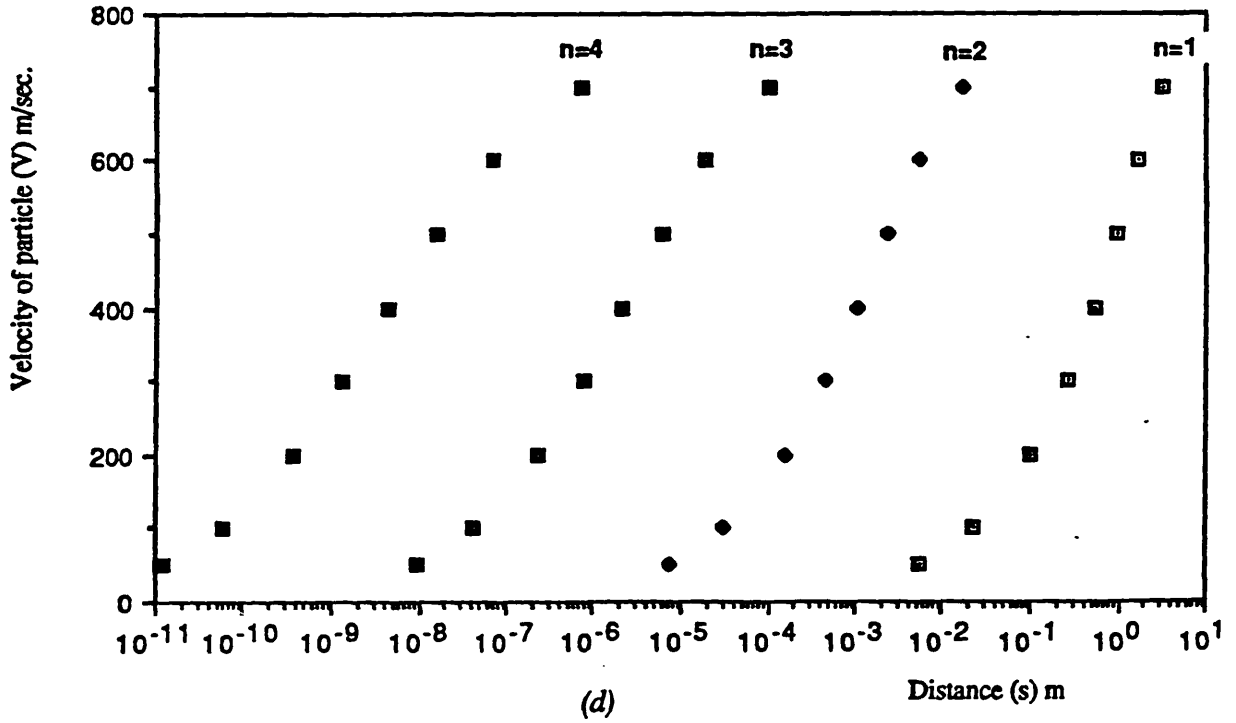
(a)


n=2
Velocity of particle (V) m/sec.
800
600
400
200
0
0.00
0.01
0.02
Distance (s) m

(b)



(c)



(d)

***Fig. 3.6** Presentation of the theoretical particle speed inside the jet*

3.5- The cutting mechanism of the abrasive water jet

The mechanism of cutting tough materials by abrasive water jet is still not completely understood. However, there are several papers dealing with repeated single particle wear . The most widely cited studies are Finnie's (Ref. 48) and Bitter's paper (Ref. 51). Bitter's approach is based on plastic energy dissipation analysis for a single abrasive particle. The wear is then postulated to equal the energy dissipation divided by a wear factor which is a material property. Both Bitter and Finnie's analysis for cutting wear yield identical results. Finnie's model of a repeated single particle wear will be adopted and modified for a stream of particles mixed with water. For such modifications to be valid, certain assumptions will be taken.

The wear of materials under impact of abrasive particles is divided into two major types of wear modes, according to the mechanical properties of the materials.

(a) **Ductile wear** which occurs in two simultaneous forms. Cutting wear or material removal by displacing action. Deformation wear in which material is removed by repeated plastic deformation.

(b) **Brittle wear** in which material is removed by the intersection of cracks which grow out from the point of impact of the particle.

Most engineering materials' mechanical properties are a compromise between very ductile and very brittle behaviour. For this reason, the erosion of such materials may be assumed as a combination of the two wear modes of wear such as wear of mild steel.

Other factors which influence the erosion process, apart from the previously mentioned mechanical properties of materials, are particle parameters such as: velocity, shape, relative hardness of the particle to the impacted material, the size and the strength of the particle and angle of impact.

3.6 - Wear of ductile materials by particle impact

a - cutting wear

Considering a single rigid abrasive particle striking a ductile material at an angle α (Fig. 3.7) and cutting or displacing a small quantity of the surface of this material.

It is assumed that:

- The particles remain rigid after material removal.
- Initial rotation of particles is zero, this implies that $x_t = x + r\theta$ and $y_t = y$.
- The ratio of the vertical force to the horizontal force on the particle during the cutting operation is taken as a constant and equal to (ϕ).
- A constant plastic flow pressure its horizontal component is σ_p.
- The depth over which the material contacts the particle is taken as twice the depth of cut

  $1/y_t = \psi = 2$.
- The volume removed is the product of the area swept out by the particle tip and the width H of the cutting face i.e,

$$\text{Volume} = H \int y_t \, dx_t = H \int_0^{t} y_t \, \dot{x}_t \, dt$$

- The vertical and the horizontal forces on the particle are taken to be located at the centre of the face having contact with the particle (Fig. 3.8).

Finnie found that a crater or scratch caused by impacting single particle has length/depth ratio of the order 10 : 1. This means that the erosion is occurring at shallow angle of attack. It is assumed that only the leading face of the particle contacts the surface of the material while the particle is in planar motion. The striking particle has a mass m_a and protruding tip which cuts a trajectory (x_t , y_t) into the surface of the ductile material (Fig. 3.7). The centre of mass C.M. travels linearly by (x_t , y_t) and rotates by angle θ into the material, thus the particle tip pushes a chip in front of the contact area with a vertical projection, A_c, and width of cut, H. The centre of mass motion can be described by $x_t = x + r\theta$, $y = y_t$. The ratio of the vertical and horizontal

contact forces' component, R_x, R_y are assumed to stay constant throughout the impact,

$$\frac{R_y}{R_x} = \phi \qquad \text{and} \qquad \frac{l}{y_t} = \psi \tag{3.24}$$

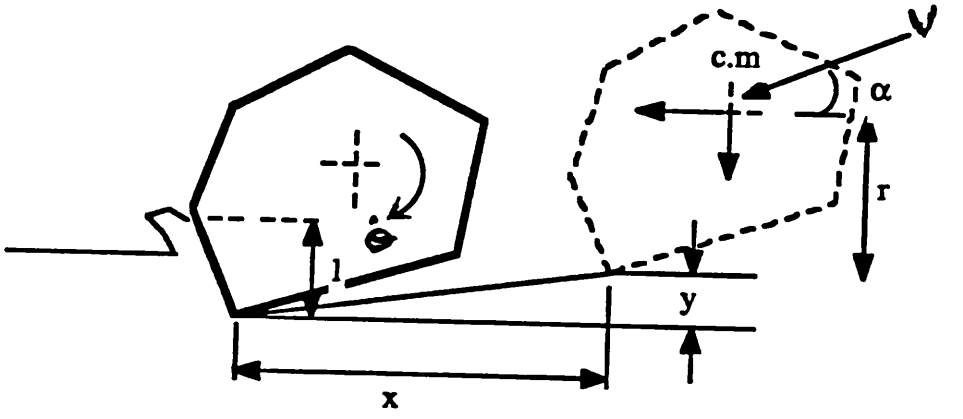


Fig 3.7 Particle cutting in a ductile material

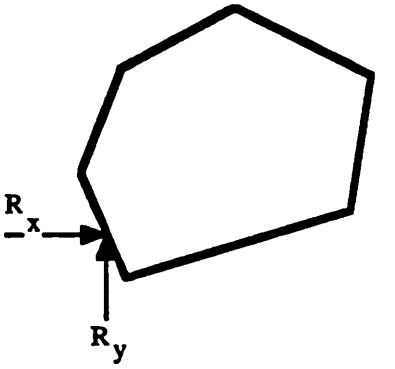


Fig. 3.8 Forces on single particle

If σ_p is the flow stress and acts horizontally then,

$$R_x = A_c \sigma_p = l H \sigma_p = \psi y_t H \sigma_p$$

hence the equation of planar motion are:-

$$m_a \ddot{x} + \psi H \sigma_p y = 0 \tag{3.25}$$

$$m_a \ddot{y} + \psi H \sigma_p \phi y = 0 \tag{3.26}$$

$$I \ddot{\theta} + \psi H \sigma_p r y = 0 \tag{3.27}$$

where I is the moment of inertia of the particle about its centre of mass

when $t = 0$, $x = y = \theta = 0$ and

$$\dot{x} = v \cos\alpha \ , \qquad \dot{y} = v \sin\alpha \ , \qquad \dot{\theta} = \dot{\theta}_0 \tag{3.28}$$

Solving the differential equations (3.25, 3.26 , 3.27),

$$x = \frac{v \sin\alpha}{\beta \phi} \sin\beta t + (v \cos\alpha) t - \frac{v \sin\alpha t}{\phi} \tag{3.29}$$

$$y = \frac{v \sin\alpha}{\beta} \sin\beta t \tag{3.30}$$

$$\theta = \frac{m_a r v \sin\alpha}{\beta \phi I} (\sin\beta t - \beta t) + \theta_0 t \tag{3.31}$$

$$\text{where} \quad \beta = \sqrt{\frac{\psi \sigma_p H \phi}{m_a}} \tag{3.32}$$

Considering the two cutting processes,

(a) The particle cuts into the ductile surface and subsequently leaves it when y_t becomes zero.

(b) The particle is stopped during its scooping action at some depth, when $x_t = 0$.

For case (a) when $y_t = 0$ then the cutting duration t^* from equation (3.30)

$$\sin\beta t^* = 0 \qquad \text{or} \qquad \beta t^* = \pi \tag{3.33}$$

and case (b) when the particle motion stops while in contact with the material

$$\dot{x_t} = \dot{x} + r\dot{\theta} = 0$$

From equations (3.29) and (3.31) approximating $I = m_a r^2 / 2$ and $\theta_0 = 0$ they

give:-

$$\cos\beta t^{*} = 1 - \frac{\phi}{3\tan\alpha} \tag{3.34}$$

equations (3.33) and (3.34) are identical when

$$\alpha = \alpha_0 = \arctan\frac{\phi}{6}$$

α_0 is called the critical angle of impingement and separates the above two cutting processes.

The volume removal by the particle of mass m_a is,

$$\delta(\text{vol}) = H\int_0^{t^{*}} y\, dx_t = H\int_0^{t^{*}} y\, d(x + r\theta) \tag{3.35}$$

Substituting equations (3.29) to (3.31) in equation (3.35) and integrating for total mass of similar particles M, hence there are two solutions.

A - for rebounding particles i.e, $\alpha \le \alpha_0$

$$\delta(\text{vol}) = \frac{M v^2}{\psi \sigma_p \phi}\left(\sin 2\alpha - \frac{6}{\phi}\sin^2\alpha\right) \tag{3.36}$$

B - For stopped particles, $\alpha \ge \alpha_0$

$$\delta(\text{vol}) = \frac{M v^2}{\psi \sigma_p \phi}\left(\frac{\phi\cos^2\alpha}{6}\right) \tag{3.37}$$

for maximum volume removed when $\alpha \le \alpha_0$, α is found from,

$$\frac{d\delta(\text{vol})}{d\alpha} = 0 \qquad \text{which gives} \quad \alpha_{\text{max.}} = \frac{1}{2}\arctan\frac{\phi}{3}$$

ϕ can be estimated from similar abrasive processes such as surface grinding and scratch hardness testing, a ratio of $\phi = R_y/R_x = 2$ is acceptable (Ref. 49). A value of the ratio $\psi=2$ is common in metal cutting (Ref. 86). This yields values for the angles $\alpha_{\text{max.}}=16.84^{o}$ and $\alpha_0 = 18.43^{o}$.

If this analysis is extended to include the hydrodynamic forces exerted on the cut surface (Fig. 3.9). And F_x, F_y are the forces resulting from water jet pressure, then the equations of motion of the particle are:

$$F_x - R_x = - m_a \ddot{x} \quad (3.38)$$

$$F_y - R_y = - m_a \ddot{y} \quad (3.39)$$

$$T_f - T_R = - I\ddot{\theta} \quad (3.40)$$

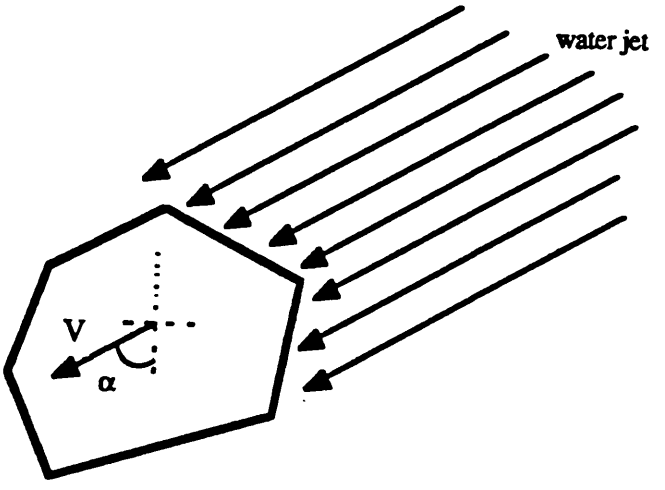


Fig. 3.9 Hydrodynamic forces on abrasive particle

The hydrodynamic forces are calculated from the drag exerted by the water jet, Viz,

$$F_x = \frac{1}{2} C_d \rho_w A_p \left(v \cos\alpha - \dot{x} \right)^2 \qquad (3.41)$$

$$R_x = \sigma_p l H \qquad \text{and} \quad l = \psi y$$

Substituting in equation (3.38), in x-diretion the equation of motion becomes,

$$\frac{1}{2} C_d A_p \rho_w \left(v \cos\alpha - \dot{x} \right)^2 - \sigma_p H \psi y = - m_a \ddot{x} \qquad (3.42)$$

and y - direction; $R_y = \phi R_x$ in equation (3.39)

$$\frac{1}{2} C_d A_p \rho_w \left(v \sin\alpha - \dot{y} \right)^2 - \sigma_p H \psi \phi y = - m_a \ddot{y} \qquad (3.43)$$

In the angular-direction, F_x and F_y are considered to pass through the centre of the particle so that $T_f = 0$ hence

$$R_y r - R_x r = - I \ddot{\theta}$$

and $\quad (\sigma_p H \psi \phi r) y - (\sigma_p H \psi r) y = - I \ddot{\theta}$

which give, $\quad (\sigma_p H \psi r)(\phi - 1) y = - I \ddot{\theta}$

The volume removal rate, due to hydrodynamic forces, is then determined by considering the initial conditions and integrating as before.

It is assumed that C_d is constant and therefore F_x and F_y are constant. But C_d at high Re is unknown and may well fluctuate up and down. For turbulent flows at low Reynold's numbers i.e Re = 10^5, for spherical shape particles C_d is about 0.5 (Fig. 3.10). At water pressures of 2000 bar, the water jet Re is around 10^6 and the predicted values of C_d at Re = 10^7 is less than 0.01, at Re > 10^7 no predictions are possible due to high turbulence in the flow (Ref. 85).

F_x, F_y can be found by estimating the static and dynamic pressure on the particle at the cut surface. The static forces can be calculated from the simple relation,

$$F = A P$$

where P is the operating pressure and A is the area this pressure. However, the static forces under the jet are experimentally measured (Ref. 13), a factor γ equal to 0.6 - 0.8 was found sufficient to compensate for losses, hence $F = \gamma A P$.

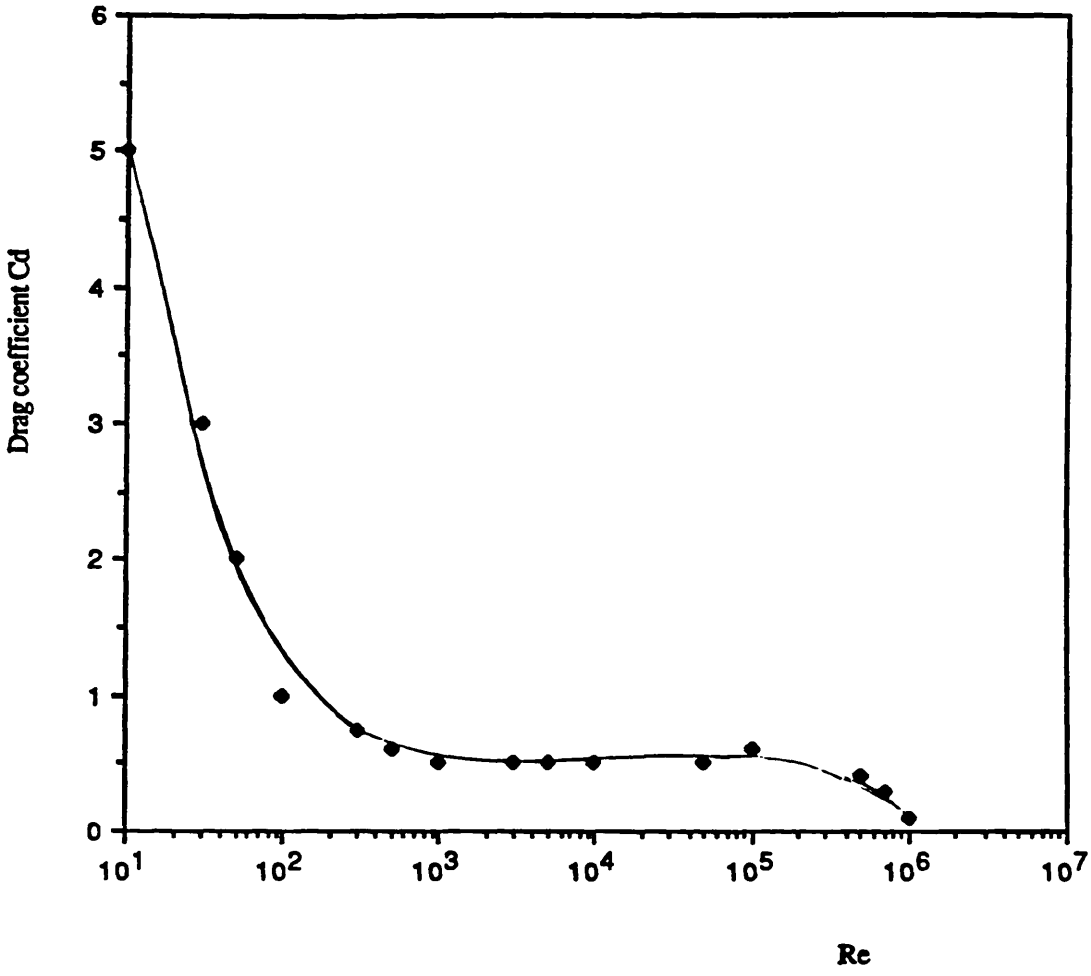


Fig. 3.10 The drag coefficient variation with jet speed

Dynamic forces are determined by several factors such as nozzle diameter and other flow conditions like jet spread and so on (Fig. 3.11).

However, from the experimental results it can be considered that the hydrodynamic forces play a secondary role in the cutting process.

Once the the volume removed (δvol) is calculated, depth of cut (h) is obtained by assuming that the particles strike the surface at shallow angles i.e $\alpha < \alpha_0$. The analysis is then is simplified by dividing the field into small elements as shown in (Fig. 3.12). The removal rate at an element, dh, which is impacted with an abrasive flow rate of dM is:-

$$\dot{\delta(vol)} = \frac{\dot{dM}\, v^2}{4\,\sigma_p} \left(\sin 2\alpha - 3\sin^2\alpha \right) \qquad (3.44)$$

substituting $\delta(vol) = dh\ u\ d_j$ and

$$\dot{dM} = \left(\frac{\dot{M}}{d_j}\right) dx$$

then integrating equation (3.44), it yields the depth of cut due to cutting wear

$$h_c = \frac{c\,\dot{M}\, v^2 \alpha_1}{4\,\sigma_p d_j\, u_x} \qquad (3.45)$$

c is the ratio of portion of the jet involved in the cutting wear to the diameter of the jet d_j. Or if $\sigma = \sigma_p / \alpha_1$, the depth of cut is expressed as:-

$$h_c = \frac{c\,\dot{M}\, v^2}{4\,\sigma\, d_j\, u_x} \qquad (3.46)$$

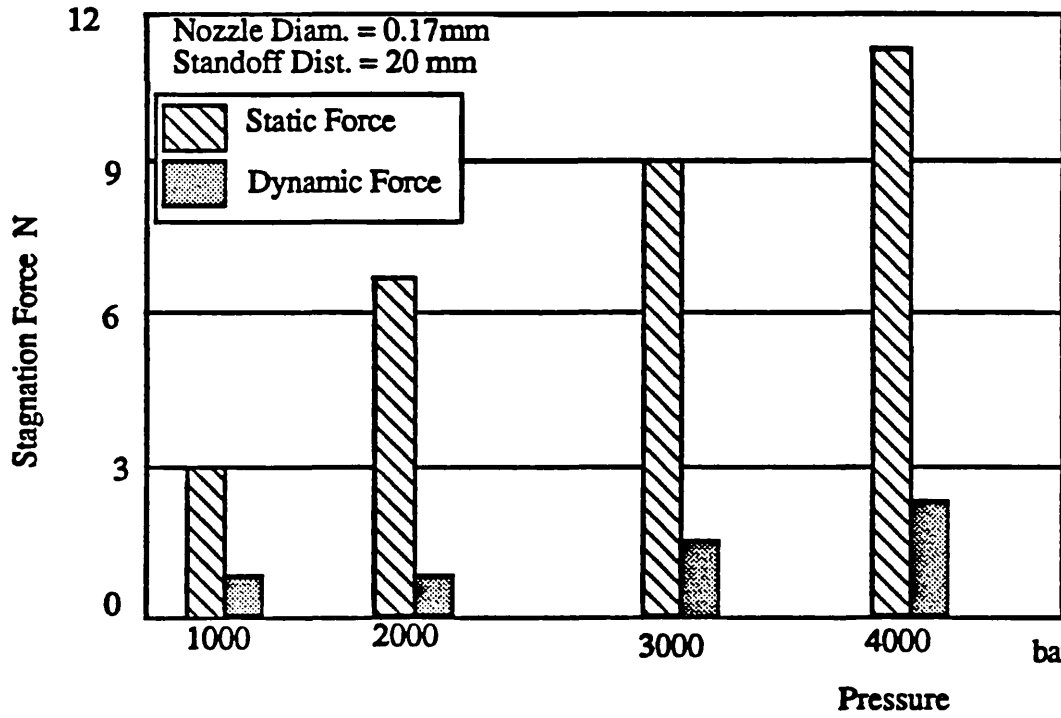


Fig. 3.11 Measured forces under jet

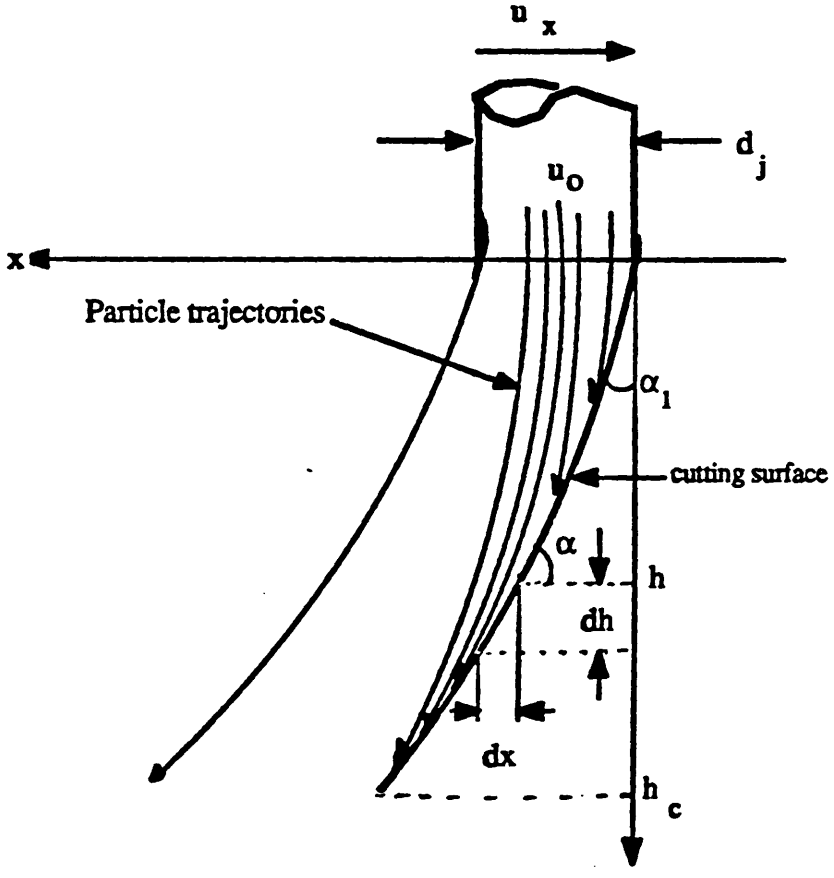


Fig. 3.12 Abrasive jet cutting model

b - Deformation wear

Bitter (Ref. 51) considered the collision of an elastic sphere (m,R) against a plane which deforms elastically and plastically (Fig. 3.13). The elastic displacement at an elastic stress σ_y is given by Hertz theory, viz,

$$x_{el.} = \frac{24.35\ \sigma_y^2 R}{E_r^2} \tag{3.47}$$

where E_r is the reduced modulus of elasticity

As σ_y increased to $\sigma_{max.}$, plastic deformation occurs and total displacement becomes,

$$x = x_{el.} + x_{pl.}$$

The total elastic energy stored in the sphere and the plane at the peak of the impact is the calculated. The kinetic energy of the rebound particles is also calculated. Hence the energy required for permanent plastic deformation can be found since $\delta(vol)_d = U_d/\varepsilon$.

However, Bitter (Ref. 51) obtained the following expression for volume removal rate of deformation wear for any mass, M, of particles.

$$\delta(vol)_d = \frac{M\,(v \sin\alpha - k_1)^2}{2\varepsilon} \tag{3.48}$$

k_1 is a constant for a given eroded surface material which is equivalent to the critical velocity.

Using the $\delta(vol)_d$, the depth of cut due to deformation wear h_d can be calculated by assuming that $\sin\alpha \approx 1$ on penetration and k_1 is small compared with v then eq. (3.48) becomes,

$$\delta(vol)_d \approx \frac{M v^2}{2\varepsilon}$$

and if

$\delta(vol) \approx \delta h\ (\pi/4)\ d_j^2$ and the abrasive flow rate involved in the cutting (1-c)M gives

$$\frac{dh}{dt} = \frac{2}{\pi d_j^2} \frac{(1\text{-}c)M v^2}{\varepsilon}$$

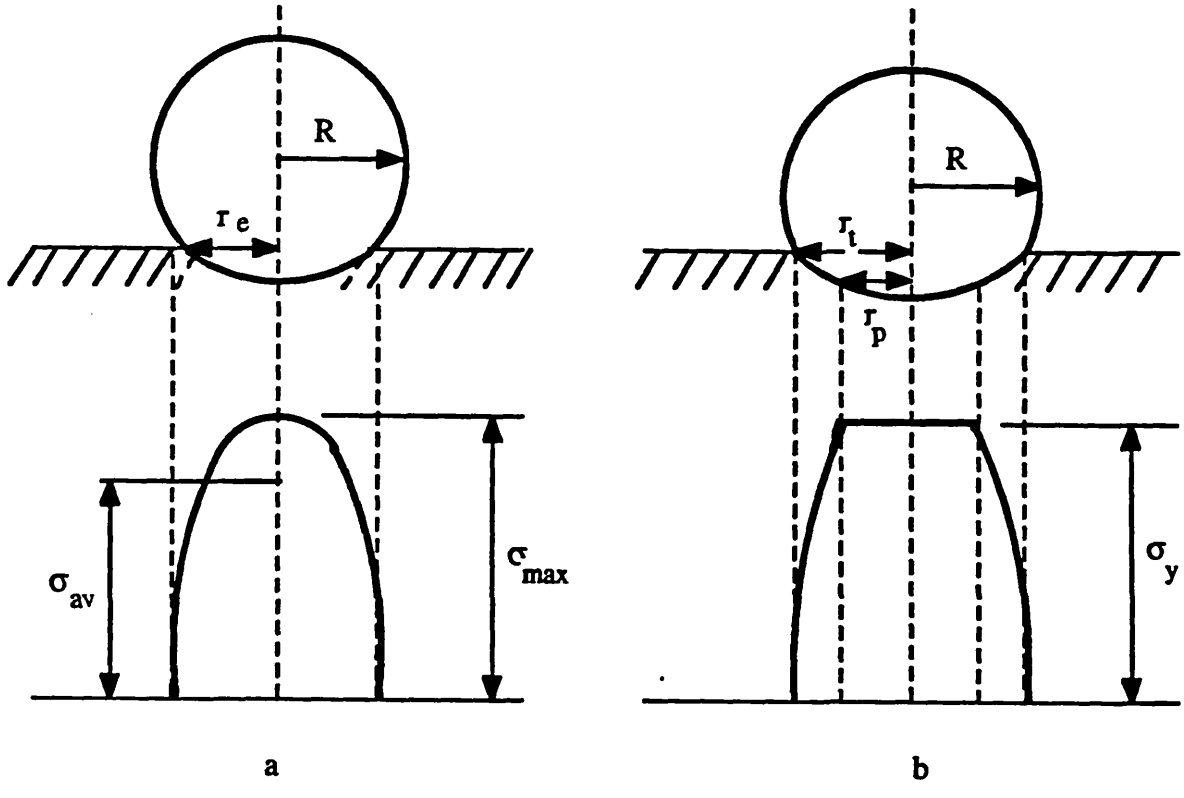


Fig. 3.13 Deformation wear model (Ref. 51)

If it is assumed that v remains constant with depth, by integrating the above equation when h=0 at t =0 and h = h_d at t = u_x/d_j,

$$h_d = \frac{2(1-c)\dot{M}v^2}{\pi d_j \varepsilon u} \tag{3.49}$$

The total volume removal and depth of cut is the sum of equations (3.44) and (3.48), also equations (3.46) and (3.49), which gives,

$$h = \frac{M v^2}{d_j u_x}\left\{\frac{c}{4\sigma} + \frac{2(1-c)}{\pi\varepsilon}\right\} \tag{3.50}$$

Equations (3.44) and (3.48) indicates the dependence of δ(vol) on velocity, angle of attack and abrasive particle properties such as shape, hardness and strength which also influence the wear process.

h_d is very small compared with h_c since ε is of the order 10^7 gfcm/cm^3. The second term can safely be ignored for sharp abrasive impact.

If we assume that c = 1.0, i.e all the jet diameter is involved in the cutting process and when pressure 2000 bar and orifice diameter 0.25 mm , V ≈ 300 m/sec at a distance of 40 mm from the orifice exit and when M = 1.6 kg/min.

v ≈ 500 cm/min based on visualisation experiments during cutting using high speed photography.

σ_p = 2700 MN/m^2 = 0.2700 MN/cm^2

σ = 0.04 MN/cm^2 when α_1 ≈ 7 at 90 degree angle of impact

d_j = 0.25 cm estimated from experimental results

u_x = 15 cm/min

then,

h ≈ 0.66 cm

volume removal rate ≈ 0.66 x 15 x 0.25 = 2.5 cm^3/min

Assuming a steel specific gravity of 7,

α_1 ≈ 20 at lower angle of impact ≈ 20 degrees (only material cutting occurs at maximum material removal rate for mild steel).

The volume removal rate increases to 7.5 cm^3/min.

3.7-. Wear of brittle materials

Brittle materials cannot deform plastically, but instead, they crack and fracture when they are subjected to large impact stresses. The stress analysis and the volume removal rate are discussed in many papers. One of the most accepted mathematical models is given in*(Appendix I)*.

It is shown that:-

The volume removed by an impacted angular particle is,

$$W = k_5 r^{a`} V^b$$

where,

$$a` = \frac{3.6\ m}{m - 2} \quad , \quad b = \frac{2.4\ m}{m - 2}$$

Since u ≈ 650 m/sec at the jet exit from continuity.

It was estimated from force recorded on a plate in front of the water jet that, u ≈ V ≈ 300 m/sec at a distance 40mm from the orifice exit, i.e assuming complete particle mixing.

m = 8 for glasses and similarly for silceram.

For particle size of mesh 70, it can be assumed that, r = 200 μm

k_5 ≈ 4000 which is the erosion parameter in erosion tests in $cm^3/ 10^9$ abrasive particles (Ref. 75).

For garnet particles of size 200 μm the density = 2.5 gm/cm^3 ,

and the abrasive flow rate = 1.6 kg/min, gives:-

W ≈ 8 cm^3/min.

Silceram specific gravity ≈ 3

Mass removal rate ≈ 24 gm/min.

It can be seen that the calculation of the theoretical volume removal of brittle material by a single particle is a function of the cut material's mechanical properties, abrasive density, size and shape of particles, flaw distribution in the brittle material and the

speed of the impacted particles.

It can be assumed the water jet forces have no effect on the cutting process, since plastic deformation does not occur.

Chapter 4

Construction of test rig

4.1- Description of testing unit requirements

- High pressure pump to deliver a flow of 4 litre/min. at pressures of up to 4000 bar.
- Clean and continuous water supply and low pressure filtering unit to filter dirts of sizes down to 0.25 μm and high pressure filter 10 μm size to stop any pump induced dirts from flowing to the nozzle.
- Cutting head holder which is capable of movement in the vertical plane and the cutting head will be required to rotate in this vertical plane by 70 degrees to either side of the vertical. Cutting head or work piece device to perform a steady X-Y movements of the cutting head or the workpiece with minimum speed ranging from 0.0 to 100 cm/min.
- Jet stopper and abrasive and water collector
- Abrasive hopper to supply the cutting head with the necessary type and flow rate of abrasive with provisions for measurement of abrasive flow rates .

4.2- Pumping unit (Fig. 4.1)

The pumping unit is of the type UHDE HP4002-11 which is designed to generate up to 6000 bars water pressure at a water flow rate up to 4 litre/min. The prime mover in this particular system is a 45 kW AC motor which drives a low pressure axial piston oil pump. This hydraulic oil pump can generate up to 130 bars and the oil flow is used to drive the low pressure side of a horizontally opposed high pressure intensifier pump. The oil pressure acts on a large piston which moves it against water pressure acting on a small piston (Fig. 4.2). The pressure is increased by the ratio of the piston area. When the piston reaches the end of the stroke the oil flow is reversed and the piston moves into the opposite direction. The reversal of the oil stream in a four way valve is accompanied by the opening of the oil line towards the depressurized end of the cylinder. The oil released flows through a pressure -relief valve into the oil sump.

The accumulator and common outlet manifold on the high pressure side ensure continuous water flow. The discharge rate of the HP pump is regulated by the number of strokes of the working piston, which depends on the amount of hydraulic oil forced into the hydraulic cylinder per unit time.

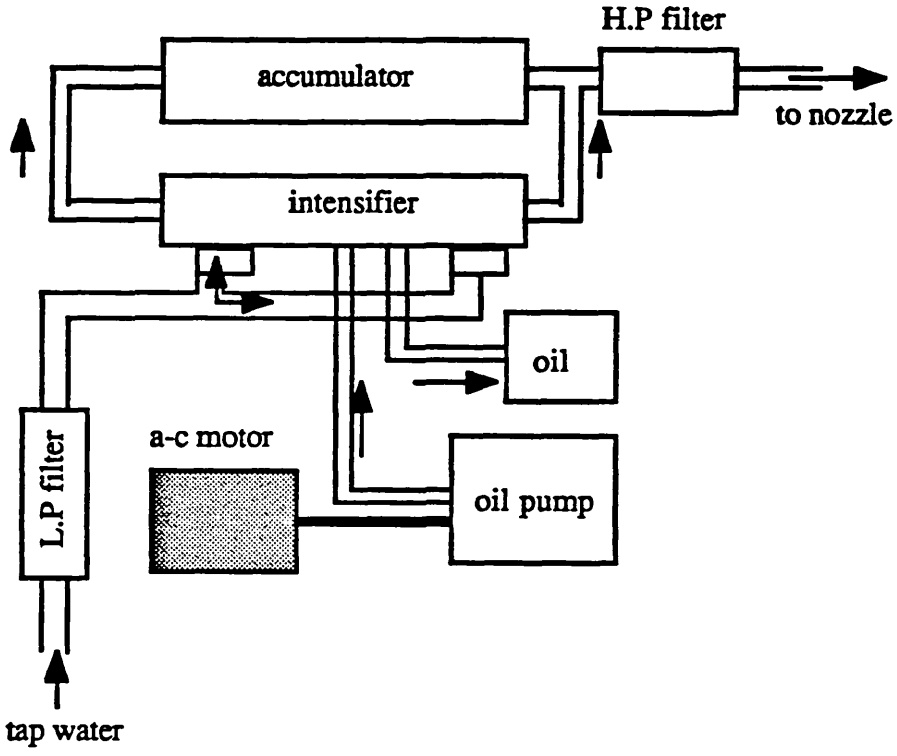


Fig. 4.1 Pumping unit layout

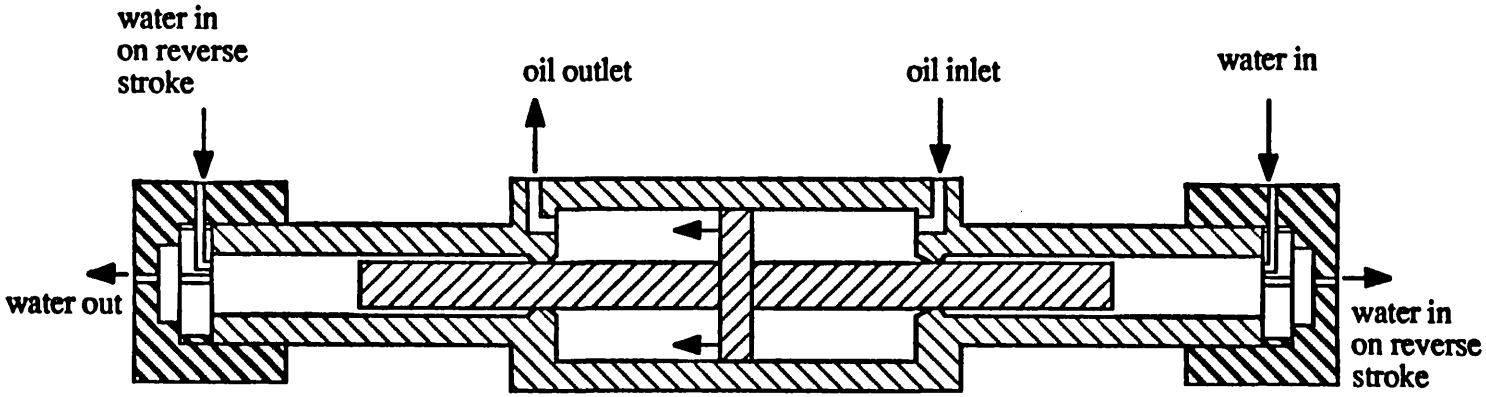


Fig 4.2 Intensifier unit

On the water suction side, a series of low pressure filters (sizes 10 to 0.25 μm) are installed to clean the supply water of impurities which can damage the cutting head sapphire orifice. A separate high pressure filter with a 10 μm screen is used in the high pressure side to collect any debris which might get detach from within the pumping system.

4.3- Rig layout *(Appendix II)*

A test rig has been built to facilitate the cutting of small samples of different materials in the X-Y direction placed in a horizontal plane. It was decided, in the test circumstances, that fixing the nozzle and moving the workpiece was much cheaper than moving the cutting head. Ideally, a better control of the cutting jet can be achieved by a 3-Degree of freedom robot arm, which allows for cutting curved surfaces in three perpendicular planes. Since the test aim was to produce straight cuts for a certain thickness workpiece, it was thought that in this instant a robot will be an unnecessary expense at this experimental stage. Also at certain stages the water pressure might have to rise above the pressure limit of any available flexible hose (2500 bars). Instead a fixed link, stainless steel pipes, which are capable of withstanding much higher working water pressure than the flexible hoses are used. However, the steel pipes allow small movements of the nozzle, such as nozzle rotation and small vertical movements, this movements are controlled by a specially made cutting head clamp.

A simple linear motion system is used to construct the X-Y table. The table is driven by two small but powerful stepping motors. The movement of the table was initially controlled by manual switches and provisions were made for eventual microprocessor control.

Since the cutting head position is fixed, plastic tanks were used for the jet obstruction and water and abrasive collection. The tanks were used instead of a water catcher which moves with the cutting head. The catcher is very expensive to use for this type of limited tests. Two tanks have been used; the first tank is used to slow down and

collect the abrasive materials of the jet (mixed jet). A piece of wood was used, which floats on the surface of the water, to act as a buffer before it penetrates the bottom of the collection tank. The second tank was used to collect water only which overflows from the collection tank, the water is then dispensed to the drain. Detailed drawings of the X-Y table, clamps and abrasive hopper are in *Appendix II.*

4.4- Abrasive hopper *(Appendix II)*

Since the abrasive is fed by suction of the abrasive materials into the cutting head mixing chamber as the result of pressure reduction in the chamber (Venturi effect), an open top abrasive hopper 0.75 m^3 capacity is mounted by 4 rubber mounts on a steel frame. A load cell is used to weigh the quantity of abrasive material inside the tank, the load cell is fixed to one edge under the tank and the tank base is hinged at the other end. Therefore the cell reading is half the actual abrasive weight in the tank. The load cell reading is recorded by a chart recorder which has to be calibrated before use. A pneumatic vibrator is fixed to the abrasive tank side, vibration of the hopper tank eases the abrasive flow from the hopper (Plate 4.1).

4.5- Cutting tests

1- Mild steel specimens (Fig. 4. 3) were used for the cutting tests, the relative speed of cut and the kerfing of the cut was observed for several cutting head designs. Since there are many parameters involved in the cutting operation, and some of these parameters were previously investigated, the aim of the tests was to improve cutting head design as far as the speed of cut is concerned without reference to the external cutting parameters such as standoff distance, angle of attack, ... etc. which were kept constant through out the tests. The angle of attack was maintained, in most tests, at 90 degrees.

2- Brittle materials such as glass and ceramics of different thicknesses were used in cutting tests to observe the quality of cut and to compare cutting speed with mild steel cutting speed.

3- Ductile materials such as nickel with different thicknesses was used in cutting tests to observe the quality of cut and the effect of angle of attack on cutting speed and compare with cutting mild steel.

4.6- Abrasive materials

Several types and grades of abrasive materials were tested, their effect on speed of cut and wear rate of focusing tube was observed. Other types of more expensive abrasive, such as silicon carbide and boron carbide could not be used because of their high cost, but small samples were obtained and examined under the scanning electronic microscope for particle shape and type of edges. The types of abrasive used here;

1- Flint (mesh 70 and 60)

2- White and pink alumina (mesh 60)

3- Reclaim alumina type S (mixed sizes, mesh 40/60)

4- Garnet (mesh 80 and 50)

4.7-Constant parameters throughout the cutting tests

- Stand off distance at 5 mm from the top surface of the specimen.
- Pressure 2000 bars.
- Sapphire orifice diameter 0.25 mm.
- Focusing tube starting bore size 2 mm.
- Number of passes ranged from 3 to 5 passes in most cases.
- Abrasive flow rate is dependent on air flow which eases the abrasive flow, attempts to keep the abrasive flow rate at 1.4 kg/min. were not successful in a few cases. However, the effect of abrasive follow rate was investigated before. Increasing air flow with the abrasive reduces the amount of abrasive fed into the jet and its believed that air flow improve abrasive and water jet mixing, hence increases the cutting speed. The wear rate of focusing tube will be quoted as gm/kg of abrasive.

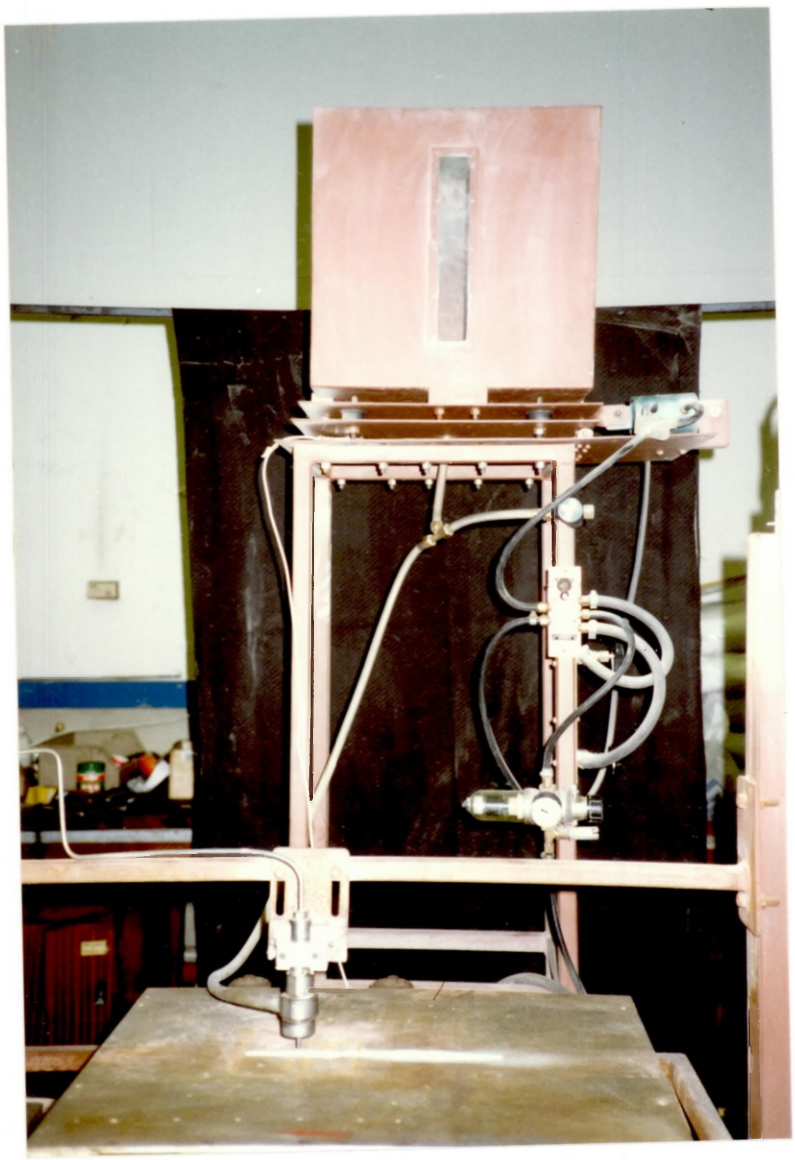


Plate 4.1 *Abrasive hopper, cutting head, clamp and table*

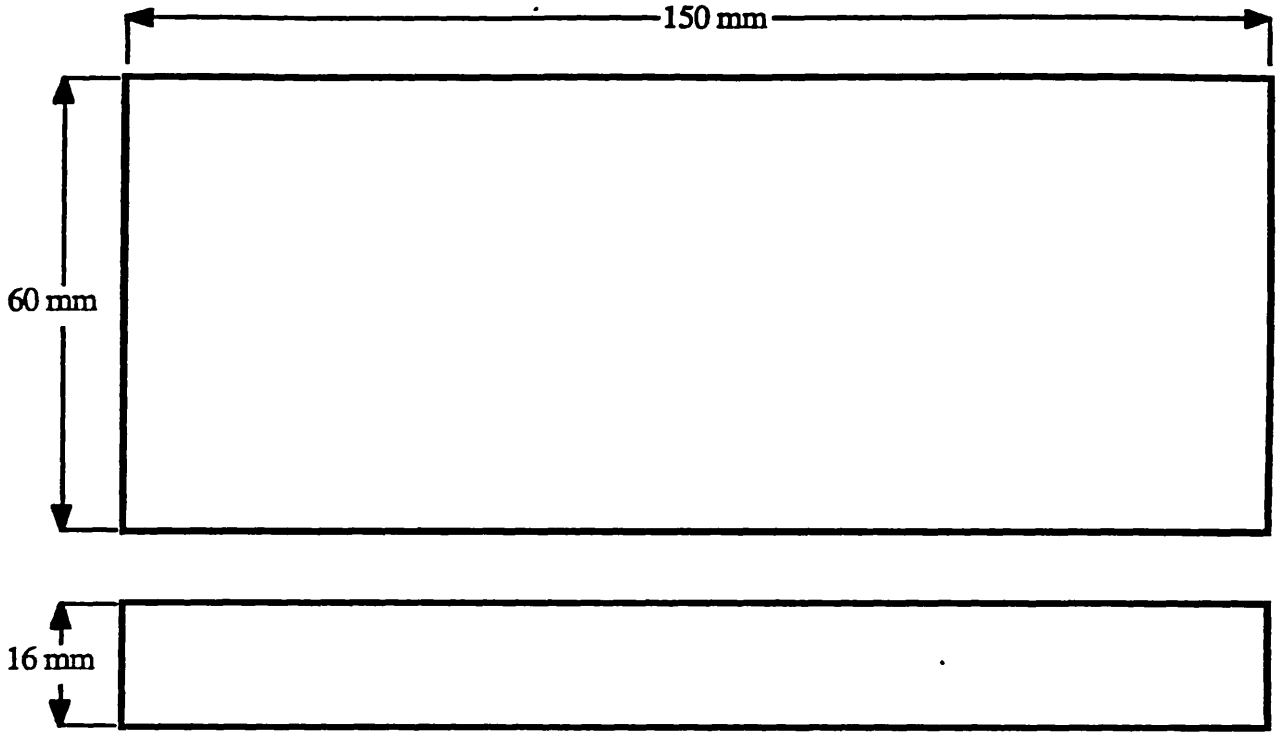


Fig. 4.3 Mild steel specimen

Chapter 5

Cutting head

5.1 - Introduction

The cutting head consists of a sapphire orifice, mixing chamber and outlet or focusing tube. Its function is to create a fine coherent water jet. This jet is then mixed with abrasive material in the mixing chamber. Finally the mixed jet is focused to perform a narrow and clean cut by the focusing tube. The abrasive particles are freely fed into the mixing chamber from the abrasive hopper. The unavoidable jet expansion inside the head results in pressure drop in the head (called Venturi effect); this pressure decrease is exploited to draw the abrasive into the head.

5.2-Cutting head design criteria

a- Fine and coherent water jet.

b- Minimum abrasive and water flow rate ($\approx$ 4 to 5 kg/min.).

c- Good abrasive mixing with the jet to give large material removal rate comparable with theoretical analysis.

d- Focused mixed jet which perform reasonable cutting speed as well as good surface finish.

e- Minimum wear of cutting head parts.

f- Low running costs i.e replaceable parts are cheap and can be replaced in a short time.

5.3- The sapphire orifice

The tests are performed on several cutting head designs, focusing the water under high pressure from the sapphire orifices (Appendix II), for the reasons which have been discussed earlier in *Chapter 2*. The jewel thickness is 2 to 3 times orifice diameter which as reported earlier gives the best coherent water jet. Other jewels with different sizes were tested and the results were found to increase the jet spread. All orifices used were inspected under the Electronic Scanning Microscope (S.E.M) before and after use (Plate. 5.1, 5.2). The time of orifice operation was also noted. Filter sizes of 10, 0.5 and 0.2μm were installed to clean the water. Before pumping, a 10μm high pressure filter is added after the pump, yet wear is occurring in the sapphire orifices. The internal wall of the hole becomes rough and irregular and this induces jet surface

eddies which increase the turbulence of the water jet.

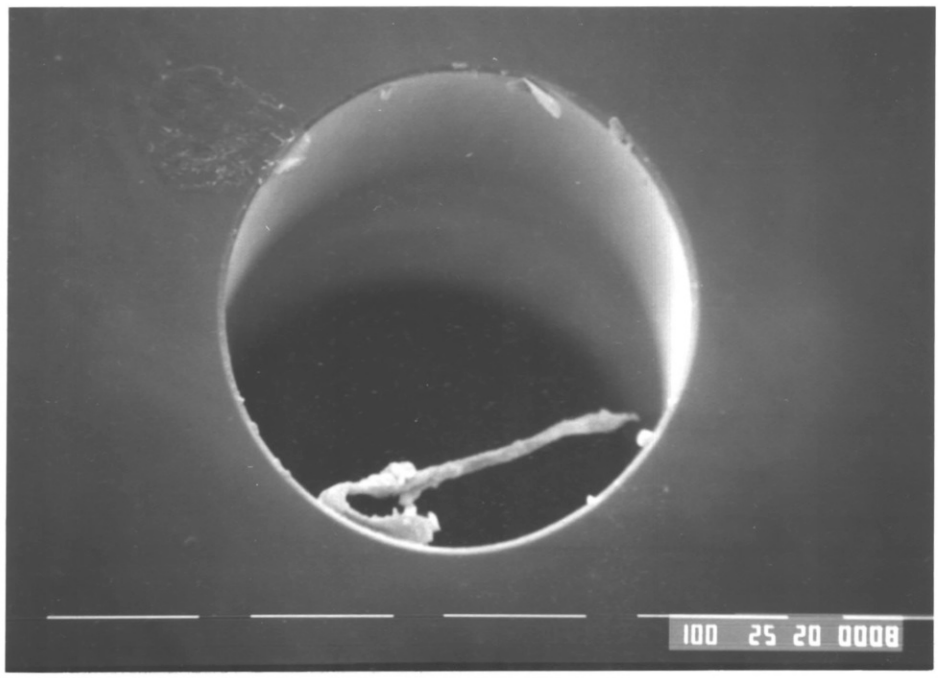


Plate 5.1 *Unused sapphire orifice x 200*

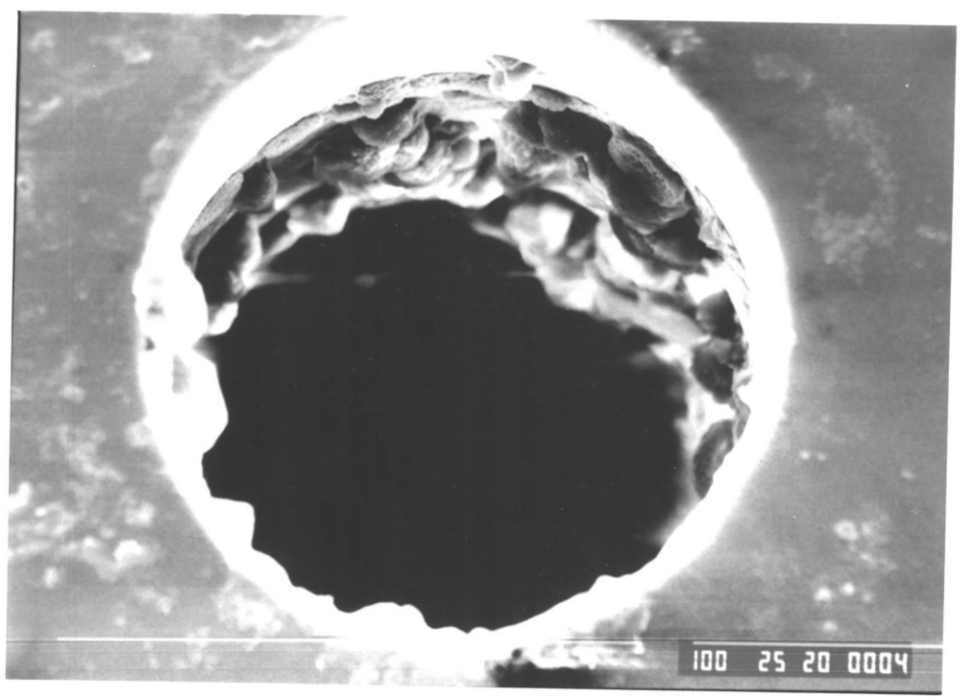


Plate 5.2 *Used sapphire orifice*

Sapphire orifices are usually replaced after 20 hours of operation time, and the time does not exceed a few minutes if the water filters are not used. The sizes of the sapphire orifices which have been tried range from 0.1 to 0.25mm hole diameter. However, most tests were carried out, using a 0.25mm orifice sizes(deliver ≈ 3 litre/min. at 2000 bars pressure), since these give a satisfactory operation time and sufficient kinetic energy in the water to be transferred to the abrasive which is fed into the abrasive mixing chamber. Preliminary cutting tests using the smaller orifices resulted in a relatively low material removal rate and the jet was very spread at a pressure of 2000 bars.

The sapphire orifice is pushed into a nylon seal in a stainless steel holder. The discontinuity on the seal-sapphire boundary induces undesirable eddies in the flow before entering the hole; this results in a less coherent jet. To minimise such eddies, the sapphire is made thicker than the seal (Fig. 5.1a) and therefore the surface of the jewel is little higher than the surface of the seal. If the jewel thickness is less than the seal thickness (Fig. 5.1b), eddies induced on the boundary will have undesirable effect on jet coherence.

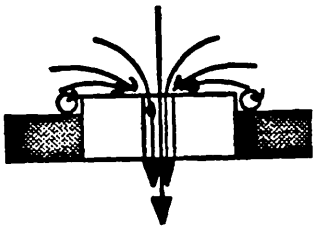
5.4- Mixing chamber

Some experiments were carried out on cutting heads without mixing chambers, that is abrasive is fed directly to the outlet tube (Fig. 5.2). It was noticed that no vacuum was generated to suck the abrasive in and the abrasive feed tube becomes blocked.

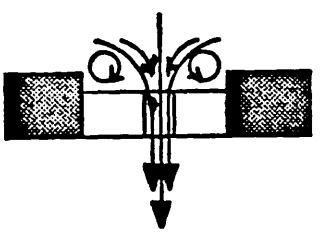
The existence of the mixing chamber is essential to create the necessary low pressure to draw the abrasive into the jet as well as to stimulate good mixing of the slow moving abrasive particles with the high speed water jet. It was found that the shape of the mixing chamber is also important for the water/abrasive mixing process. A square sectioned chamber (Fig. 5.3) is not as good in mixing as a conical section (Fig. 5.4) or concave section (Fig. 5.5).

It was also noticed that blockage of abrasive feed pipes was more frequent when a cutting head with a square section mixing chamber is used, because abrasive particles

tend to accumulate and create a wall around the water jet rather than mixing with it. Whereas conical and concave sections cause the abrasive to slide into the lower part of the mixing chamber and towards the focusing tube entrance.



a



b

Fig. 5.1 Sapphire orifice in the rubber seal

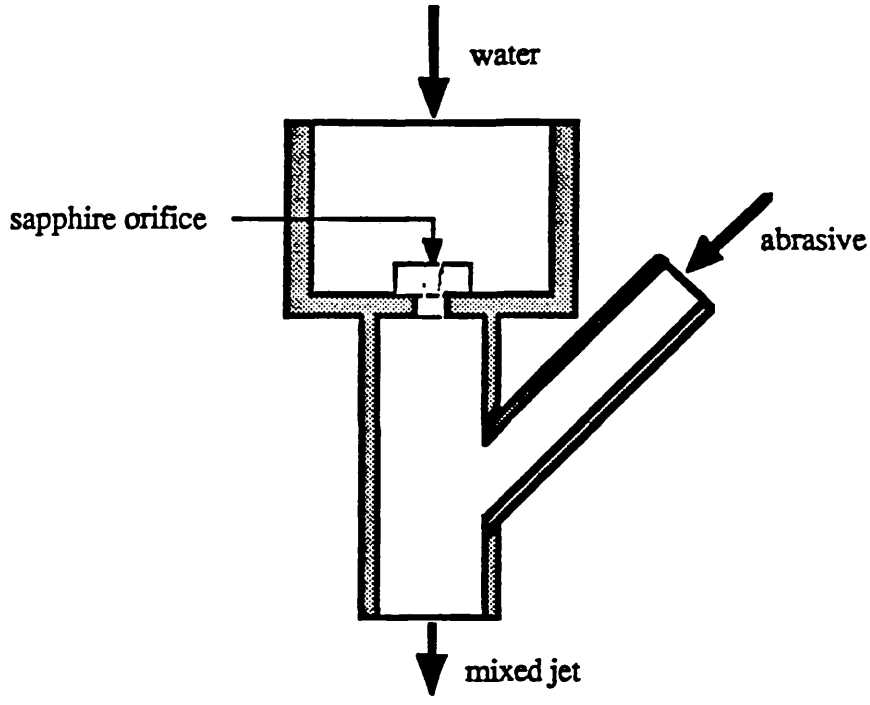


Fig. 5.2 Cutting head without mixing chamber

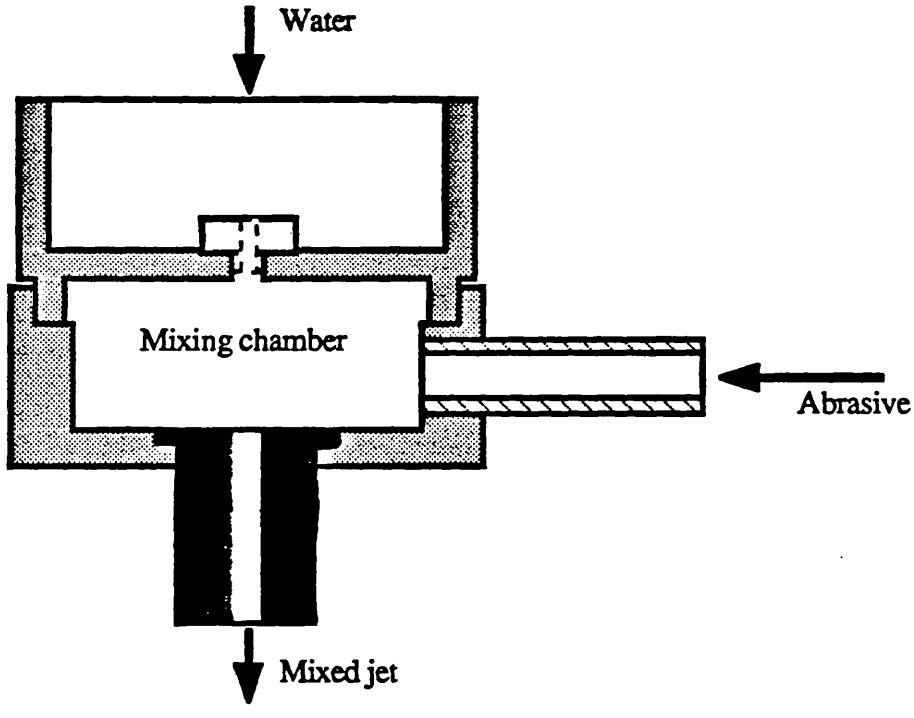


Fig. 5.3 Cutting head with a square section mixing chamber

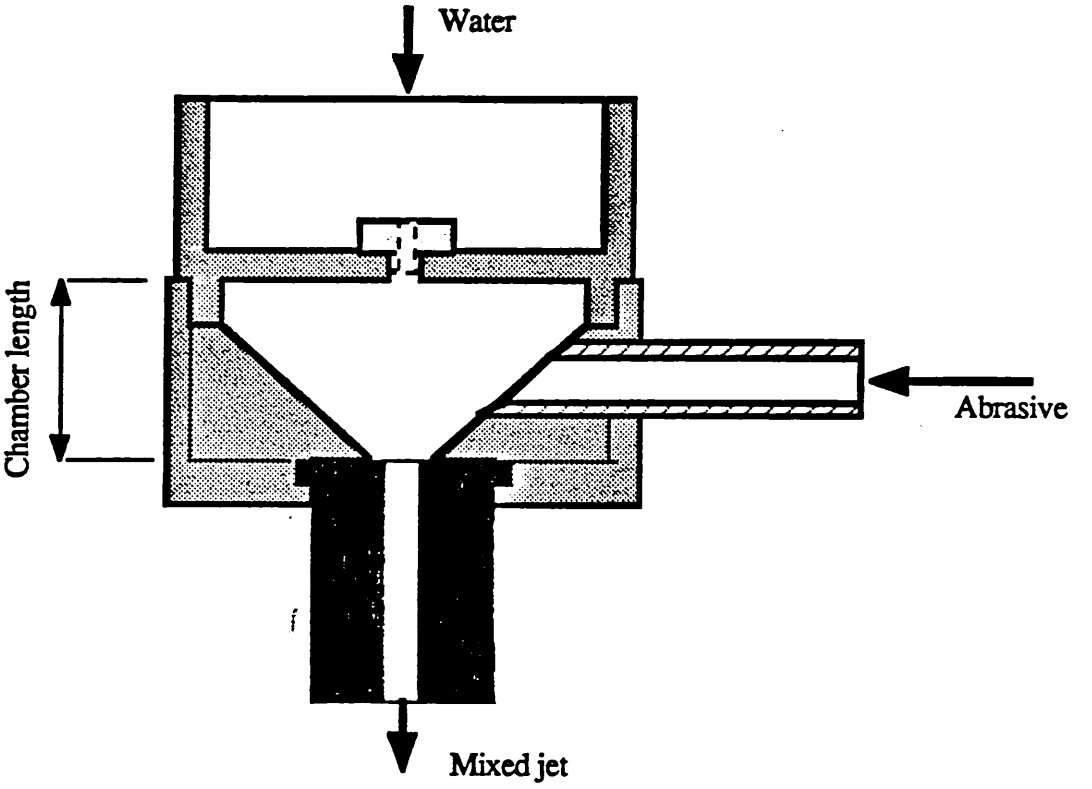


Fig. 5.4 Conical cutting head

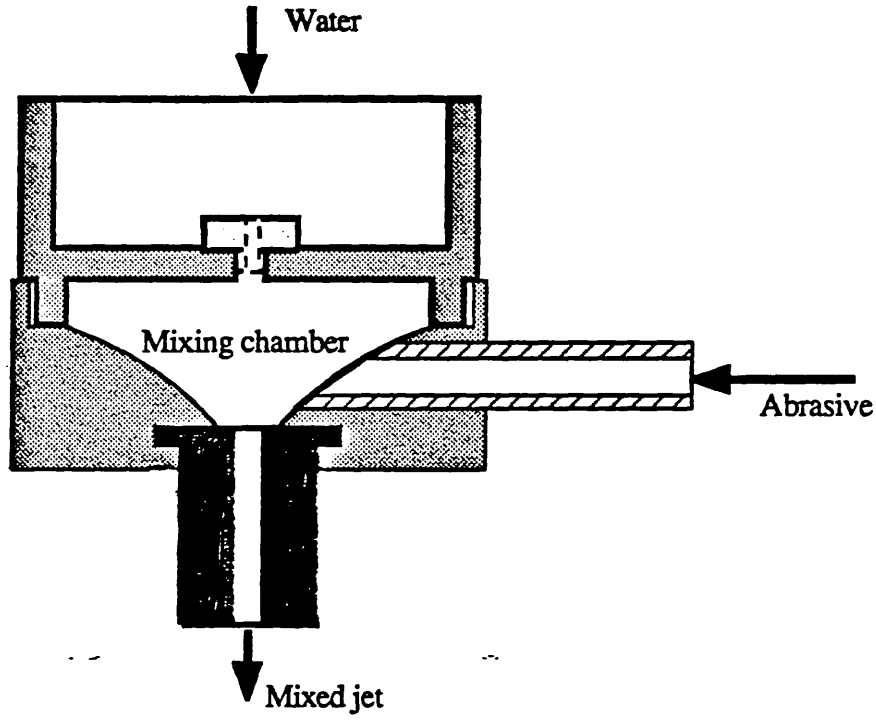


Fig. 5.5 Curved internal surface mixing chamber

The pressure in the mixing chamber was measured, using a mercury barometer connected to the abrasive feed tube. It was found that the pressure is a function of the water mass flow rate and the focusing tube bore (Fig. 5.6) .

As the water pressure increases or the sapphire orifice diameter increases, the mixing chamber pressure decreases. When the focusing tube bore increases, the mixing chamber pressure was increased because large tube bore allows the air to flow back into the mixing chamber and replace the air which is entrained in the jet. This entrained air in the jet is the cause of the low pressure in the chamber. Conical and concave sections give the same mixed jet unlike the square section. However, conical section heads are easier to fabricate than concave internal shape mixing chambers. There are other advantages for a low pressure mixing chamber. It was observed that at very low chamber pressure the speed at which the abrasive particles approach the water jet is greatly increased. Increasing the speed of the particles may improve their ability to penetrate through the water jet which results in improved mixing, whereas, low speed particles tend to bounce on the jet outer surface and the particles can not gain the full speed of the water jet core. Moreover, at lower mixing chamber pressure blockages of the abrasive feed pipe are unlikely to occur.

5.5- Tests on mixing chamber length

Three mixing chamber lengths were tested on cutting steel samples, 30 mm and 20 mm lengths and the shortest possible mixing chamber length of 10 mm was also tested. a mixing chamber length of 10 mm gave fastest cutting operation and the same time resulted in lowest outlet tube wear.

It is known that the water jet spread increases with the increase of distance from the exit of the jet. For this reason, short length mixing chambers are more desirable since they limit abrasive mixing to the coherent part of jet, which is at short distance from the water exit.

Short mixing chambers should result in a decrease of the focusing tube wear rate, because the water jet spread in short chambers is less than long mixing chamber.

Therefore short mixing chamber decreases the water and abrasive friction along the focusing tube inner wall.

Short mixing chambers affect the cutting ability of the jet because at short distance from the orifice the jet is coherent, hence inefficient mixing of abrasive. An increase of the focusing tube length might be required to increase the cutting speed.

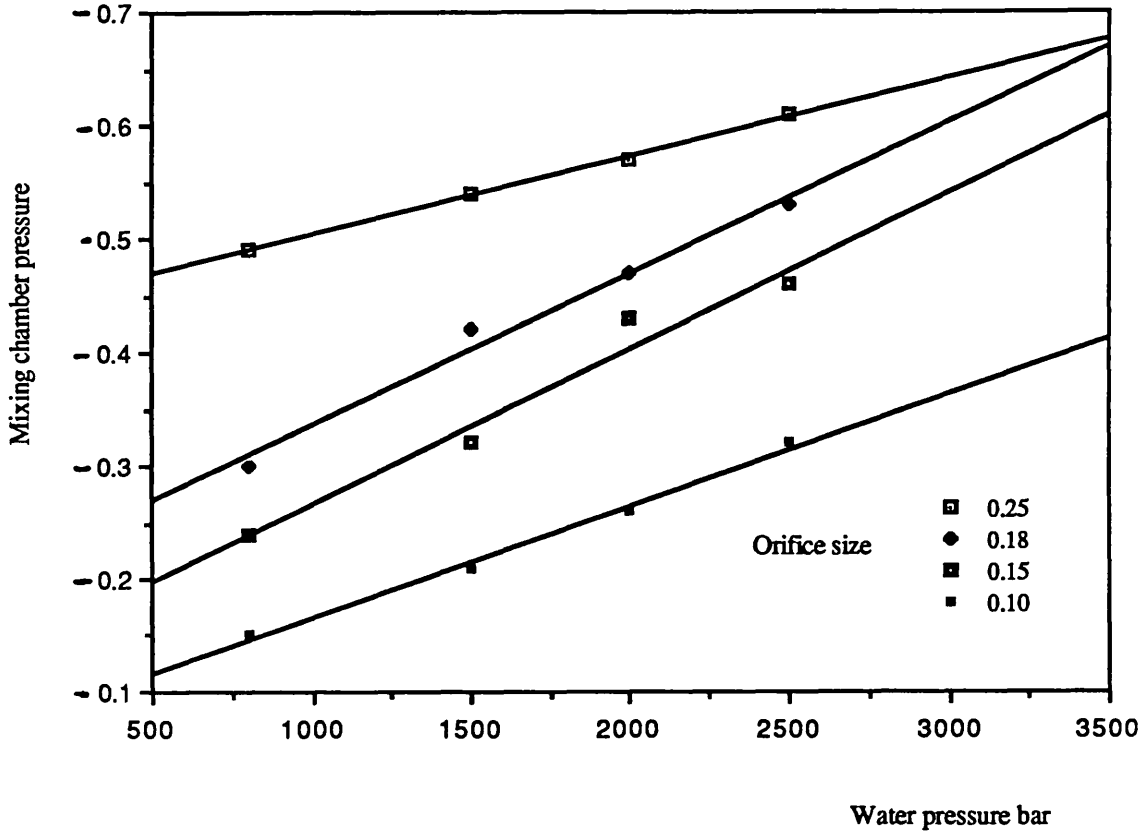


Fig. 5.6 Mixing chamber suction pressure variation with operation pressure

5.6- Focusing tube

Without the focusing tube, little cutting was achieved. Initial observations indicate that abrasive particles remains on the periphery of the water jet and can be seen piling on the workpiece and without any cutting taking place. The tube focuses the mixed jet and hence accelerates the particles for this reason the length of the tube is critical (as it will be shown later). Since the abrasive particles flow parallel to the tube inner wall, severe wear is expected. This wear can be reduced by a combination of head design and outlet tube material selections. Tungsten carbide or boron carbide are the usual choice because of their hardness and strength. However, there are no substantial forces exerted on the tube to demand a tube made of a high strength material. Some of the newly developed ceramic materials possess acceptable strength and in some cases a high hardness equal to the carbide alloys. Ceramics are relatively easy to form or machine before firing and cost much less than the carbides. An example of such ceramics is zirconia. Generally, ceramics are very brittle, more than tungsten or boron carbide, for this reason, they are potentially useful in making the focusing tube. The inner of the tube can be considered to be subjected to intensive particle sliding and rubbing and little particle impacts.

5.7- Materials considered and tested for making the outlet tube

a-Tungsten carbide *(Carbide Tools, LTD)*

10 tungsten carbide (Nickel binder) tubes of diameter 2 mm and of lengths 19.6, 21.5, 23.4, 25.3, 27.4, 29.4, 31.5, 33.5, 35.9 and 38.2 mm used to test effect of the length of focusing tube on speed of cut. The tubes are made with a conical end to be fixed into the mixing chamber by threaded nut which normally fastened by hand (Plate 5.3).

b-Partially stabilised zirconia *(Powder,Toya Soda Manufacturing Co., LTD)*

Several grades of zirconia powders were supplied. The powders were then pressed in an especially designed hard steel die in a shape of solid cylinder. Then the cylinder was iso-statically pressed up to 3000 bars inside an oil pressure vessel.

A suitable hole was drilled in the compacted cylinder. The produced tubes were fired for 24 hours at temperature of 1500^{o}C and cooled gradually to room temperature,

allowance for material shrinkage was calculated.

It was found that the powder may shrink up to two thirds of the original dimensions to produce the final tubes. Outlet tubes 2 mm bore and lengths of 12 to 20 mm were made and tested (Plate 5.4).

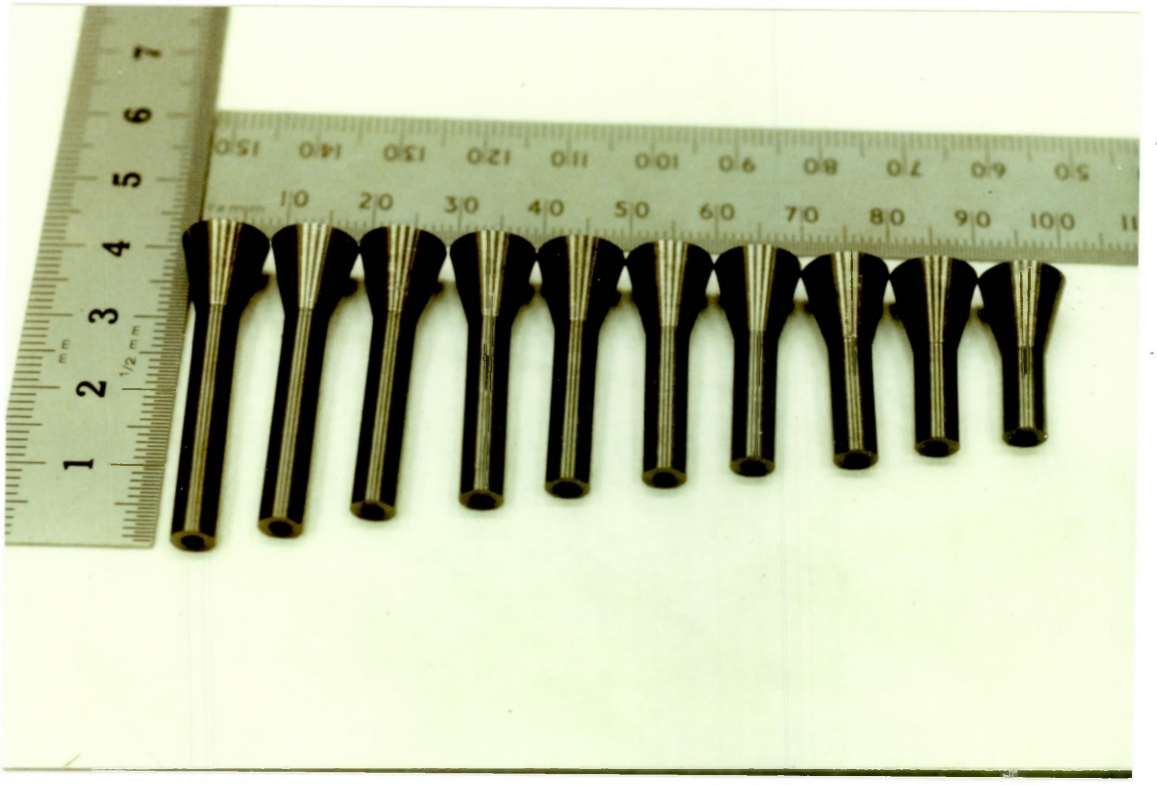


***Plate 5.3** Tungsten carbide focusing tube*

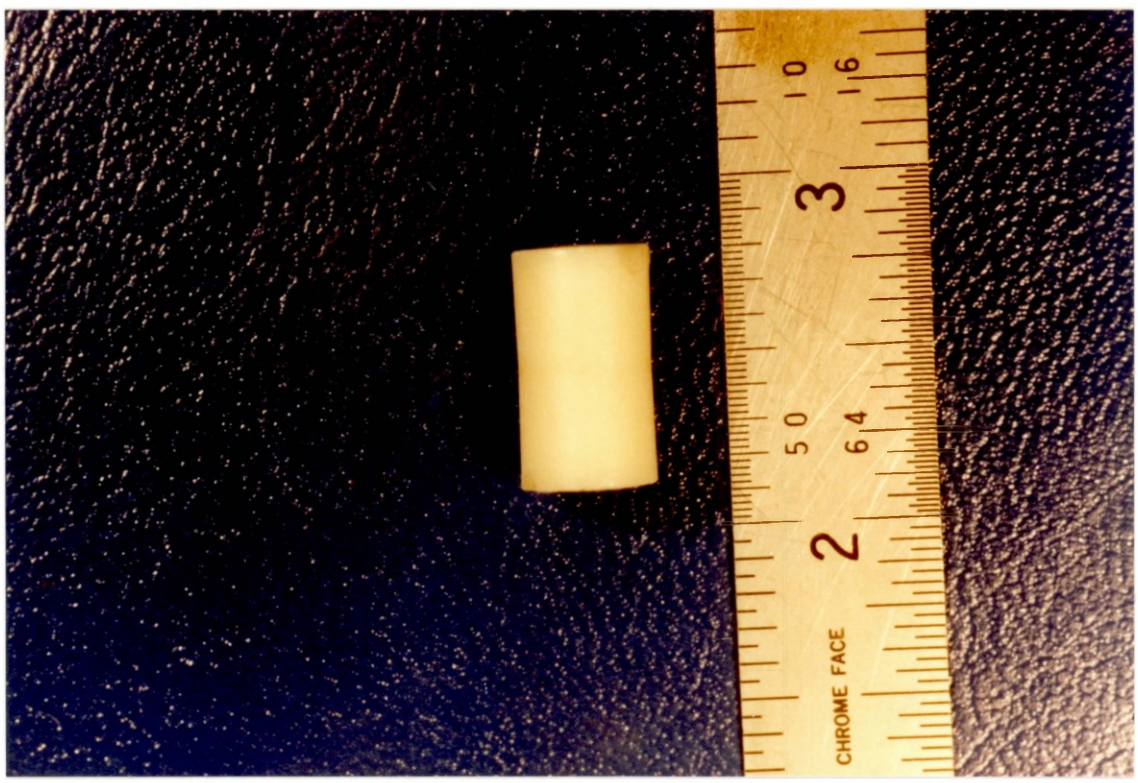


***Plate 5.4** Zirconia focusing tube*

c-Alumina *(Coors Ceramics Wales Limited)*

Standard pure alumina tubes of 2 mm bore and 25 mm length were supplied. Several tubes of the same length were tested.

d-Silceram, glass ceramic *(developed and produced by The Metallurgy and Material Science Department, I. C.)*

This material was obtained as solid blocks.Tubes of 2 mm bore and 25 mm length were cut and drilled, by diamond drills.

A comparison of the mechanical properties of the focusing tube materials are shown in (Table 5.1)

	Tungsten carbide	Zirconia	Alumina	Silceram
Density kg/m^3	16331	5800 - 6200	3500 - 3900	2900
Hardness kg/mm^2	1200 - 1450	1200 - 1400	1000 -1200	800
Tensile strength kg/mm^2	120 -200	100 - 130	15 - 40	10 - 20

Table 5.1 Mechanical properties of materials used for making focusing tube

Chapter 6

Results of cutting tests

Full description of tests and results are given in Appendix III

6.1 - Introduction

The optimum cutting head, as described in the previous Chapter, is used in all of the following cutting trials. The cutting head has a conical shaped mixing chamber and the length of the chamber is 10 mm (Fig. 5.4).

Further cutting tests on mild steel specimens were carried out to examine the nozzle design and its effect on mixing of abrasive inside the mixing chamber, hence the speed of cut of the mild steel specimen. Wear of the focusing tube is examined, tube material wear and length of the tube are two areas of interest.

The speed of cut and wear of focusing tube are related to the abrasive material type and particles shape used in the trials.

The results are presented in table and graphical forms.

6.2- Focusing tube (outlet tube)

To increase the speed of the abrasive particles and limit the spread of the mixed jet a focusing tube is added to the cutting head. This tube is subjected to severe wear because of particles impact on the tube internal wall and occasionally ploughing of the internal wall of the tube occurs. Tubes must be made of hard wear resistant materials to minimise the wear and produce coherent jet for cutting. Tungsten carbide has been tested (Tables 6.1, 6.2, 6.4 and 6.5) as well as hard ceramics such as zirconia and alumina (Table 6. 3). It was found that wear rate of the focusing tube is also related to the the bore diameter. High wear was observed at small bores and the wear decreases rapidly at large tube bores (Fig. 6.1). In (Table 6.1) wear of the T.C. tube in gm/kg is shown to decrease when the bore of the tube is increased. It is also shown (Table 6.1, 6.2) that wear of the inlet of the tube is always less than the wear of outlet of the tube.

Variable lengths of the tubes were tested to determine the required length to produce a well focused jet on the outlet of the mixed jet (Table 6.4). It was found that a tube length larger than 30 mm produces a well focused mixed jet and sufficient to achieve the maximum removal rate.

Focusing tube mat.	T.C.	T.C.	T.C.	T.C.	T.C.	T.C.
Length mm	19.6	19.6	19.6	21.5	21.5	21.5
Tube inlet bore before mm	2.46	2.8	3.1	2.25	2.3	2.5
Tube outlet bore before mm	2.5	3	3.4	2.35	2.45	2.75
Water Pressure. Bar	2000	2000	2000	2000	2000	2000
Type of Abr.	Flint-70	Flint-70	Flint-70	Flint-70	Flint-70	Flint-70
WT of tube Before gm	8	7.4	6.7	8.64	8.43	7.933
Operation time mins.	20	55	40	15	60	35
Tube inlet bore after mm	2.8	3.1	3.15	2.3	2.5	2.86
Tube outlet bore after mm	3	3.4	3.5	2.45	2.75	2.94
WT After gm	7.4	6.7	6.13	8.43	7.93	7.534
WT Loss gm.	0.6	0.7	0.57	0.21	0.5	0.399
Wear rate gm/min	0.030	0.013	0.014	0.014	0.008	0.011
Volume wear rate cc/min. mm	0.00011	0.00005	0.00005	0.00005	0.00003	0.00004
Abrasive flow rate Kg/min	0.930	0.850	1.075	0.400	0.400	0.600
Wear rate gm/Kg	0.032	0.015	0.013	0.035	0.021	0.019
Wear rate gm/Kg. mm.	0.002	0.001	0.001	0.002	0.001	0.001
Wear rate gm/min.mm	0.002	0.001	0.001	0.001	0.001	0.001

Table 6.1 Wear results of T.C. tubes using flint as abrasive

Kilograms	Kg.
Grams	gm.
Millimetre	mm. length of tube
Minute	min.
Cubic centimetre	cc

Focusing tube mat.	T.C.	T.C.	T.C.	T.C.	T.C.
Length mm	19.6	21.5	21.5	21.5	23.42
Tube inlet bore before mm	3.3	2.86	3	3.04	2.3
Tube outlet bore before mm	3.74	2.94	3.3	3.5	2.3
Water Pressure. Bar	2000	2000	2000	2000	2000
Type of Abr.	W.Al. 60	W.Al. 60	W.Al. 60	W.Al. 60	W.Al.- 60
WT of tube Before gm	6.117	7.53	7.089	6.737	9.188
Operation time mins.	3	3	3	9.5	15
Tube inlet bore after mm	3.44	3	3.04	3.4	2.96
Tube outlet bore after mm	3.94	3.3	3.5	4	3.84
WT After gm	5.886	7.089	6.737	5.93	6.724
WT Loss gm.	0.231	0.441	0.352	0.807	2.464
Wear rate gm/min	0.077	0.147	0.117	0.085	0.164
Volume wear rate cc/min. mm	0.00028	0.00049	0.00039	0.00028	0.00050
Abrasive flow rate Kg/min	1.4	1.4	1.4	1.4	1.4
Wear rate gm/Kg	0.055	0.105	0.084	0.061	0.117
Wear rate gm/Kg. mm.	0.003	0.005	0.004	0.003	0.005
Wear rate gm/min.mm	0.004	0.007	0.005	0.004	0.007

Table 6.2 Wear results of T.C. tubes using white alumina abrasive

Focusing tube mat.	Zirconia	Zirconia	Zirconia	Zirconia	Zirconia	Zirconia	Zirconia
Length mm	17	12.8	12.8	12.8	16.1	16.1	16.1
Tube inlet bore before mm	2	2	2.56	3	2.16	2.6	2.84
Tube outlet bore before mm	2	2	3.5	4.16	2.16	3.34	4.04
Water Pressure Bar	2000	2000	2000	2000	2000	2000	2000
Type of Abr.	W.Al.- 60	W. Al.- 60	W. Al.- 60	W.Al.-60	W.Al. 60	W. Al. 60	W.Al. 60
WT of tube Before gm	7.037	5.927	5.518	5.342	7.342	6.857	6.587
Operation time mins.	7.5	3	3	3	3	3	3
Tube inlet bore after mm	2.96	2.56	3	3.08	2.6	2.84	3
Tube outlet bore after mm	3.9	3.5	4.16	4.24	3.34	4.04	4.62
WT After gm	6.280	5.518	5.342	5.279	6.857	6.587	6.388
WT Loss gm.	0.757	0.409	0.176	0.063	0.485	0.270	0.199
Wear rate gm/min	0.101	0.136	0.059	0.021	0.162	0.090	0.066
Volume wear rate cc/min. mm	0.00096	0.00171	0.00074	0.00026	0.00162	0.00090	0.00066
Abrasive flow rate Kg/min	1.4	1.4	1.4	1.4	1.4	1.4	1.4
Wear rate gm/Kg	0.072	0.097	0.042	0.015	0.115	0.064	0.047
Wear rate gm/Kg. mm.	0.004	0.008	0.003	0.001	0.007	0.004	0.003
Wear rate gm/min.mm	0.006	0.011	0.005	0.002	0.010	0.006	0.004

Table 6.3 Wear results of zirconia tubes using white alumina abrasive

Focusing tube mat.	T.C.	T.C.	T.C.	T.C.	T.C.	T.C.	T.C.
Length mm	25.32	27.42	29.44	31.48	33.5	35.9	38.2
Water Pressure Bar	2000	2000	2000	2000	2000	2000	2000
Type of Abr.	Flint 70	Flint 70	Flint 70	Type S	Type S	Type S	Type S
WT of tube before gm	9.7	10.1	10.6	11.1	11.5	11.8	12.4
Operation and cutting time mins.	24	25	21	16	15	13	15
WT after gm	9	9.4	9.9	8.9	9.1	8.8	7.9
WT loss gm	0.7	0.7	0.7	2.2	2.4	3	4.5
Wear rate gm/min.	0.029	0.028	0.033	0.138	0.160	0.231	0.300
Volume wear rate cc/min. mm	0.00008	0.00007	0.00008	0.00031	0.00034	0.00046	0.00056
Abrasive flow rate kg/min.	0.625	0.600	0.840	0.875	0.700	0.900	1.200
Wear rate gm/Kg	0.046	0.047	0.039	0.158	0.229	0.257	0.250
Wear rate gm/min. mm	0.001	0.001	0.001	0.004	0.005	0.006	0.008
Wear rate gm/mm.Kg	0.002	0.002	0.001	0.005	0.007	0.007	0.007
Time to cut specimen mins	24.	20.	17.	13.	8.	7.	10.
Volume removal rate cc/min.	0.300	0.360	0.424	0.554	0.900	1.029	0.720
Sample	B	M	W	D	A	L	Q

Table 6.4 Speed of cut using flint and alumina abrasives and tests of several lengths of focusing tubes

Focusing tube mat.	T.C.	T.C.	T.C.	T.C.	T.C.	T.C.
Length mm	27.42	27.42	27.42	29.44	29.44	29.44
Tube inlet bore before mm	2.5	2.5	2.6	2.5	2.5	2.5
Tube outlet bore before mm	2.46	2.47	2.5	2.46	2.46	2.5
Water Pressure Bar	2000	2000	2000	2000	2000	2000
Type of Abr.	Garent 50	Garent 50	Garent 50	Garent 80	Garent 80	Garent 80
WT of tube before gm	9.53	9.47	9.38	9.94	9.9	9.67
Operation time mins.	2.25	3.3	9	1.45	9.2	6.45
Tube inlet bore after mm	2.5	2.6	2.6	2.5	2.5	2.6
Tube outlet bore after mm	2.47	2.5	2.6	2.46	2.5	2.66
WT After gm	9.47	9.38	9.18	9.9	9.67	9.5
WT Loss gm.	0.06	0.09	0.2	0.04	0.23	0.17
Wear rate gm/min	0.027	0.027	0.022	0.028	0.025	0.026
Volume wear rate cc/mim.mm	0.00007	0.00007	0.00006	0.00007	0.00006	0.00006
Abrasive flow rate Kg/min	1.6	1.6	1.6	1.4	1.4	1.4
Wear rate gm/Kg	0.017	0.017	0.014	0.020	0.018	0.019
Wear rate gm/Kg. mm.	0.001	0.001	0.001	0.001	0.001	0.001
Wear rate gm/min.mm	0.001	0.001	0.001	0.001	0.001	0.001
Specimen cut time min.	cut in 5 min.	cut in 5 min.	cut in 5 min.	cut in 5 min.	cut in 5 min.	cut in 5 min.
Volume removal rate cc/min.	1.44	1.44	1.44	1.44	1.44	1.44

Table 6.5 Cutting speed using garnet as abrasive

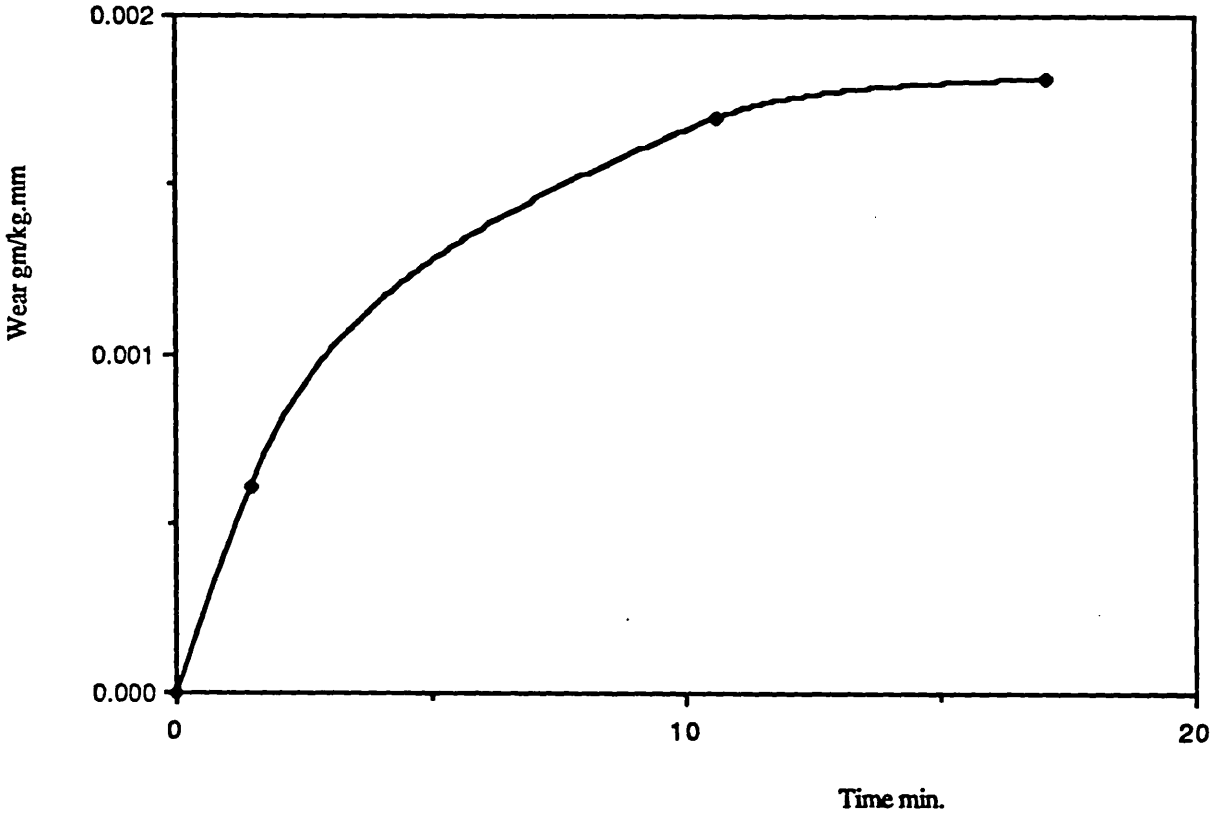


Fig. 6.1 Wear of tungsten carbide outlet focusing tube using garnet 80 abrasive

Tube lengths longer than the optimum length (30 to 35 mm) are found to be unnecessary and result in an increase of the total wear rate of the tube. After the sapphire orifice, the jet disperses downstream of the flow, especially, inside the mixing chamber. This spread increases the friction between the jet and the inner wall of the focusing tube which results in more wear of the focusing tube and a decrease in the cutting capabilities of the emerging jet.

The internal shape of the worn out tubes (Fig. 6.2 a and b) indicate that wear is maximum downstream in the direction of increasing jet spread because friction impact between the tube wall and abrasive particles will increase downstream of the flow. The focusing tube wear varies according to the tube's material. This occurs because the material's mechanical properties which respond to particle erosion with different wear modes. For example, an examination of tungsten carbide tubes shows that more wear occurs at the outlet of tube than the inlet. However the increase in wear along the tube is linear or uniform. Whereas, zirconia tubes show little wear at the inlet and higher wear than in the case of tungsten carbide tubes at the outlet.

The internal surface of the used zirconia tubes is curved, i.e. wear along the inner wall of the tube is not uniform, unlike tungsten carbide tubes where the wear is uniform. Brittle materials are more wear resistant at shallow angle of particle attack and wears easily at large angle of attack. The internal shape of the used zirconia tube confirmed this and the down stream wear is larger than the up stream wear of the tube. This is because the spread of the jet and the rebounding of the abrasive particles from the jet surface increases the angle of attack down stream of the tube.

Tests show that the spread of the jet is also affected by the amount of air flow into the mixing chamber. It is an advantage to prevent air flow into the chamber and to have low suction pressure to encourage abrasive flow and prevent blockage of the abrasive pipes, an increase of air in the chamber increases jet entrainment and hence the jet spread is increased. Tests and photographic observations were conducted when the abrasive feed pipe is blocked and when the pipe is open for only air flow (Plates. 6.1 , 6.2). It can be seen that increasing air entrainment results in an increase in the jet spread.



(a) *(b)*

***Fig. 6.2** Worn out focusing tubes (a) tungsten carbide (b) zirconia*

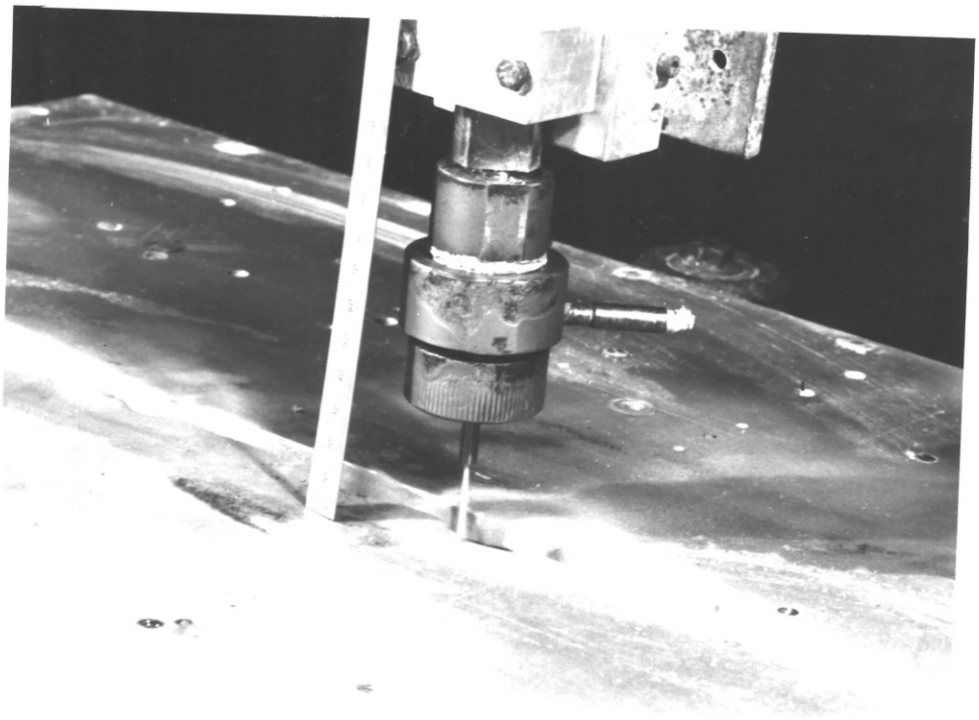


***Plate 6.1** Jet spread when abrasive pipe is closed*

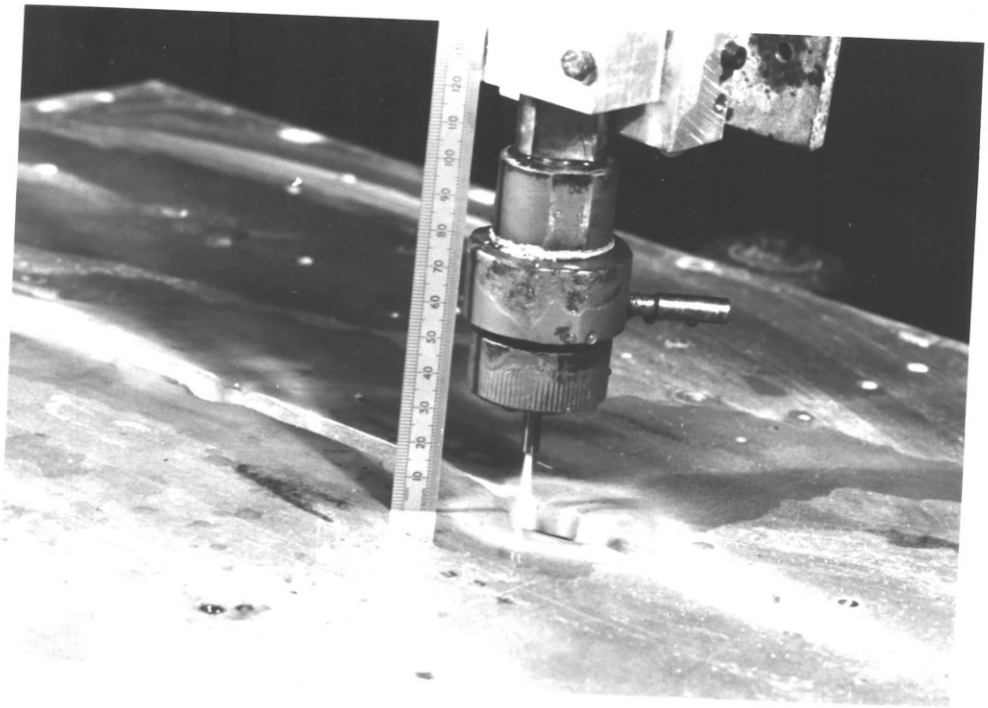


***Plate 6.2** Jet spread when abrasive pipe is open*

6.3- Cutting tests

From the trials on cutting heads and cutting tests, the following was observed;

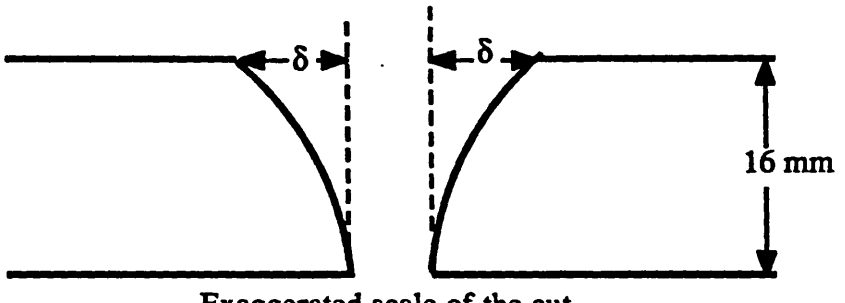
- Generally a cone shaped mixing chamber gives best cutting results, the conical chamber focuses the abrasive towards the jet centre, as a result more abrasive can be be fed to the chamber. It was noticed that conical shaped chambers reduces the chances of abrasive feed pipe blockage. The shorter the cone, the more efficient the cutting operation and the better the quality of cut, since the water jet spreads with distance from the sapphire orifice exit, short length chambers reduce the overall distance between the sapphire orifice and the workpiece.
- A replaceable focusing tube made from wear resistant hard materials is essential to focus and to mix abrasive and water. Tubes made of soft materials wears out very quickly (less than 5 minutes when mild steel focusing tubes were used).

- 30 to 35 mm length of the focusing tube was sufficient to give fully mixed water and abrasive jet and more than this length is unnecessary expense. However, this length may change slightly if the operating pressure changes.

- Kerfing of cut increases when the standoff distance increases and when the focusing tube bore is large. Almost no kerfed cuts are observed in cutting 16 mm thick mild steel when the operation pressure was 2000 bars with a stand off distance of 5 mm (Fig. 6.3).

- The angle of inclination of abrasive feed pipe to the direction of the jet was found to have no effect on the cutting operation. Cutting heads with several abrasive feed pipes inclination angles were tested. There was no evidence to suggest that the inclination angle has any effect on the performance of the cutting head.

- Increasing the air flow which is mixed with the abrasive results in increasing the focusing tube wear. When the air inlet valve attached to the abrasive feed pipe was fully open, it was observed that the water jet spread increased. Increased wear of the focusing tube was also apparent.



Exaggerated scale of the cut

Sample	δ mm	Focusing tube bore mm
HP 50	0.8	2.6
HP 80	0.2	2.4
W	0.1	2.2
M	0.9	2.6
A	0.0	2.0
D	0.4	2.4
L	0.0	2.0
B	0.6	2.5

Fig 6.3 Kerfing in 16 mm mild steel specimen related to focusing tube bore

- Large bore focusing tubes result in less focused jet and hence produces an unmixed jet and low quality cut surface as well as large kerfing in the cut .

- All parts of the cutting head can be made from ordinary stainless steel except the replaceable focusing tube which is subjected to severe wear is made from a harder materials. Examining the cutting heads after trials no material wear has been detected in the mixing chamber. wear was limited to the focusing tubes and was maximum at the outlet of the focusing tubes

- Focusing tubes made of tungsten carbide and zirconia have lasted approximately equal operation time while tubes made of alumina and silceram lasted for few seconds

- Sparks can be seen during cutting, however they are in the inside of the jet stream

- Width of cut is dependent on jet spread focusing tube bore, in most cutting cases it ranged from 2.5 to 3.0 mm. When the focusing tube bore was 2 mm width of cut was limited to 2.5 mm

- Speed of cut of the mild steel specimen has increased to a rate of 15 cm /min at angle of attack equal to 20 degrees (volume removal rate of $\approx$ 6.0 cm^3/min.)

- Tests on cutting brittle material such as silceram shows that the quality of cut is not as good as in mild steel (Plate 6.3 and 6.4). Cutting silceram was found to be sensitive to the cutting angle.While an eight mm thick piece was cut at a rate of 32.5 cm/min at 90 degrees angle of attack (volume removal rate of 6.5 cm^3/min.), it took 10 cm/min. to cut similar piece at 40 degrees angle of attack (volume removal rate of 2.0 cm^3/min.), garnet was the cutting abrasive in both cases.

- Test on cutting very ductile material such as nickel shows that the garnet mixed jet could not cut 1 mm thick nickel at 90 degrees angle of attack, where as the same

thickness was cut at a rate of 40 cm/min. at 40 degrees angle of attack (volume removal rate of 1.0 cm^3/min.)

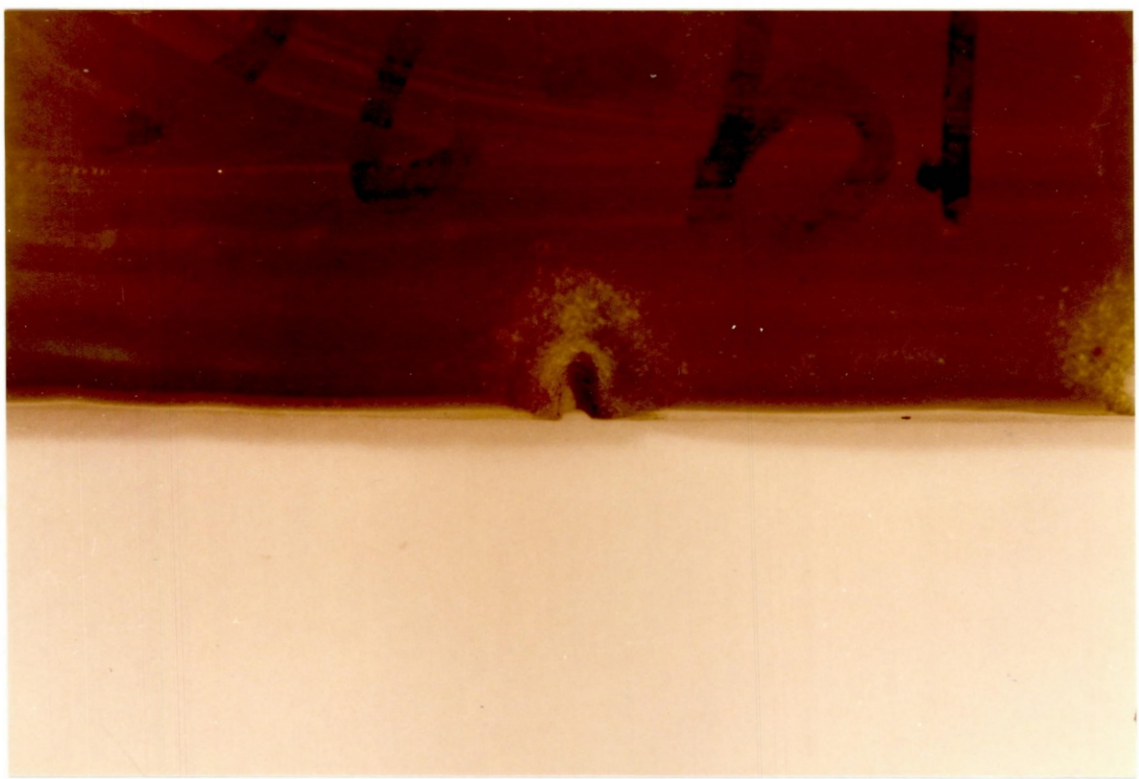


Plate 6.3 *Cut through silceram*

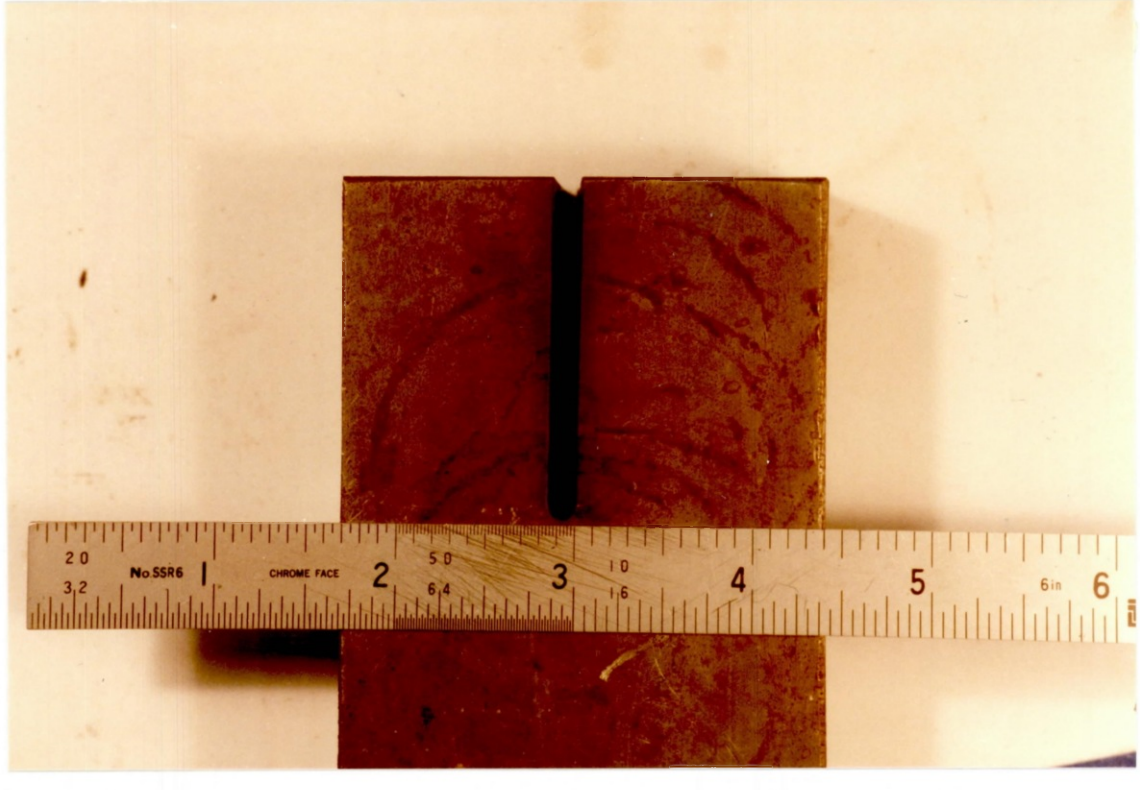


***Plate 6.4** Cut throught 25 mm mild steel*

6.4- Abrasive materials shapes and types

1- Flint (mesh 70 and 60)

Cutting mild steel using flint as the abrasive is slow but the focus tube wear rate is very small compared with other abrasive materials (Fig. 6.4) and (Fig. 6.5). The flint particles shapes are long and possess dull edges (Plate. 6.5), it also has a low density. The particles collected after the cutting operation are much finer than the particles before the cutting which suggest crushing of the particles on impact is occurring. Using abrasive mesh size 70 or size 60 make no difference to the observed cutting results. However, flint is cheap compared with the other abrasive materials and can be economical in cutting material with lower hardness than mild steel. The disposal of the flint after use is a cause of concern from an environmental point of view because flint contains free silica.

2- White alumina (mesh 60)

White alumina particles are thin laminates and have many sharp and jagged edges (Plate. 6.6). Alumina particles are harder than flint particles hence cut faster than flint (Fig. 6.4). The jagged edges however, result in a high wear rate of the focus tube, much more than in the case of using flint as cutting abrasive material (Fig. 6.5).

3- Reclaimed alumina type S (mesh 40/60)

This type of alumina abrasive is bulky and has sharp edges (Plate. 6.7). Its large hardness gives it the high cutting speed (Fig. 6.4), but the round particles possess less sharp edges for this reason the focus tube wear in this case is less than the wear if the white alumina is used (Fig. 6.5).

4- Garnet (mesh 50 and 80)

The two sizes of garnet particles tested gave the same results, the particles have sharp and smooth edges (compared with jagged edges in alumina particles). The garnet particles are cubic in shape (Plate. 6.8) and have less sharp corners than the alumina particles. Although garnet particles arenot as hard as that of alumina, the results shows faster cutting speed than the alumina (Fig. 6.4) and more importantly, garnet particles

cause less wear to the focusing tube than alumina (Fig. 6.5). The results show that garnet causes less wear to the focusing tube than any type of alumina abrasives and similar to the wear rate caused by flint. Garnet is the natural form of alumina and has no health hazard to be used in any cutting operation.

In all type of abrasive materials used in the cutting trials, the abrasives broke and crushed on impact with the workpiece. The produced particles after impact were very fine which render any further recycling process to recover the abrasive to be financially pointless, because fine particles reduced the speed of cut and it is costly to recover the abrasive.

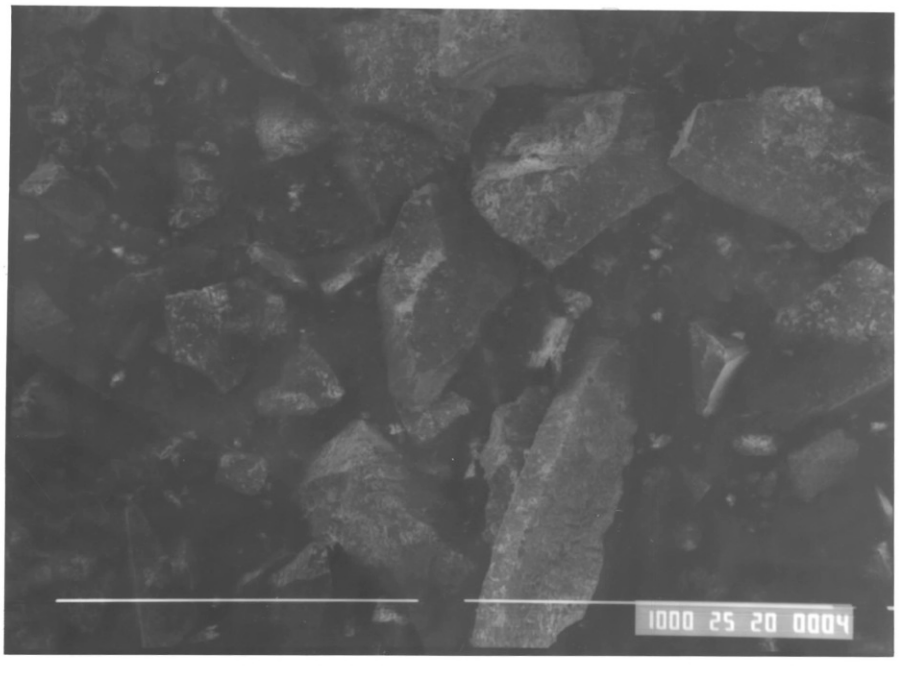


***Plate 6.5** Flint particles x 100*

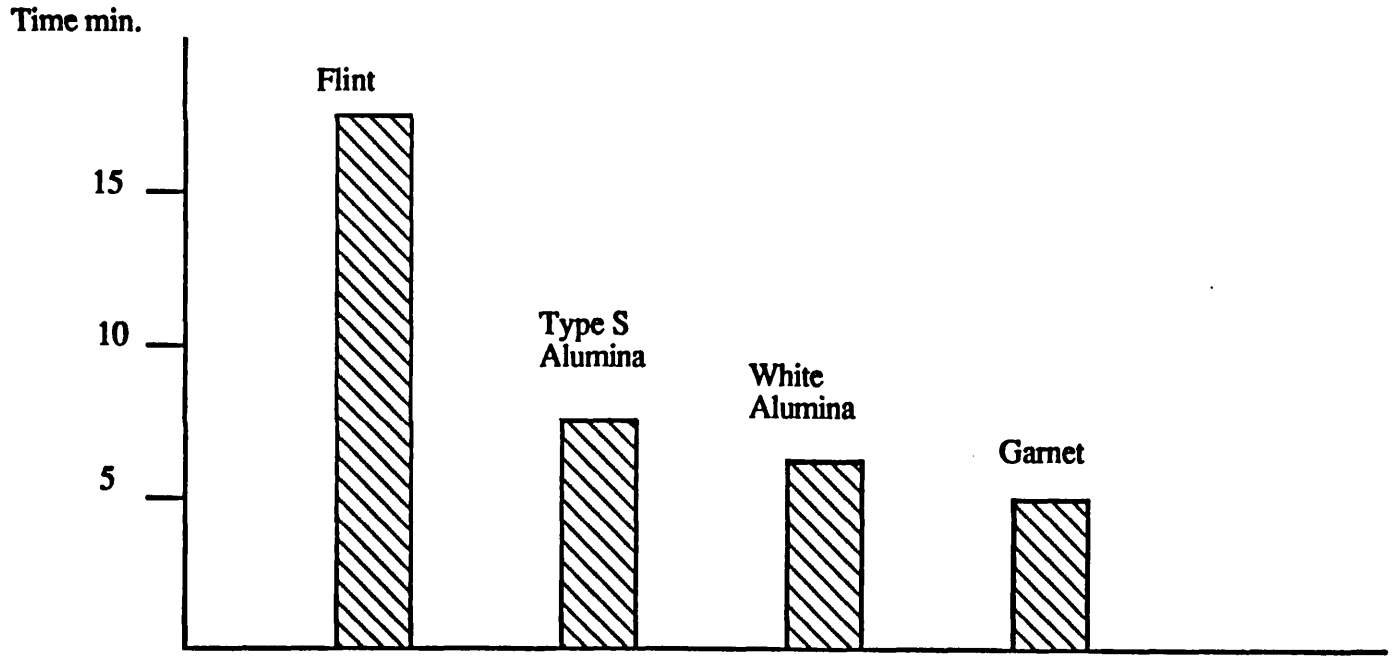


Fig. 6.4 Cutting time of specimen using different abrasive types

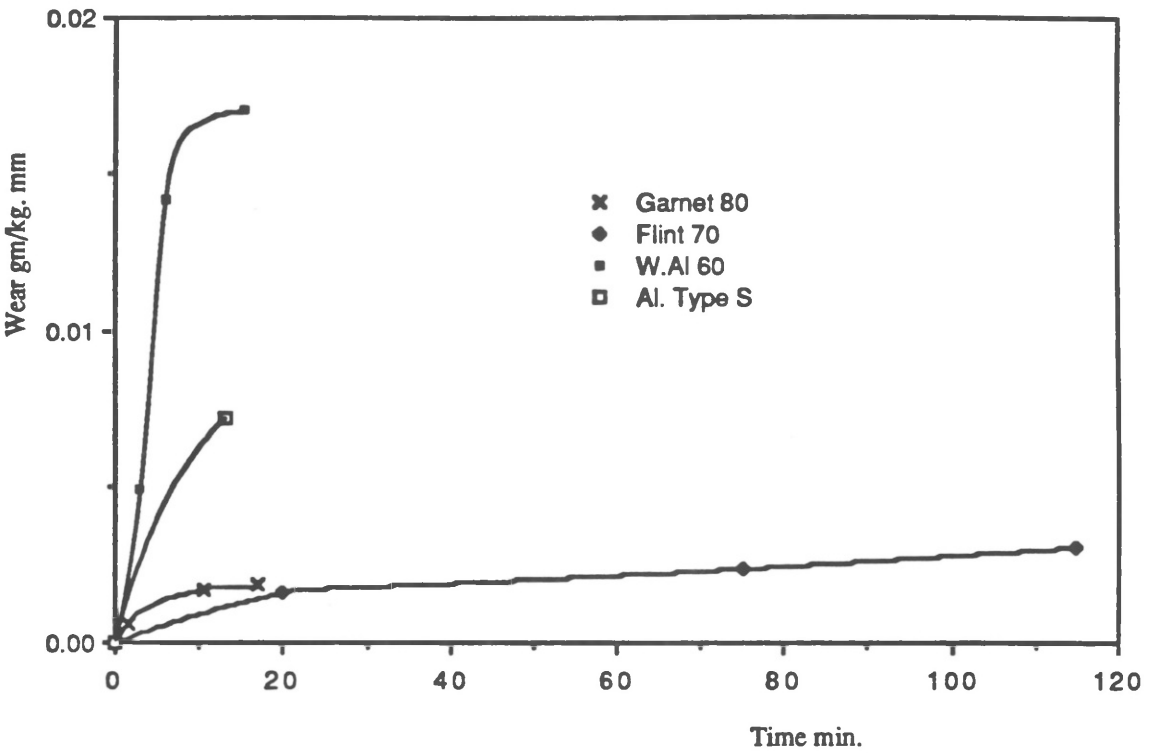


Fig. 6.5 Wear of tungsten carbide focusing tube with different types of abrasives



Plate 6.6 White alumina particles x 100

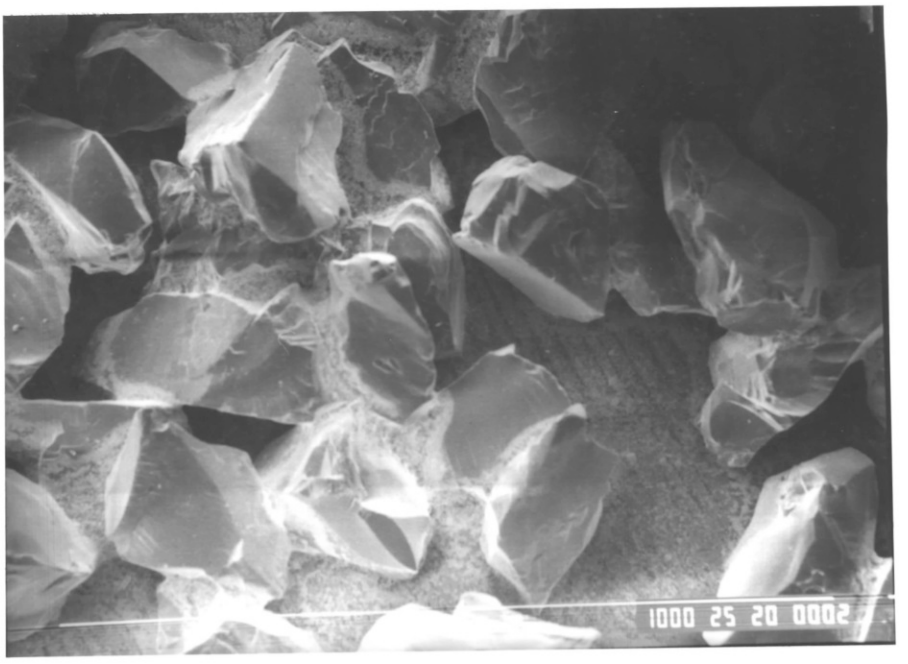


***Plate 6.7** S. type alumina particles x 50*



***Plate 6.8** Garnet particles x 100*

Chapter 7

Discussion of results

7.1- Introduction

The phenomena of jet spread caused by the flow of high speed dense media, water and abrasive in this case, into a stationary and less dense medium (air) is probably the most important phenomena in abrasive water jet cutting techniques which has engaged researchers for the last three decades.

The spread can effectively be reduced if the operating pressure is reduced and the orifice hole diameter is increased (or mass flow rate increase), this has been applied in operations such as mining and rock cutting However, for certain cutting operations it is required that only a small amount of cutting debris is produced (e.g.in nuclear industry) and at the same time a high cutting speed. Therefore, increasing the water pressure and decreasing the nozzle orifice are essential factors for any of such precision cutting operations. The limitations of the pressure increase are pump power and intensifier seals, an upper pressure limit of 4000 bar have been successfully used for a long time without significant leakage or seal failure.

Operation pressure of 2000 bar and sapphire orifice size of 0.25 were used in the tests. Smaller sizes are also used and resulted in very low cutting speed. This pressure and orifice size deliver approximate water mass flow rate of 3 kg/min. A maximum abrasive flow rate of 1.6 kg/min. was consumed in some cutting tests which make the maximum total abrasive and water flow rate 4.6 kg/min. About half of any reported cutting test.

The theoretical volume removal rate will be compared with the experimental results to evaluate the cutting head efficiency and discuss any scope for improvement in cutting operation (volume removal rate will be used in the comparison instead of mass removal rate to eliminate the effect of material specific weight) .

7.2- Jet spread

Sapphire orifices have been proven to reduce the jet spread. The dimensions of sapphire steel mounting are as shown in (Appendix II). Orifices which were used have a standard thickness equal to 0.45 mm which is 2 to 3 times the diameter size as reported earlier (Ref. 4) Nozzles which have $L_d/d = 3$ gave most coherent jet. Nozzles with longer stabilisers were used and either increased the jet spread or did not have any effect on the jet structure. However, short length stabilisers are preferred to reduce the over all contact between water stream and rough surfaces.

At this range of pressure and the small size of the orifice, the water upstream of the orifice can be considered to be turbulence free, since the water pipe before the orifice is long and has a diameter 20 times larger than the orifice size. For these reasons the pipe acts to eliminate or decrease turbulence in the water created from the pump action and from the flow along the pipe wall.

From observations of the high speed jet emerging from sapphire orifices and other nozzle holes such as mild steel and stainless steel. The sapphire orifices results in a significant reduction of the jet spread. However, this reduction is more apparent when the orifice hole is small. The wall roughness of the nozzle wall influences the jet spread especially at small orifice sizes. It is also evident that the effect of wall roughness increases at high pressure as well as when the orifice diameter is small.

The theoretical analysis assumes that the jet spread mainly due air entrainment of the water jet stream, and suggest that the jet spread in air is linear at low Re (Re < 2000). However, tests *(Section 3.2)* show that the spread is not so and the spread along the flow is given by the empirical formula

$$b = k_1 \sqrt{x} \qquad \text{where} \quad k_1 \text{ is a constant} = 0.237$$

This means the jet spread reaches a width (b) of 2 mm at a distance $x \approx 55$ mm which is much longer than any focusing tube used. In fact tests show that a tube length of 30 mm added to the cutting head length of 10 mm is sufficient to produce a focused

mixed jet. This is assuming that for good mixing to take place 'b' must be bigger than the diameter of the tube at tube inlet i.e. $b \geq 2$ mm at $x = 10$ mm. The apparent increase in the jet spread may due to the low pressure in the mixing chamber.

Examining used focusing tubes, it was apparent that wear of the tubes was maximum at a fixed length of the tubes (pressure and water and abrasive mass flow rates are constant). At this distance, the mixed jet spread reaches maximum. Beyond this distance, the wear of the tube is decreased (Plate 7.1) or remains constant. This indicates that for a certain orifice size, the jet expansion is maximum at a fixed distance from the orifice exist.

7.3– Mixing the abrasive with the water jet

The dense water jet is used to speed up abrasive particles, which in turn carry out the cutting by abrasion of the material. Very little cutting of any hard materials is done by the water jet alone. Soft material such as some polymer, paper and thin wood sheet are usually cut by water alone.

In abrasive water jet cutting, the water jet role can be reduced to a source of kinetic energy to be supplied to the abrasive particles, for this reason the water kinetic energy is increased enormously in the hope that most of this kinetic energy would be transferred to the abrasive particles.

From the theoretical analysis *(Section 3.4)*, it was shown that for high speed jet, as in the case of abrasive water jet cutting, the drag law becomes less important since the constant 'n' becomes larger than 2 and the particle, according to the drag law, approaches the speed of the jet instantaneously.

It is found that mixing abrasive particles with the water jet is difficult to achieve. The general slow speeds particles are not capable of penetrating the jet and they tend to reflect from the surface of the jet. Increasing the particles speed would improve the mixing operation, for this reason the abrasive chamber is incorporated in the cutting

head design. The inevitable spread of the water jet results in a low pressure in the mixing chamber. This pressure is a function of the water mass flow rate and the outlet tube bore. The maximum particle speed is reached at the lowest chamber pressure. A large mass flow of water and small outlet tube bore gives low chamber pressure. The largest orifice hole used was 0.25 mm and the minimum bore was 2 mm pressure of 0.65 bar below the atmospheric pressure was recorded (Fig. 5.6).

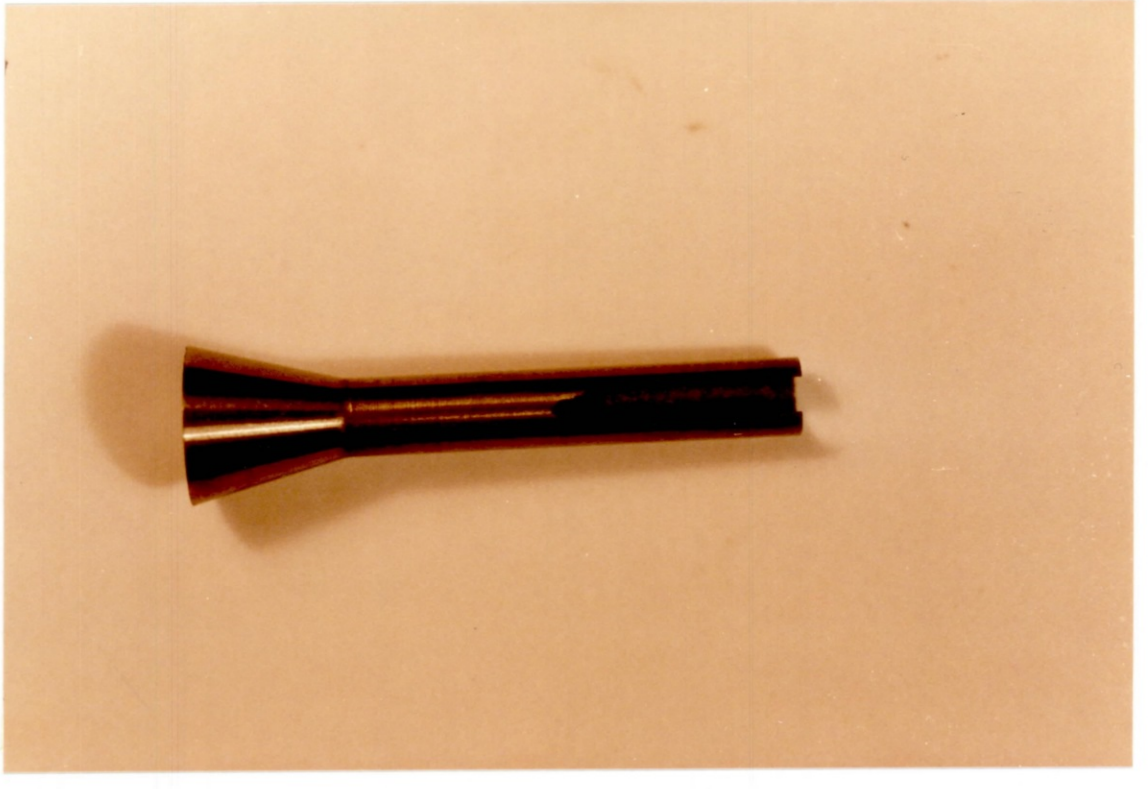


Plate 7.1 *Worn out tungsten carbide focusing tube*

However, the pressure inside the chamber will start to rise as soon as the outlet tube start to wear and its bore increases. Air flows from the outside to inside of the chamber through the worn tube and increases the chamber pressure.

Decrease in the mixing chamber pressure could decrease the outlet tube wear rate, very low pressure in the chamber forces the air through the outlet tube to the chamber. This air flow presents an air cushion between the jet and the wall of the tube. This air cushion acts to protect the wall of the outlet tube from severe wear. The air flow between the jet and the tube's inner wall and in the opposite direction of jet flow, creates a less spread mixed jet, as it was demonstrated earlier when the abrasive feed pipe was completely blocked (Plate. 6.1, 6.2).

The minimum chamber pressure of 0.65 bar below atmosphere is unlikely to be reached and maintained during cutting operation. This is because the abrasive flow into the chamber will increase the pressure and more significantly, it is always essential to let some air flow with the abrasive particles to prevent abrasive pipe blockages and to increase the speed in which the particles approaches and meet the water jet.

Trials have been conducted to feed abrasive in the form of wet abrasive or slurry, these trials gave poor cutting results and at some instants no cutting was observed. Feeding abrasive mixed with water results in injecting a large amount of low energy water, instead of preserving the jet energy to be transferred to the abrasive alone. In slurry feed, this energy is used to accelerate the water in the slurry as well as abrasive. Slurry generally reduced the overall cutting jet speed.

The outlet tube wear increases rapidly from 2 mm bore to about 3 mm bore in a short time (Fig. 6.1). The tube total wear rate then levels to a constant with the increase of the bore, no wear was detected at tube bore of 4 mm for this particular orifice (0.25) and cutting head.

A long mixing chamber increases the cutting abilities of the mixed jet because of large jet expansion in the chamber hence it is easier for abrasive particles to penetrate the jet, but long mixing chamber will increase the focusing tube wear because of good abrasive/water mixing and because of larger jet expansion which increases the mixed

jet friction with the tube. While a short chamber confines the abrasive particles penetration to a short coherent jet near the orifice exist, which is dense and has faster water speed which will resist abrasive particle penetration. The particles are more likely to bounce from the jet surface rather than mix with the it.

Mixing also takes place during the cutting operation. After the initiation of the cut in the cut material surface, a kerfed surface is created and this acts to focus the jet and abrasive to the lower parts of the cut (Plate 7.2). But the kerfing decreases or does not exist when the jet is more coherent especially when using 2 mm bore focusing tube (Fig. 6.3) and (Plate 7.3)

In the tests all cuts are carried out by 3 to 5 passes, but the effect of number of passes on cutting steel was studied by Hashish (Ref. 27) which indicate an increase in the speed of cut by increasing the number of passes. This confirms that local mixing and focusing is occurring inside the slot.

One of the very few advantages of the spread jet is improved mixing of abrasive particles. In the spread jet more air is entrained in the water which makes it easier for abrasive particles to penetrate the jet.

Since there was no single method to assess the degree of mixing independent of other parameters, the mass flow rate of abrasive, which can be fed to the jet, is not an accurate indication of the degree of mixing. The speed of cut or cutting head efficiency may be used to a certain extent to indicate the degree of mixing if all other parameters remain constant. However, it is difficult to examine the effect of shape and size of the particles on mixing since speed of cut is also a function of the particle shape, size and the mechanical properties of the particles.
Analysis of water drag forces on two basic shapes of particles namely, spherical and tetrahedral shapes shows that irregular shaped particles absorb more kinetic energy from the water jet (Fig. 7.1) than the spherical shaped particles. Hence they mix easier with the jet.

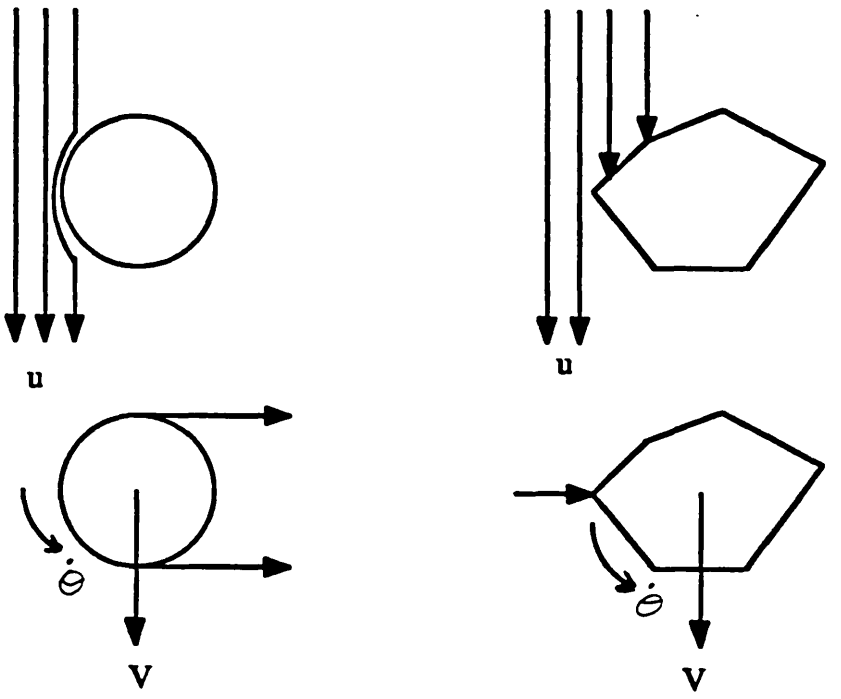


Fig. 7.1 Forces on two particles shape during jet penetration

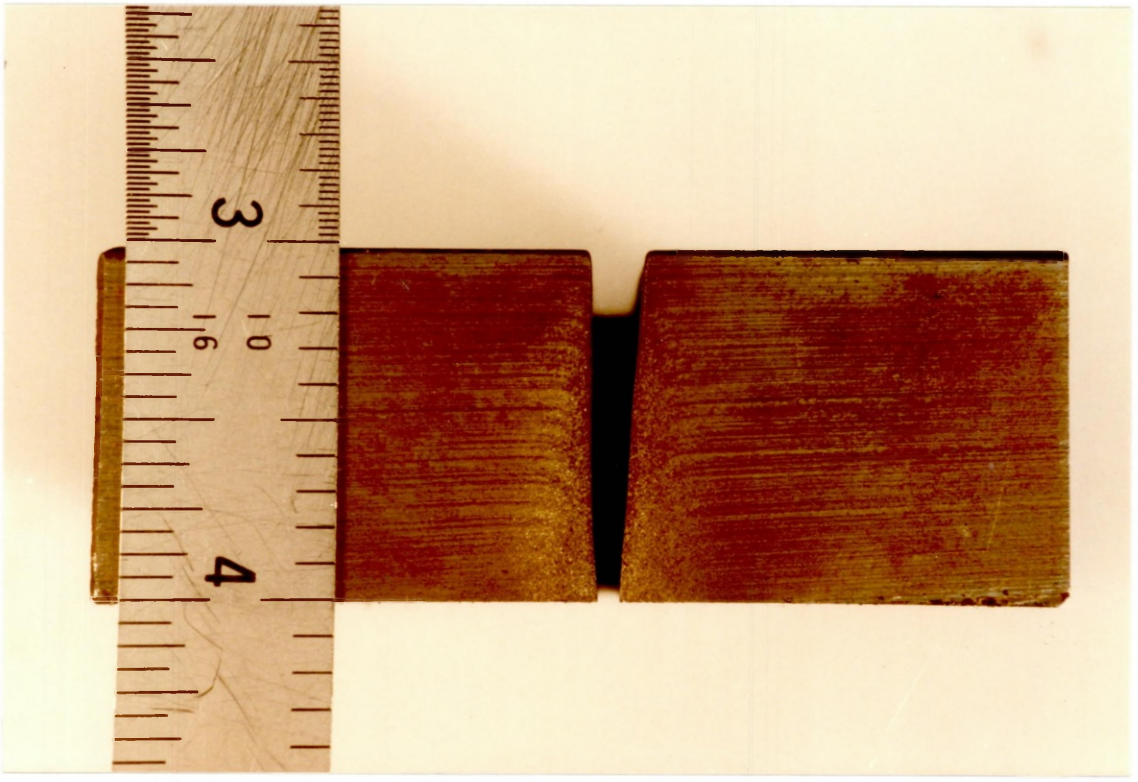


***Plate 7.2** Kerfing in thick mild steel*



Plate 7.3 *Cut in 16 mm thick mild steel* $\delta = 0.2$ *mm*

7.4– Cutting head design

The internal shape of the cutting head is critical as far as the mixing of abrasive with the jet is concerned. As was stated earlier a square shaped chamber gives poor mixing results and in some cases no abrasive particles were observed to flow with the water jet. A square section causes the abrasive feed pipe to block because of abrasive accumulation around the jet supported by the lower parts of the chamber.

Conical shaped chambers, in general, perform better and result in higher cutting speeds, the angle of the cone is related to the chamber length. However, most heads used in the course of this work have had conical shaped chambers and half cone angles between 20 to 45 degrees, and are of length between 10 to 40 mm. A cutting head with a short mixing chambers (10 mm) followed by 30 mm long focusing tube gave highest cutting speed. To assess the performance of this cutting head at 2000 bars pressure and abrasive and water flow rate of 4.5 kg/min., the head efficiency can be defined as follows:-

$$\text{Head efficiency} = \frac{\text{experimental volume removal rate}}{\text{theoretical volume removal rate}} \times 100$$

(Theoretical volume removal rate as calcutated in section 3.6)

From (Table 6.5), the highest cutting rate of mild steel achieved was 1.44 cm^3/min using garnet as the abrasive material and water and abrasive flow rate of ≈ 4.5 kg/min. at 90 degrees angle of attack.

$$\text{Cutting head efficiency} = \frac{1.44}{2.5} \times 100 = 58\ \%$$

Mild steel is a material with certain degree of ductility, and as shown earlier, material ploughing dominate the removal process (Plate 7.4). The volume removal rate increases when the specimen was cut at angle = 20^o (maximum theoretical removal rate Ref. 47).

$$\text{Efficiency at } 20^o \text{ angle of attack} = \frac{6.0}{7.5} \times 100 = 80\ \%$$

(For nickel which is very ductile no cutting occurs at 90^o angle of attack while at 40^o

the volume removal rate was 1.0 cm^3/min. *Section 6.3*)

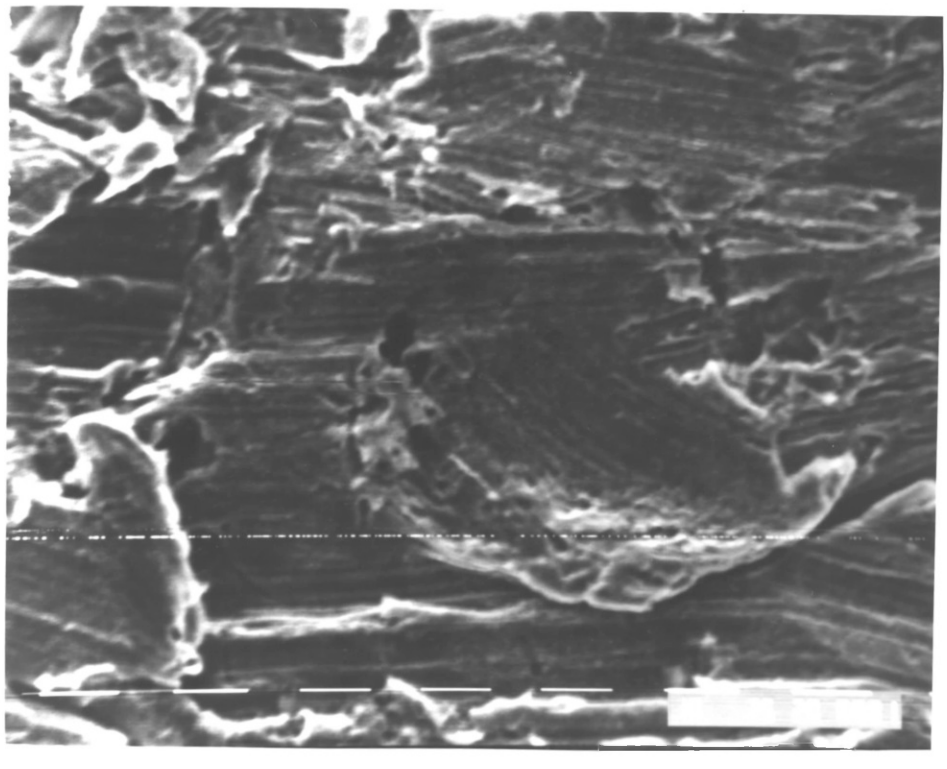


Plate 7.4 *Surface of cut of mild steel shows ductile cutting x 1000*

It can be seen that to increase the cutting capabilities of the head the mixing of abrasive material may have to improve further by 20 %. Increasing the water flow rate is one way as shown (Table 2.1), similar cutting head produced efficiency reached 90 % but the flow rate of water and abrasive was more than 8 kg/min (cutting rate of 6.75/8 = 0.84 cm^3/ kg), while in this test the cutting rate was 1.33 cm^3/ kg (8.6 gm/gm)

The efficiency decreases as the focusing tube bore wears out because the jet becomes less focused and the mixing is incomplete.

For cutting a brittle material (silceram) at 90° angle with the angular garnet particles;

$$\text{Efficiency of cutting head} = \frac{6.5}{8.0} \times 100 = 81\ \%$$

The volume removal rate of silceram as expected reduced when the angle of attack decreases. At 40° angle of attack the removal rate was 2.4 cm^3/min .

The variations of the ductile and brittle materials removal rates with the angle of attack follows the same material response in qualitative terms as for single particle erosion reported in the literature review. A quantitative comparison indicates that the volume removal rate in water jet cutting is at least 3 to 4 times larger than for single particle erosion tests. The water jet cutting test are at much higher particle impact speed 900 to 600 m/sec compared with single particle speed of 200 m/sec. The material removal rate of the abrasive water jet is expected to be higher than the reported single particle erosion tests because of the following factors:- Speed of particles in the abrasive water jet is 2 to 3 times higher than the reported tests. Water during the cutting operation is believed to increase material removal rate.

The reduced experimental volume removal rates compared with the theoretical results are largely due to factors such as incomplete mixing of abrasive in the cutting head chamber. Particles collisions before and during cutting which can interfere in the cutting process and fracture of particles on impact. In the calculations of the theoretical removal rate it was assumed that the whole mixed jet is taking part equally in the wear operation. But the fact is that one half of the jet could be in direct contact

with the surface of the cut material. However, there are factors which are not fully considered in evaluation of the theoretical volume removal rate, such as the exact effect of jet static and dynamic forces during cutting material deformation, repeated impact erosion and secondary erosion which resulted from fracturing of particles on impact.

Cutting heads are designed in a way to reduce wear to a small and replaceable part of the focus tube. All the cutting head, a part from the focusing tube, can made of mild steel or stainless steel, while hard materials are required for the focusing tube.

A comparison of the two hard materials extensively tested as focusing tube material, namely tungsten carbide and zirconia was carried out. The cost may justify opting for zirconia. The wear rates of a unit length of zirconia tubes $\approx 1.0 \times 10^{-3}$ cm^3/min. compared with 0.6×10^{-3} cm^3/min. of a unit length of tungsten carbide for the same abrasive (w.alumina), (Tables 6.2 and 6.3). Cost estimates of the average tube of zirconia is about £2.00 while tungsten carbide tube coasts £17.00. Cutting tests using garnet abrasive reveal that tungsten carbide tube wears out (bore becomes 4 mm) in 15 hours, while zirconia tube at the same operation conditions lasts for 12 hours.

Decreasing the mixing chamber pressure has been shown to decrease the water jet spread because either the low pressure chamber reduces air entrainment in the jet or low pressure in the chamber forces air through the the focusing tube hence reduces the jet spread by creating an air cushion between the jet and the wall of the tube. or it could be a combination of the two.

As a result of the above observation cutting heads with multiple cavities(or more than one mixing chamber) inside were made and tested (Fig. 7.2). It was hoped that more cavities would decrease the internal pressure further still. The somewhat inconclusive results showed a further decrease in pressure inside the cavities and more importantly the effect of the air cushion around the jet resulted in slight decrease in the focusing tube wear rate. It was thought that because the new multi-cavity heads are longer than

the single chamber head, wear rate of the tube will increase. More tests on this area are required for a new cutting head to be designed.

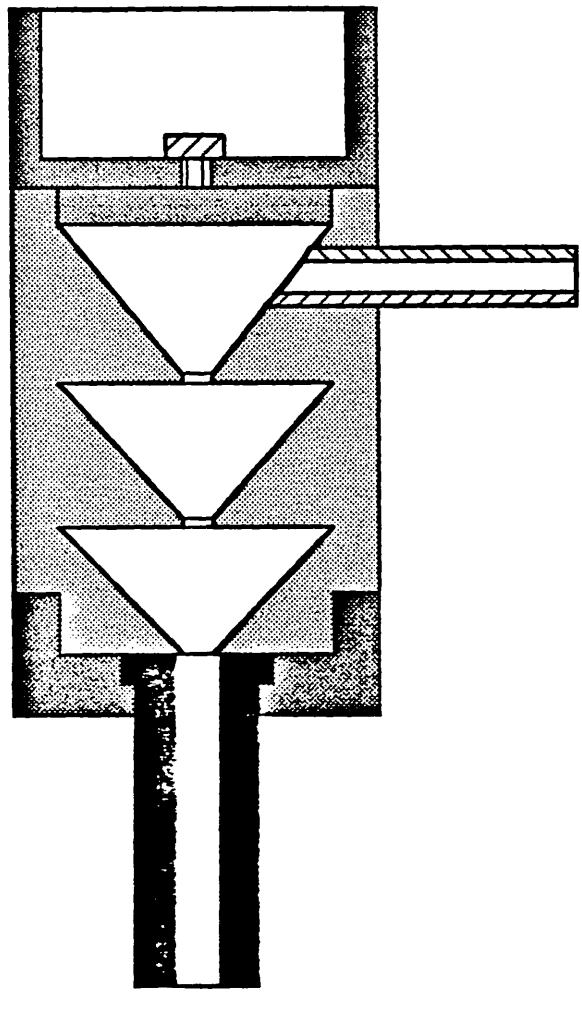


Fig. 7.2 3 cavities (mixing chambers) cutting head

7.5– Abrasive particles

The results shows that garnet particles are the most effective abrasive material to cut mild steel. Garnet mesh 50 and 80 produced the same cutting speed, however, there are other factors, other than mechanical properties of the cut materials, to be taken into consideration when selecting the type of abrasive, one of these factors is the wear of the focusing tube.

It has been shown earlier that garnet particles give the fastest cutting speed and produce the lowest wear rate of the focusing tube compared with alumina particles. The lowest wear in the focusing tube was recorded when flint particles are used, but flint gave slow cutting speeds compared with the rest of abrasive materials used, moreover flint contains silica in a free form which is a health hazard.

Alumina particles are as hard as garnet which has the same chemical composition and usually is considered as alumina but in its natural form. From the scanning electron microscope observation of alumina and garnet it was concluded that alumina particles have many more edges than garnet and that these edges are sharper and jagged whilst garnet particles are bulky with fewer edges. This explains the difference between the performance of the two types during cutting. Garnet cuts mild steel faster than alumina, but alumina wears the focusing tube faster than garnet. The large number of sharp and jagged edges of the alumina contributes to the increase of the wear of the focusing tube. The thin, long and irregular shape of the alumina particles render fracture and shattering of alumina on impact a more likely occurrence compared with garnet particles.

The impact of the jagged alumina particles on the work piece surface at 90 degrees, a multiple edge contact occurs in comparison with garnet particle impact in which single point contact is more likely to take place. This makes garnet faster than alumina in cutting mild steel (Fig. 7.4). Likewise, when the abrasive particles are flowing parallel to the focusing tube's inner wall, the alumina particles with its many and sharp edges predictably cause increase in wear (Fig. 7.3) compared with garnet.



Fig 7.3 Particles sliding inside the focusing tube

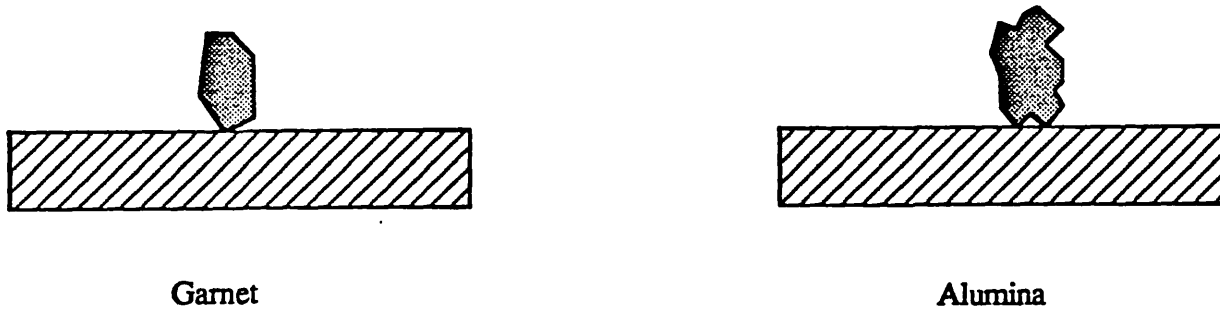


Fig. 7.4 Presentation of particles on impact with the specimen

The shape of the abrasive particles must be taken in consideration in any cutting operation, sharp edges cut ductile materials faster while round abrasive particles are more suitable for cutting brittle materials. These considerations are also applicable to the focusing tube material. One can predict that brittle ceramics (in this tests zirconia) last long enough as tungsten carbide tube when sharp abrasives are used, while tungsten carbide tubes are more suitable for round and spherical abrasive particles.

7.6– Material removal process

Tests show that very ductile materials are difficult to cut by any type of abrasive if the angle of attack is 90 degrees. In fact, it was impossible to cut a thin sheet of nickel (1 mm thick) with garnet or alumina abrasive at 90 degrees angle of attack and 2000 bar operating pressure. But the sheet was easily cut at 40 degrees angle of attack.

The mechanical properties of the cut materials dictate the operational parameters of the cutting which must be optimised for an efficient cutting process.
The tests confirm the theoretical analysis in that the abrasive particles have to be harder than the cut material for cutting to takeplace. Flint abrasive is ineffective to cut a piece of silceram or zirconia, a small marking was left on the zirconia which indicates small amount of material removal by erosion rather than cutting (ploughing) or fracturing (spoiling) of the material surface.

The combination of ductile cutting, intersection of surface fracture and micro-erosion of material are probably occurring simultaneously. However, one of these modes of material removal usually dominates the removal process and this largely depends on the mechanical properties of the cut material. The type, shape and angle of attack of the abrasive particles have no influence on what mode dominates the material removal process.

The efficiency of the cutting head can be maximised by adjusting the conditions for maximum material removal rate once the dominant mode of wear is known. For example, ductile material removal is dominated by cutting or ploughing which is

sensitive to particle shape and angle of attack. To increase the rate of removal of such materials, optimisation of those factors is essential.
Brittle materials are sensitive to particle strength and shape, strong particles do not easily fracture or shatter on impact with the cut material surface, bulky and round particles are more suitable for cutting brittle materials.

Water jet without an abrasive, in relative terms to abrasive water jet cutting, has a minor effect in erosion of material during abrasive water jet cutting process. However. increased water erosion can be stimulated by bubbles in the jet. The bubbles burst on the surface of the material and hence micro-erosion is increased in this way (Refs. 87, 88). Encouraging bubbles growth means increasing air entrainment which result in increasing jet expansion which is fundamentally against the idea of coherent jet for precision cutting.

Chapter 8

Conclusions and Proposals for Future Research

Cutting by abrasive water jet remains limited to special cutting and dismantling jobs where heat and flame cannot be allowed. Recently, as a result of the development of the abrasive water jet systems a wider range of cutting operations are carried out. A great deal of research is required to perfect the system and make it even more competitive with the conventional cutting methods.

A wide area of research is covered in this thesis and many of the results are inconclusive. The large number of parameters involved can be classified in to two distinguishable fields, a fluid mechanics related parameter and the cut material mechanics parameters.
The findings of the research which were presented and discussed in Chapter 5, Chapter 6 and Chapter 7 are listed here and recommendations and proposals for any future work to improve the overall cutting operation using abrasive water jets are also listed below.

8.1- Water jet expansion

a-Minimum air entrainment reduces the jet spread. However, air flow into the jet is unavoidable since abrasive feed is eased by allowing air to flow with the abrasive particles and stop any blockages of abrasive feed pipe. Further research is required to reduced air flow with the abrasive or alternatively to find other methods of introducing the abrasive particles to the water jet.

b-A sapphire orifice reduces the water surface turbulence but requires careful inspection of the mounting of the jewel in the rubber ring in which the jewel must be thicker than the rubber and the hole which must be smooth and free of any surface cracks before used to give the expected coherent water jet and minimal turbulence.

c-Filtering the supply water by a 0.2 μm filter size increases the working life of the sapphire orifice 10 times (from 2 hours to more than 20 hours)

d-Water flow rate of 3 kg/min.and pressure = 2000 bars are sufficient to perform a fast cutting operation after mixing with abrasive.

e-At 2000 bars the water jet speed is very high and the theoretical analysis predicts that if the particle penetrates the jet, it reaches the water speed instantaneously.

8.2- Cutting head

a-Cutting head with a conical mixing chamber of 10 mm length and 30 mm long focusing tube, can cut mild steel at a rate of 6.0 cm^3/min. (15 cm/min. of 16 mm thick plate) and maximum abrasive and water flow rate of 4.5 kg/min.

b-Cutting head efficiency can reach a maximum of 80 % at this flow rate of abrasive and water. To increase the efficiency further the mixing of abrasive material with the water jet has to improve

c-The width of cut is limited to 2.5 mm, but increases as the bore of the focusing tube increases

d-In tests when the tube bore equals 2 mm there was no cut kerfing.

e-More research on optimising air flow into mixing chamber is required. Tests indicate that there is a certain amount of air flow which produces minimum focusing tube wear and gives maximum cutting speed. For this reason optimisation of parameters such as air flow into the mixing chamber, speed of cut and focusing tube wear rate would be of interest.

8.3- Focusing tube

a-No serious cutting was performed without the focusing tube since it is believed that the abrasive particles mix and gain speed in the tube. The necessary length of the tube is found to be 30 mm for 0.25 mm orifice size and 2000 bar operating pressure. Larger lengths are found not have any improvements on the cutting speed and long

tubes can result in increasing the wear, hence, the cutting cost.

b-The tube material can be either tungsten carbide or hard ceramics as zirconia which give the wear rates similar to the tungsten carbide. But zirconia is much cheaper and faster to form to the required shapes in special dies.

c-The wear rate of tungsten carbide and zirconia tubes varies with types of abrasive materials. More wide ranging tests, using several of the more available abrasive materials, are required to find the wear rate of both materials, tungsten carbide and zirconia. Since some of the results indicate sharp abrasive particles cause tungsten carbide to wear faster than zirconia, similarly round particles wear zirconia faster than tungsten carbide.

8.4- Abrasive Materials

a-Garnet 50 and garnet 80 gave by far the fastest cutting speed and garnet particles also produced relatively low wear rate of the focusing tube. Cheap and low hardness abrasive such as flint produces less wear rate of the focusing tube but cutting speed of mild steel is slow compared with garnet. Flint is cheap compared with other abrasive materials, but using flint can be uneconomical because separation, safe handling and disposing of the abrasive is required after use, since flint contains free silica.

b-Sharp and hard abrasive materials increases wear rate of focusing tube such as alumina, while abrasive with fewer sharp edges with the same hardness such as garnet, causes less wear of the tube and at the same time cuts a mild steel plate faster.

c-The abrasive particles are not suitable for recycling. Microscopic examination of the used particles show that they are crushed to a very fine dust

Appendix I

Removal of brittle materials by impact (Refs. 71, 75)

To predict volume removal by studying the interaction of eroding particle and surface of the material.

Maximum depth x_m

$$F = - m_a \ddot{x} \quad \text{Equation of motion}$$

Hertz equation

$$F = x^{3/2} \gamma^{3} \; r^{1/2} \qquad (1)$$

where

$$\gamma = \left[\frac{3}{4} \left(\frac{1-\nu}{E} \right) \right]^{1/3}$$

after integration

$$\frac{1}{2} \left(x^2 - u^2 \right) = - \frac{3 r'^{\frac{1}{2}} x^{\frac{5}{2}}}{10\pi r^3 \rho_p \gamma^3}$$

at maximum indentation $x = 0$

$$x_m = \left(\frac{5\pi}{3} \right)^{\frac{2}{5}} \left(\rho_p \gamma^3 \right)^{\frac{2}{5}} \left(\frac{r^6}{r'} \right)^{\frac{1}{5}} \quad u^{\frac{4}{5}} \qquad (2)$$

Initial fracture due to particle impact

when spherical indenter is pressed against a plane elastic surface, then

$$\sigma_a = \frac{1- 2\nu}{2\pi} \frac{F}{a^2} \qquad (3)$$

at distance R greater than a (Fig. 2.7)

$$\sigma_R = \sigma_a \left(\frac{a}{R} \right)^2$$

Initial fracture occurs when when the maximum tensile stress reaches a value equal to the tensile strength of the material corresponding to the size and stress distribution in the region exposed to tensile stress.

According to weibull's theory (Ref. 89), the mean fracture strength of a material with a volume distribution of flaws is given by;

$$\sigma_f = \sigma_u + \int_{\sigma_u}^{\infty} s \, d\sigma$$

$$s = e^{-B}$$

$$B = \int_{vol.} \left(\frac{\sigma - \sigma_u}{\sigma_0}\right)^m d(vol.)$$

$h_s = k_1 x$

then

$d(vol.) = 2\pi k_1 x R \, dR$

the depth may be eliminated from this expression by noting that when a surface intersects a sphere of radius r' as in (Fig. 2.7) then $a^2 \approx 2 r' x$

if

$$\frac{x}{r'} \ll 1 \text{ then}$$

$$d(vol.) = \frac{k_1 a^2 \pi R \, dR}{r'}$$

the risk of rupture becomes

$$B = \int_a^{Ru} \left(\frac{\frac{\sigma_a a^2}{R^2} - \sigma_u}{\sigma_0}\right)^m \frac{a^2 \pi}{r'} k_1 R \, dR$$

σ_u may be expressed as

$$\sigma_u = \sigma_u' \frac{a^2}{R^2}$$

where σ'_u is the maximum zero stress at R = a

then

$$B = \frac{k_1 \pi a^{2m+2}}{r'} \left(\frac{\sigma_a - \sigma'_u}{\sigma_0}\right)^m \int_a^{Ru} R^{1-2m} \, dR$$

which gives

$$B = \frac{k_1 \pi a^4}{2r`(m-1)} \left(\frac{\sigma_a - \sigma`_u}{\sigma_0}\right)^m \left[1 - \left(\frac{\sigma_u}{\sigma_a}\right)^{m-1}\right]$$

using the fracture stress in bending, a relation may be obtained by equating the risk of rupture, for the hertzian stress state, to that for a pure bending stress state

where

$$B = \left[\frac{v_b}{2(m+1)\sigma_0^m}\right]\left[\frac{(\sigma_b - \sigma_u)^{m+1}}{\sigma_b}\right]$$

putting B=0 and σ_u=0 and approximating a^2=2r`x and replacing σ_a by S_H gives

$$S_H = k_2 (r\, x^2)^{\frac{-1}{m}} \qquad (4)$$

where

$$k_2 = \sigma_b V_b^{\frac{1}{m}} \left[\frac{m-1}{4\pi(m+1)k_1}\right]^{\frac{1}{m}}$$

At the time of failure, the fracture strength given by equation 4 must equal the maximum induced contact stress given by equation (3). Equating 3 and 4 and using (1) to eliminate F gives the following relation between the indentation depth at the time of initial cracking and the particle contact radius r`

$$r` = \left(\frac{k_3}{\gamma^3 k_2}\right)^{\frac{2m}{m-2}} x^{\frac{m+2}{m-2}} \qquad (5)$$

where

$$k_3 = \frac{1-2\nu}{4\pi}$$

Damage after initial cracking for a ball

Replacing r` by r^* in (5)

$$r` = \left(\frac{k_3}{\gamma^3 k_2}\right)^{\frac{2m}{m-2}} x_m^{\frac{m+4}{m-2}} \qquad (6)$$

to examine the validity of (6) experimental measures were taken for r^* and using $a^{*2} = 2r^* x_m$ in (6)

$$a^* = \sqrt{2}\left(\frac{k_3}{\gamma^3 k_2}\right)^{\frac{m}{m-2}} x_m^{\frac{m+1}{m-2}} \qquad (7)$$

the maximum indentation depth in static tests could be estimated from the Hertz equation (1) thus (7) may be written as

$$a^* = \left(\frac{k_3}{k_2}\right)^{\frac{m}{m-2}} \frac{\sqrt{2}\, F^{\frac{2(m+1)}{3(m-2)}}}{\gamma r`^{\frac{m+1}{3(m-1)}}}$$

Tests using 1/8 inch diameter steel ball and a glass surface for which m=8 in bending and approximating k_1 with unity gives $a^* = 1.24 \times 10^{-4} F^{0.99}$

Volume removed by an impacted particle

the volume removed per particle, $d(Vol)_p$, will be taken as proportional to $\pi a^{*2} x_m/2$, the volume of the spherical cap defined by r^*, a^*, and x_m thus;

$$W = c_2 \frac{\pi}{2} a^{*2} x_m \qquad (8)$$

the value of c_2 should be of the order of unity and may be estimated from measurements of volume removal per particle in erosion tests and calculations of a^* and x_m

For angular particles

$r`$ is probably independent of r and can be denoted as a constant quantity. Then for angular particles

$$W = k_5 r^{a`} V^b \qquad (9)$$

where

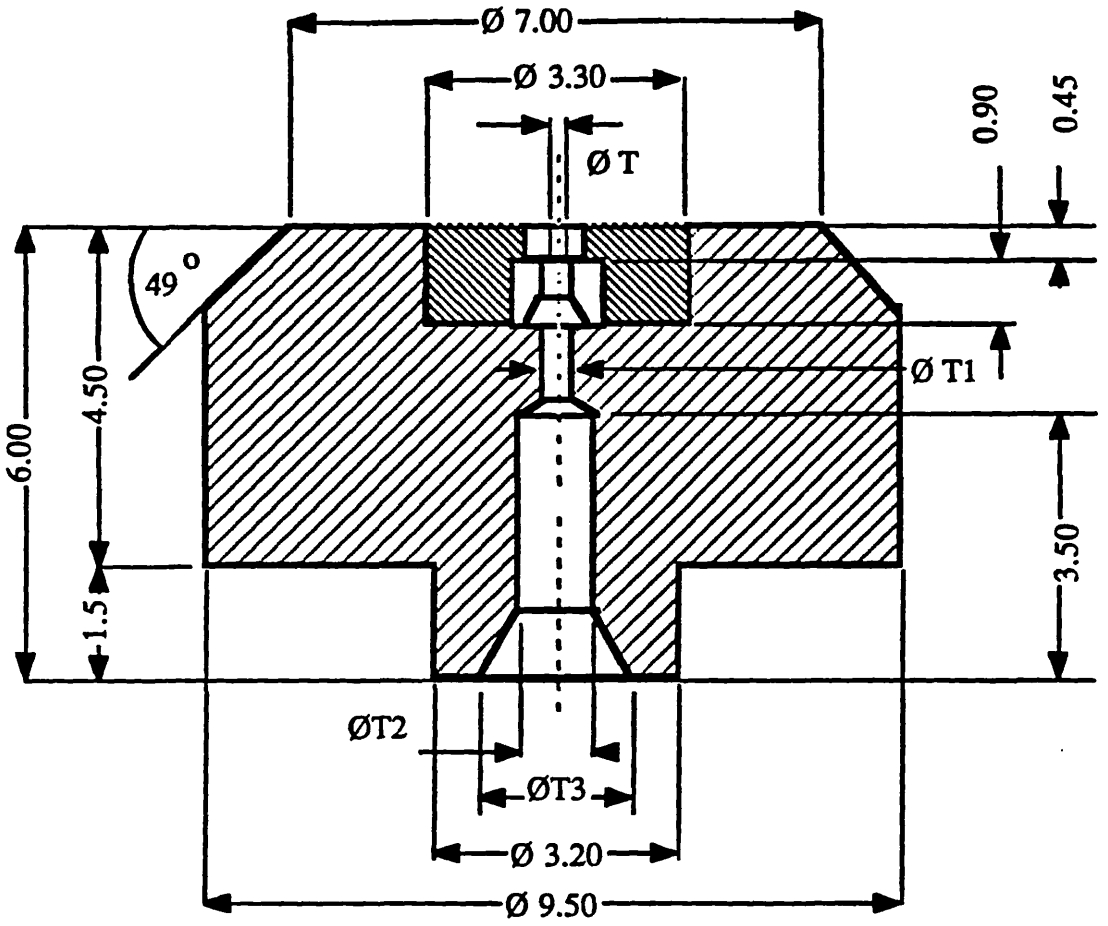
$$k_5 = \frac{k_4}{\frac{0.6m}{r`^{m-2}}} \quad , \quad a` = \frac{3.6m}{m-2} \quad , \quad b = \frac{2.4m}{m-2}$$

and

$$k_4 = c_2 \pi \left(\frac{k_3}{k_2}\right)^{\frac{2m}{m-2}} \left(\frac{5\pi}{3}\right)^{\frac{1.2m}{m-2}} \left(\frac{\rho_p}{\gamma^2}\right)^{\frac{1.2m}{m-2}}$$

Appendix II

1-Sapphire orifice (Fig. 1)



Ø T	ØT1	ØT2	ØT3
.0.08	0.40	1.00	2.00
0.10			
0.12			
0.13			
0.15			
0.17			
0.18			
0.20			
0.25	1.00	2.00	2.40

All dimensions are in mm

Fig. 1 Sapphire orifice in a steel holder

2- X–Y table and control equipment

It is essential that the feed rate of work piece is accurately controlled, hence X–Y table is built, the table is mounted on a metal frame about one metre high from the ground level. Feeding the X- direction and the same time the Y- direction curved shapes cuts are produced. The X and Y- directions movements may also be controlled by a Microprocessor which make cutting curves an easier task.

The table is made of two aluminium plates with holes and slots drilled in the plates to allow the jet to pass through during the cutting operation. The X- direction (upper plate) stroke is 300 mm and the Y- direction (lower plate) is 400 mm, 4 micro-switches (2 for each table) are used to reverse the the tables movements at the end of strokes. The plates are guided by precision 8 linear motion wheels (4 for each table) and track system (Fig. 2). The tables system is mounted on a metal frame over a water collection tank ($1m^3$ capacity) to collect the jet after the cutting operation.

The tables are driven by two small stepping motors (90 mm length x 55 mm diameter) fixed under the tables. The motors drive ballscrews fixed to the plates, the ballscrews and the track-wheel system reduces surfaces friction and results in a smooth table feed. The ballscrews are protected from the outside environment by rubber bellows hence require minimum service. The motors are linked to the screws via two flexible coupling, the flexible couplings eliminate any misalignment between the ballscrew profile and the edge of the tracks hence reduces the resistance to the table feed force.

The number of electrical pulses can be controlled, the speed of the motors can be varied and hence the speed of the two tables. The ballscrews are of 5 mm pitch i.e. the table travels 5 mm each revolution of the motor/screw. A frequency counter is used to measure the number of motor input pulses. The selected motor types require a 200 pulses for each shaft revolution.

The number of pulses which directly read by a frequency count, are used to indicate the traverse speed of the tables as follow;

$$\text{Speed of table} = \frac{\text{number of pulses x pitch of screw}}{\text{number of pulses required for one revolution}}$$

The motors are capable of transmitting a torque of 1.27 N.m and a variable speed up to maximum speed of 4,500 rpm (i.e. 0.375 m/sec linear speed).

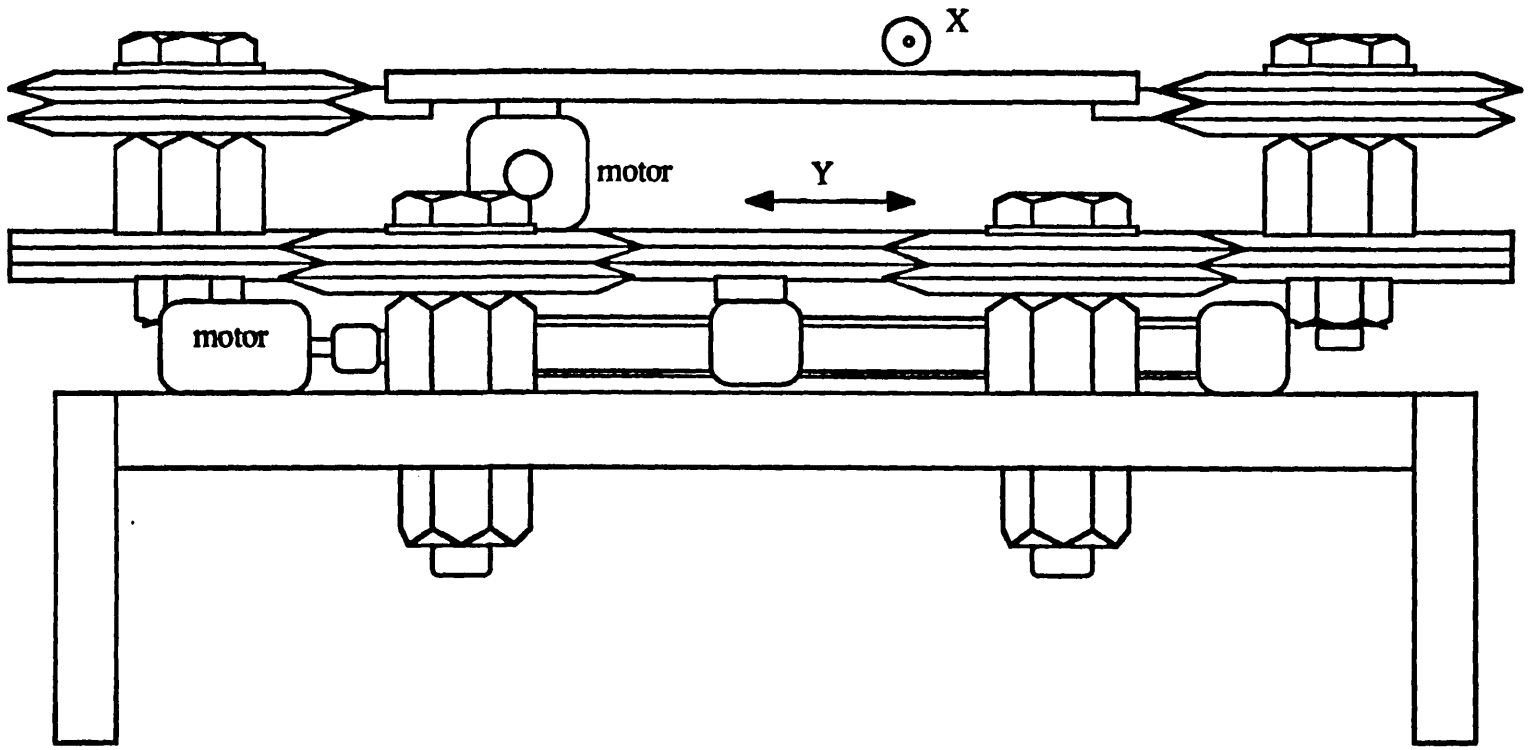


Fig. 2 X-Y table

3-Parts of drive unit

Part & Type	Number Required
Stepping Motor (21-2235 D200 F037)	2
Transformer (T 0119)	1
Rack (SR20)	1
Bipolar stepper drive (SD3)	2
Blank front panel (FB5)	4

4-Stepping motor drive board (Figs. 3, 4)

This board provides drive pulses to the stepping motor output card SD3. Two boards are provided to give independent drives to X & Y coordinate motors.
The card has provision for switching from an internally derived clock source and direction control to an external drive which can be an I/O buss of a microprocessor system.

On internal control, the condition of a microswitch connected as a limit switch on each end of the motor traverse is sensed. When the microswitch is activated by a mechanical sensor at end of travel, the motor direction is changed and the mechanical assembly ramps in the opposite direction until a second microswitch is activated, again changing motor direction.

After sensing the microswitch, the frequency of the clock pulses is ramped down and steps for short period of time until the motor has changed direction; the clock pulses then ramp up to the set operating rate again clock is varied from a front panel fine variable control, a coarse range switch over the range 100 - 1000 steps/sec. in two

ranges. the front panel fine control has a switch incorporated inhibiting clock pulses and hence stopping the motor.

Under microprocessor control the card interfaces to an I/O bus. Four active levels are required for each card so that only one 8 bit I/O buss is required.

The I/O signal are:

Input to card	I/O_0 (I/O_2)	–Microprocessor generated clock pulses
	I/O_1 (I/O_3)	–Direction control level
	I/O_4 (I/O_6)	–Sensing output to microprocessor
	I/O_5 (I/O_7)	–Requesting change of direction

All connections to the limit switch and I/O bus are available from screw terminals at the rear of the rack.

5-Terminal connections

	X		Y	
Clock pulse	7	I/O_0	7	I/O_2
Direction level	8	I/O_1	8	I/O_3
Direction Change 1	9	I/O_4	9	I/O_6
Direction Change 2	10	I/O_5	10	I/O_7
Microswitch 1	3	N.C	3	N.C
	6	N.O	6	N.O
Microswitch 2	4	N.C	4	N.C
	5	N.O	5	N.O
Common 0v	1, 2		1, 2	

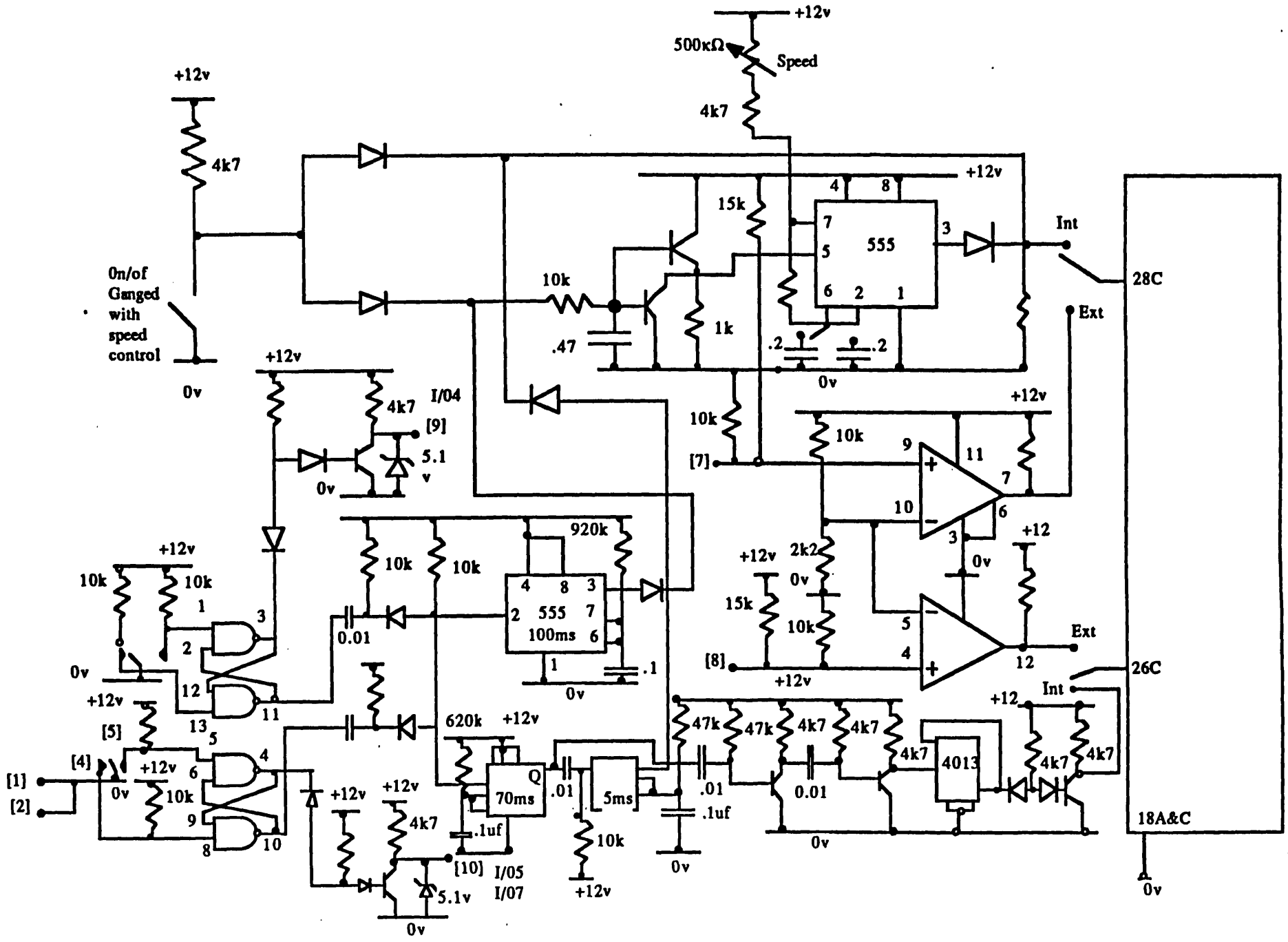


Fig. 3 Motor drive unit

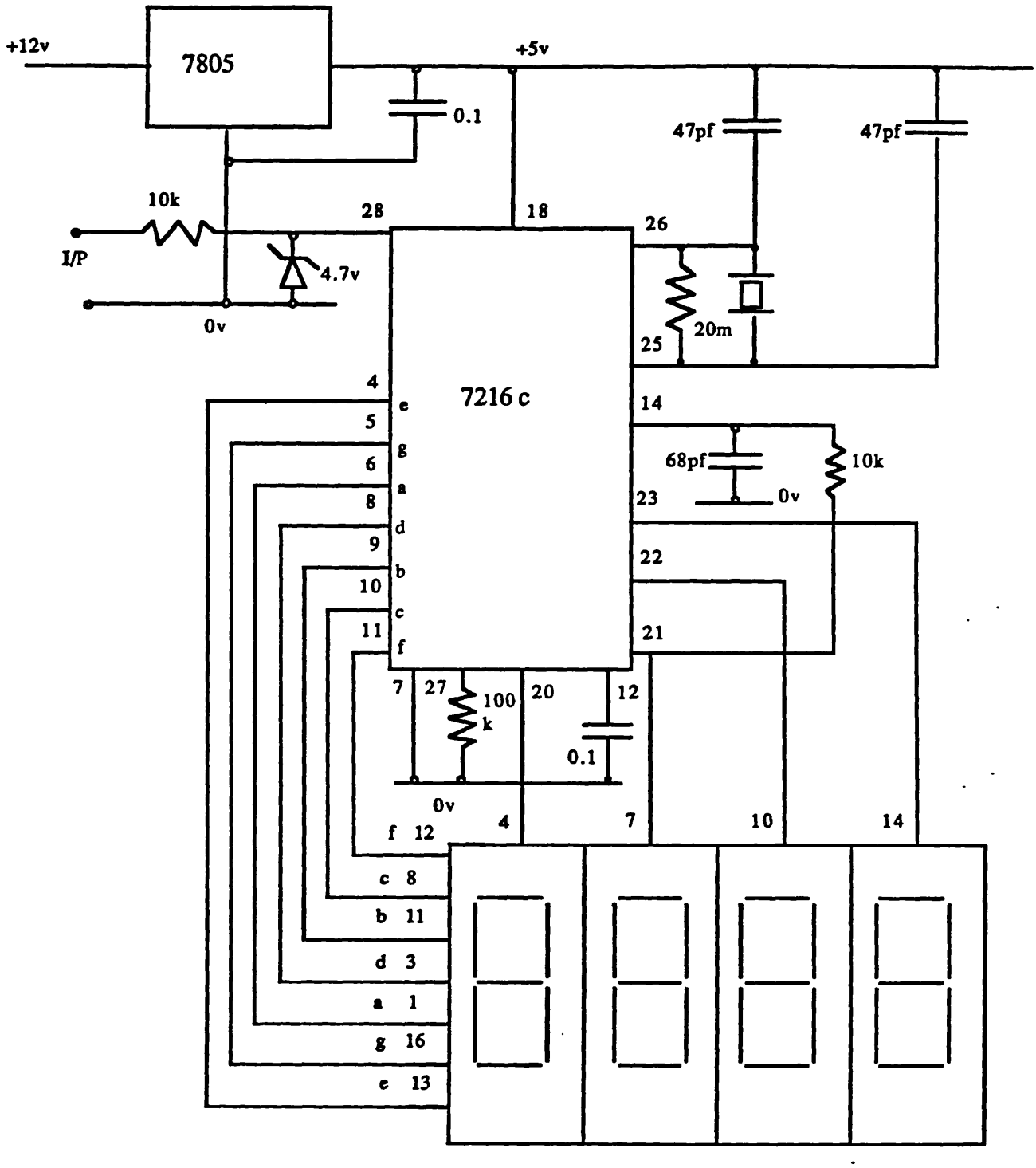


Fig. 4 Frequency counter 1-9999 pps

6- Nozzle clamp

Since parameters such as standoff distance and angle of attack are variable, these can influence the cutting operation, these parameters have to be changed for some tests. A clamp suitable for this purpose has been made, the clamp consist of 4 parts;

Part I (Fig. 5a).

A 100 X 135 mm mild steel plate slotted at equal distance from the plate centre line. This plate is bolted to a cross beam above the table. The slots allow for 70 mm vertical movement of the plate and the attached clamp units and also the cutting head.

Part II (Fig. 5b)

A circular disc 50 mm diameter and 20 mm thick, small holes drilled and tapped in the side of the two opposing quarters of the disc at angles 0, 10, 20, 30, and 40 degrees from the horizontal line. The disc is fitted to part I by two screws through the other two quarters of the disc.

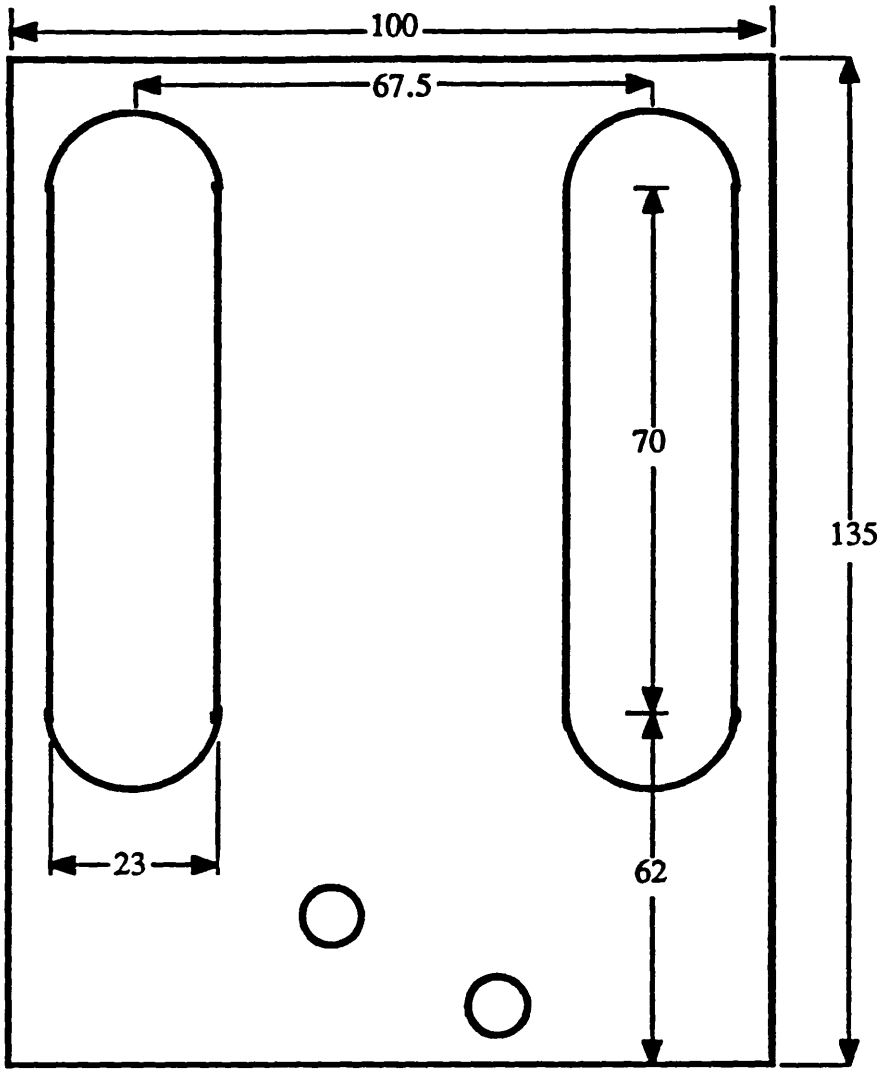
Part III (Fig. 5c)

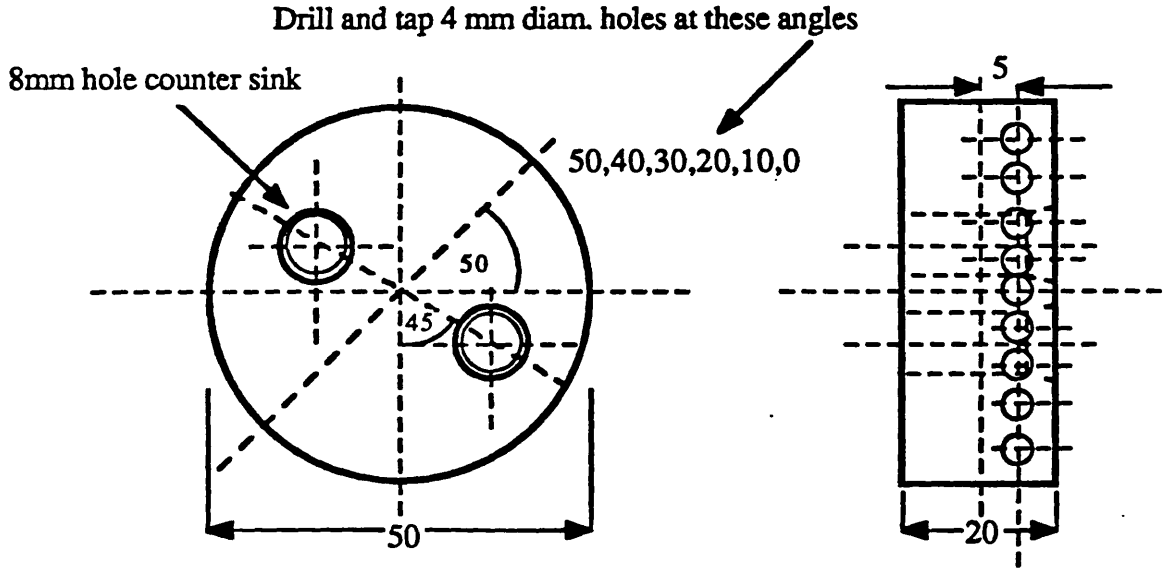
Rotating bracket, fitted on the circular disc. The bracket rotation angle correspond to the circular disc holes angle. A further 24 mm vertical adjustment is added as a result of having 5 screw holes alongside the bracket.

Part IV (Fig. 5d)

Nozzle bracket, fitted to the rotating bracket (III). Part III and part IV are used to catch the cutting head, then the cutting head can be rotated and adjusted to the desired angle by rotating part III around the circular disc part II.

Fig. 5a Part I





All dimensions are in mm

Fig. 5b Part II

All dimensions are in mm

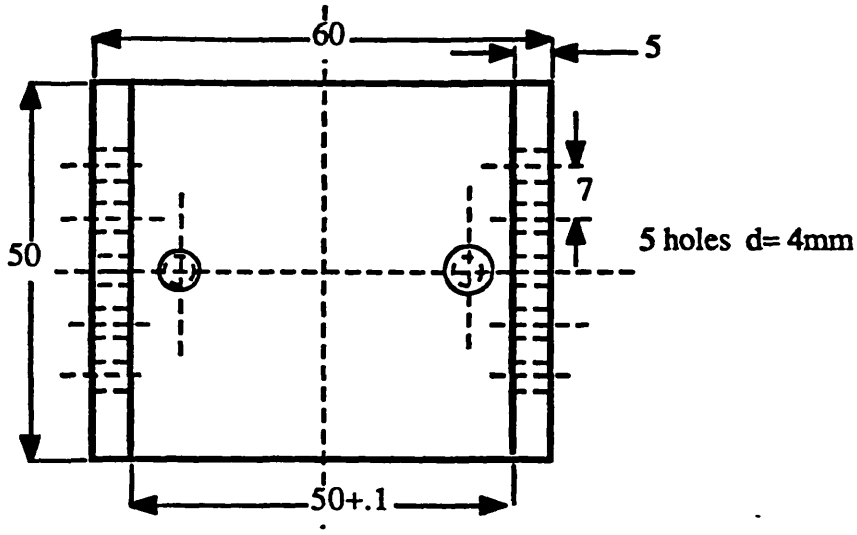
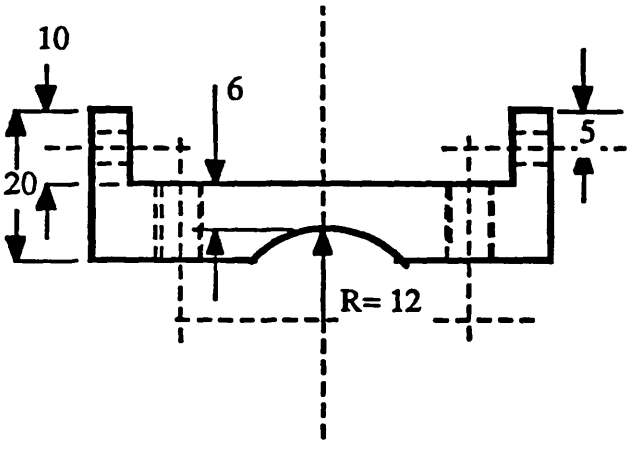


Fig. 5c Part III



All dimensions are in mm

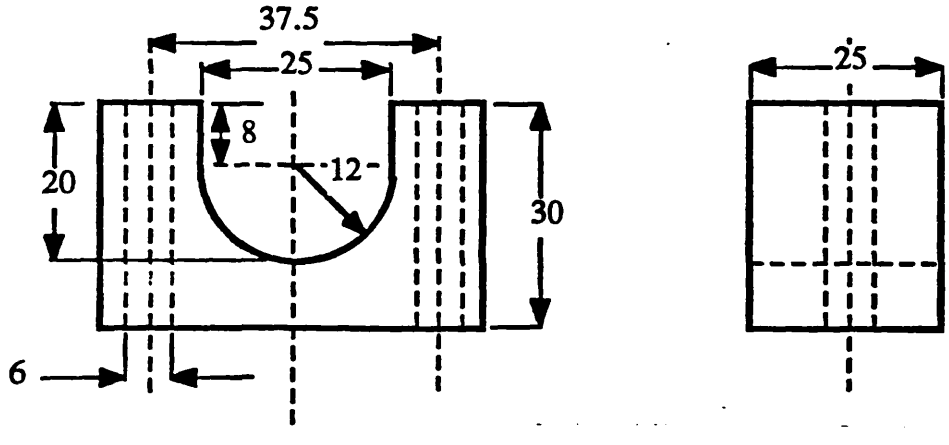


Fig. 5d Part IV

7- Abrasive hopper (Fig. 6)

Abrasive hopper made of 1 mm thick metal sheet capable of volume capacity of 0.75 m^3 of abrasive materials. The hopper is mounted on a steel frame.

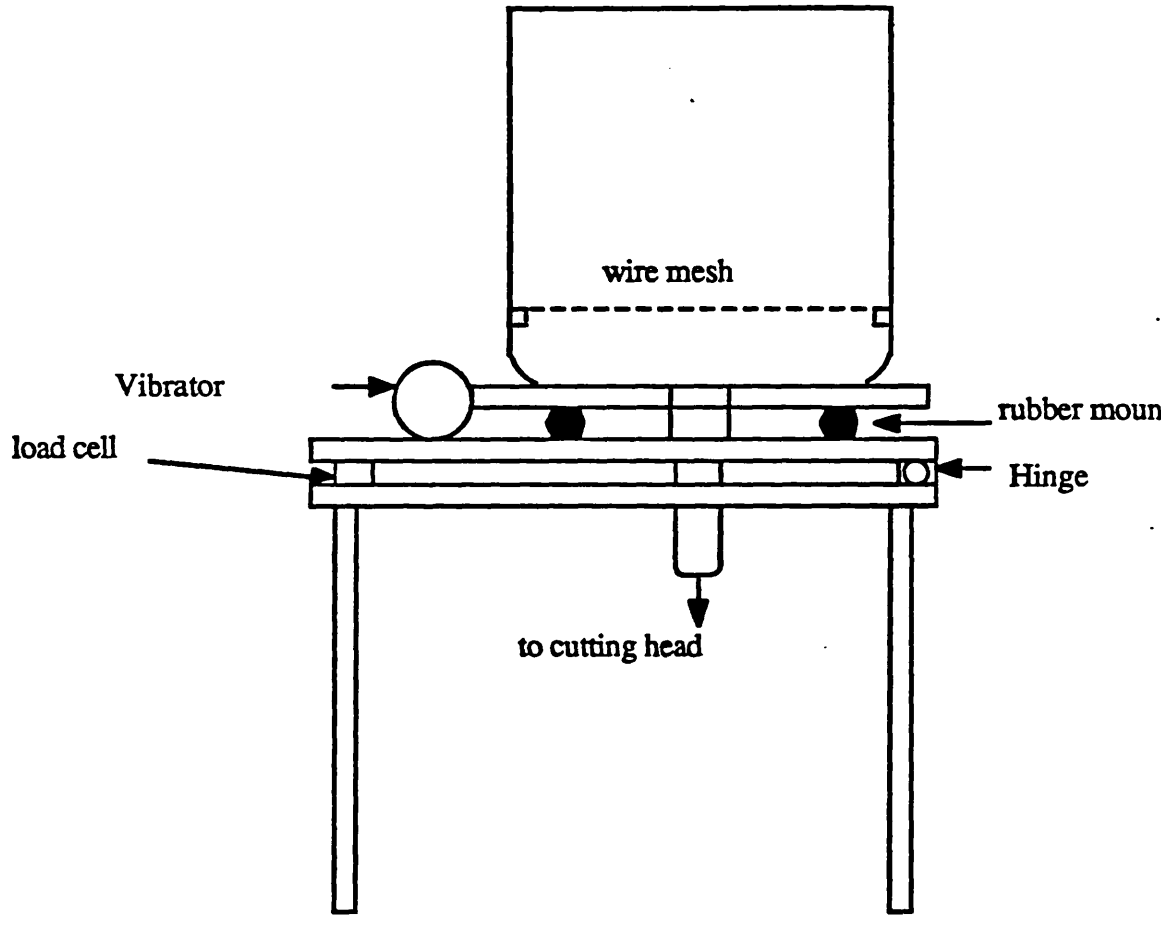


Fig. 6 Abrasive hopper

REFERENCES

1- B. V. Voitsekhovskii , V. P. Nikolaev, V. M. Ludin , O. F. Maier and G. P. Chermenskii.
Some results of breaking up rock with an impulse jet monitor (in Russian)
Izv. Sib. otd. Akad. nauk SSR, no.2, 1963, p. 7-11.

2- I. W. Farmer and P. B. Attewell
Experiments with water as adynamic pressure medium.
Mine & Quarry Engng., Vol. 25, Dec. 1963, p. 524-530

3- E. L. Bryan.
Steel and Coal 1962, 185, (4913), 530.

4- S . J . Leach ; G . L . Walker .
Some aspects of rock cutting by high speed water jets .
Royal soc. London, Phil. Trans. Ser. A, Vol. 260 , no 1110, Jul. 1966, pp 295-308

5 - B . V . Voitsekhovsky, E . B . Solovkin, O . I . Grebennik, V . A . Kuvshinov, G . Ya. Shoikhet, V. P . Nikolaev, N . P . Lesic.
On destruction of rocks and metals by high pressure jets of water
In. proc. 1st Int. Symp. on Jet cutting Technol. (Cranfield U.K : Apr. 5-7, 1972),Cranfield, U.K, BHRA Fluid Engng., 1972, Paper G8-93 .

6- B . Crossland; J . G . Logan
Development of equipment for jet cutting
In. proc. 1st Int. Symp. on Jet Cutting Technol. (Cranfield U.K: Apr. 5-7, 1972), Cranfield, U.K., BHRA Fluid Engng., 1972, Paper C1, 12P .

7- U . H . Mohaupt ; D . J . Burns .
Machining with continuous fluid jets at pressure of 2 to 7 kbar .
In. Proc. 1st Int. Symp. on Jet cutting Technol. (Cranfield U.K: Apr. 5-7, 1972) , Cranfield, U.K, BHRA Fluid Engng.,1972, Paper G4, P. G4, 37 - G4, 48 .

8- H . D . Harris ; W . H . Brierley
Application of water jet cutting
In. Proc. 1st Int. Symp. on Jet cutting Technol. (Cranfield U.K : Apr. 5-7, 1972)
Cranfield U.K , BHRA Fluid Engng., 1972, Paper G1, P. G1 ,1-G1, 12 .

9- M. J. McCarthy and N. A. Molloy
Review of stability of liquid jets and the influence of nozzle design.
The Chem. Eng. Journal, 7, 1974, p. 1-20.

10- P . D . Lohn and D . A . Brent
Nozzle design for improved water jet cutting
In. Proc. 3rd Int. symp. on Jet cutting Technol. (Chicago , U.S.A. May 11-13 , 1976), Cranfield , U.K. , BHRA Fluid Engng. ,1976 , P. A3 , 33-A3 , 46

11- K . Yanaida and A . Ohashi
Flow characteristics of water jets in air
In. Proc. 5th Int. Symp. on jet cutting Technol. (Hanover , FRG . June 2-4 ,1980) Cranfield , U.K. , BHRA Fluid Engng. ,1980 , P 33 -44 .

12- R . S . Amano and K . F . Neusen .
A numerical and experimental investigation of high-velocity jets impinging on a flat plate.
In. Proc. 6th Int. Symp. on Jet Cutting Technol. (Guildford, England ,Apr. 6-8, 1982), Cranfied , U.K , BHRA Fluid Engng ,1982 , P 107 - 122 .

13- W . Konig and CH. Wulf
The influence of the cutting parameters on jet forces and the geometry of the kerf
In. Proc. 7th Int. Symp. on Jet Cutting Technol. (Ottawa , Canada , June 26 -28, 1984), Cranfield , U.K , BHRA Fluid Engng , 1984 , P 179 - 191 .

14- R. S. Amano and V. S. Kodali.
A numerical study of turbulent plane jet flowing into a dead-end passage.
In. Proc. 7th Int. Symp. on Jet Cutting Technol. (Ottawa, Canada , June 26 -28, 1984), Cranfield, U.K, BHRA Fluid Engng , 1984 , Paper P6, P. 537 .

15- K. Przyklenk and M. Schlatter.
Simulation of the cutting process in water jetting with the finite element method.
In. Proc. 8th Int. Symp. on Jet Cutting Technol. (Durham, England, 9-11 Sept., 1986), Cranfield, U.K, BHRA Fluid Engng, 1986, P. 125-136 .

16- E. Gelfort, J. Mischke, C. Boltze, H. Haferkamp and W. Schikorr.
Application of jet-cutting on spent fuel elements of nuclear power plants.
In. Proc. 7th Int. Symp. on Jet Cutting Technol. (Ottawa, Canada, June 26 -28, 1984), Cranfield, U.K, BHRA Fluid Engng , 1984 , P 135-152.

17- E. Gelfort, J. Mischke, C. Boltze, H. Blickwedel, H. Haferkamp.
Submerge cutting of nuclear fuel element by high speed water jets.
In. Proc. 8th Int. Symp. on Jet Cutting Technol. (Durham, England, 9-11 Sept., 1986), Cranfield, U.K, BHRA Fluid Engng, 1986, P. 315-322.

18- T . J . Labus
Energy requirements for rock penetration by water jets
In. Proc. 3rd Int. Symp. on Jet cutting Technol. , (Chicago , U.S.A , May 11-13, 1976), Cranfield , U.K , BHRA Fluid Engng. , 1976 , P. E3 , 29- E3 , 40 .

19- M . Mazurkiewicz , Z . Sebastian and G . Galecki
Analysis of the mechanism of interaction between high-pressure water jet and the material being cut .
In. Proc. 4th Int. Symp. on Jet Cutting Technol.,(Canterbury U.K , Apr. 12-14, 1978) Vol.2 Cranfield , U.K , BHRA Fluid Engng. , 1979 , Paper F3 , P . F3 ,31 -F3 , 36 .

20- J. W. Callahan
Abrasive jet deburring
Dearborn, U.S.A., Soc. Manuf. Engrs., 1976, P 14.

21- J. D. Tighe.
A comparison of coventional and airless abrasive blasting techniques.
(1) In. North sea corrosion- What we have learnt, (Paper presented Edinburgh, U.K. : 23-25 Oct. 1978), London U.K., Inst. Mar. Engrs. 1978, Paper C3.
(2) Trans. Inst. Mar. Engrs. (C), Vol. 91, Conf. no. 1, 1979, Paper C3, P. 19 -23.

22- Hodge Clemco Ltd. U.K.
Trends in abrasive blast cleaning.
Anticorros. Method & mater., vol. 27, no. 7, Jul. 1980, P. 5-7.

23- Maasberg , W . , et al .
Sand blasting apparatus .
U.S. Patent 3,424,386 January 28 , 1976 .

24- Watson , J . D .
Fluid-abrasive nozzle device .
U.S. Patent 4,080,762 March 28 , 1978 .

25- Hart , B. E.
Guns for forming jets of particulate material .
U.S. Patent 3,972,150 August 3 , 1976 .

26- Easton , N.
Wet abrasion blasting .
U.S. Patent 4,125,969 November 21 , 1978 .

27- M . Hashish
Steel cutting with abrasive water jets
In. Proc. 6th Int. Symp. on Jet Cutting Technol., (Guildford , U.K. Apr. 6-8 , 1982) , Cranfield U.K. , BHRA Fluid Engng. , Paper K3 , P.P. 465-487 .

28- M. M. Lyashchukov and A. O. Gerasimova.
A hydroabrasive jet mashine for working the channels of centrifugal pump rotors and stators.
Chem. & Pet. Engng., vol. 15, no. 11-12, Jul. 1980, P. 944- 945.

29- V. N. Morozenko, A. E. Provolotskii, I. M. Nesterenko, V. S. Grishin.
Hydroabrasive cleaning process of vulcanizing molds.
Chem. & Pet. Engng., Vol. 9, no. 11-12, Jan.- Feb. 1973, P. 144- 145. (Transl. from Russian: Khin. i Neft. Machinostroenie no. 2 Feb. 1973, P. 26).

30- A. N. McKelvie
Water/abrasive blasting for preparation of surfaces before painting.
(1) In: North Sea Corrosion-What we have learnt, (Papers presented Edinburgh, U.K.; 23-25 Oct. 1978), London, U.K., Inst. Mar. Engrs., 1978, Paper C2.
(2) Trans. Inst. Mar. Engr. (c), Vol. 91, Conf. no 1, 1979 Paper C2, P. 10-18.

31- Development of "Ishiclean" a new technology for descaling hot strip coil.
Technocrat, Vol. 12, no. 1, Jan. 1979, P. 59.

32- M. Hashish
The application of abrasive jets to concrete cutting
In. Proc. 6th Int. Symp. on Jet Cutting Technol., (Guildford , U.K. Apr. 6-8 , 1982) , Cranfield U.K. , BHRA Fluid Engng. , 1982, Paper K2, P. 447.

33- M. Hashish
On the modeling of abrasive-water jet cutting
In. Proc. 7th Int. Symp. on Jet Cutting Technol. (Ottawa, Canada, June 26 -28, 1984), Cranfield, U.K, BHRA Fluid Engng , 1984, Paper E1, P. 249 .

34- M. Hashish
Aspects of abrasive-water jet performance optimization
In. Proc. 8th Int. Symp. on Jet Cutting Technol. (Durham, England, 9-11 Sept., 1986), Cranfield, U.K, BHRA Fluid Engng, 1986, P. 297.

35- D. H. Saunders
A safe method of cutting steel and rock in hazardous atmospheres
In. Proc. 6th Int. Symp. on Jet Cutting Technol., (Guildford, U.K. Apr. 6-8 , 1982), Cranfield U.K. , BHRA Fluid Engng., 1982, Paper K5, P. 503- 518.

36- R. E. P. Barton and D. H. Saunders
Water/abrasive jet cutting of concrete and reinforced concrete
In. Proc. 6th Int. Symp. on Jet Cutting Technol., (Guildford, U.K. Apr. 6-8 , 1982), Cranfield U.K., BHRA Fluid Engng., 1982, Paper K4, P. 489-502.

37- D. H. Saunders
Water/abrasive cutting of slate
Report no. 1677 BHRA Fluid Engineering Cranfield (March 1981)

38- D. H. Saunders, N. J. Griffiths and K. Moodie
Water abrasive cutting in flammable atmospheres
RR 1608, BHRA Fluid Engineering, Cranfield (June 1980)

39- Gene G. Yie
Cutting hard materials with abrasive-entrained water jet
In. Proc. 7th Int. Symp. on Jet Cutting Technol. (Ottawa, Canada, June 26 -28, 1984), Cranfield, U.K, BHRA Fluid Engng., 1984 , Paper P1, P 481.

40- R. M. Fairhurst, R. A. Heron, and D. H. Saunders.
DIAJET- A new abrasive water jet cutting technique
In. Proc. 8th Int. Symp. on Jet Cutting Technol. (Durham, England, 9-11 Sept., 1986), Cranfield, U.K, BHRA Fluid Engng, 1986, Paper 40, P. 395.

41- M. Hashish
Critical and optimum traverse rates in jet cutting
In. Proc. of the first U.S. water jet Smposium, Golden, Colorado, Colorado School of Mines. April 7-9, 1981.

42- M. Nakaya, et al.
Concrete cutting with abrasive water jet
In. Proc. 7th Int. Symp. on Jet Cutting Technol. (Ottawa, Canada , June 26 -28, 1984), Cranfield, U.K, BHRA Fluid Engng , 1984 , Paper E3, P 281.

43- M. Hashish
A modeling study of metal cutting with abrasive-water jets
ASME Transactions, Journal of Engineering Material and Technology, January 1984, P. 88-100.

44- D. K. M. Tan
A model for the surface finish in abrasive water jet cutting.
In. Proc. 8th Int. Symp. on Jet Cutting Technol. (Durham, England, 9-11 Sept., 1986), Cranfield, U.K, BHRA Fluid Engng, 1986, Paper 31, P. 309.

45- M. Mellor
Some general relationships for idealized jet cutting
In. Proc. 1st Int. Symp. on Jet cutting Technol. (Cranfield U.K : Apr. 5-7, 1972), Cranfield, U.K , BHRA Fluid Engng.,1972, Paper A2, P. A2-25.

46- M. Hashish
Experimental studies of cutting with abrasive water jets
Proceedings of the 2nd U.S. Water Jet Symposium, Rolla, Missouri, 1983, P. 379.

47- R. Wellinger
Z. Metallk., 40 (1949) 361

48- I. Finnie
The mechanism of erosion of ductile metals
Proceedings of the 3rd National Congress of Applied Mechanics, ASME, 1958, P. 527-532.

49- I. Finnie
Erosion of surfaces by solid particles
Wear, Vol. 3, 1960, P. 87-103

50- I. Finnie
Erosion by solid particles in a fluid stream
Erosion and cavitation ASTM STP 307, 1962, P. 70-82.

51- J. G. Bitter
A study of erosion phenomena.
Part I, Wear, 6 (1963) 5-21, and Part II 169-190

52- P. A. Engle.
Impact wear of materials
Elsevier Scientific Publishing Company, Amsterdam 1976, 333 PP (see chapters 4 and 5).

53- C. Preece, Ed.
Treatise on materials science and technology.
Erosion, vol. 16, Academic press, New York, 1979, P. 69-126.

54- I. Finnie, and D. H. Mcfadden.
On the velocity dependence of the erosion of ductile metals by solid particles at low angles of incidence.
Wear, Vol. 48, 1978, P. 181-190.

55- J. H. Neilson, and A. Gilchrist
Erosion by a stream of solid particles
Wear, Vol. 11, 1968, P. 111-122.

56- G. P. Tilly
A two stage mechanism of ductile erosion
Wear, Vol. 23, 1973, P. 87-96.

57- J. Maji, and G. L. Sheldon
Mechanisms of erosion of a ductile material by solid particle
Erosion : Prevention and useful applications (W. F. Adler, Ed.), ASTM STP 664, 1979, P. 136-147.

58- L. K. Ives and A. W. Ruff.
Electron microscopy study of erosion damage in copper.
Erosion: Prevention and useful applications (W. F. Adler, Ed.), ASTM STP 664, 1979, P.5-35

59- R. E. Winter, and I. M. Hutchings
Solid particle erosion studies using single angular particle.
Wear, Vol. 29, 1974, P. 181-194.

60- R. E. Winter, and I. M. Hutchings.
The role of adiabatic shear on solid particle erosion.
Wear, Vol. 34, 1975, P. 141-148.

61- I. M. Hutchings
Deformation of metal surface by the oblique impact of square plate.
International Journal of Mechanical Science. Vol. 19, Pergamon Press, NewYork, 1977, P. 45-52.

62- I. M. Hutchings
Mechanism of the erosion of metals by solid particles.
Erosion: Prevention and useful application (W. F. Adler, Ed.) ASTM STP 664, 1979, P. 59-76.

63- G. L. Sheldon, and A. Kanhere
An investigation of impingement erosion using single particles
Wear, Vol. 21, 1972, P. 195-209.

64- I. Finnie, J. Wolak, and Y. Kabil.
Erosion of metals by solid particles
Journal of Materials, Vol. 2, no. 3, September 1967, P. 682-700

65- G. L. Sheldon.
Effect of surface hardness and other materials properties on erosive wear of metals by solid particles.
ASME Journal of Engineering Materials and Technology, Vol. 99 Apr. 1977, P 133-137.

66- P. Ascarelli
Relation between the erosion by solid particles and the physical properties of metals.
U.S Army material Research Centre Technical Report 71-74, 1971.

67- G. E. Smeltzer, M. E. Gulden, and W. A. Compton.
Mechanisms of metal removed by impacting dust particles.
ASME Journal of Basic Engineering, Vol. 92, 1970, P. 639-654.

68- I. M. Hutchings
Prediction of the resistance of metals to erosion by solid particles
Wear, Vol. 35, 1975, P. 371-374.

69- R. H. Barkalow, J. A. Goebel and F. S. Pettit.
Erosion-corrosion of coatings and superalloys in high velosity hot gases
Erosion: Prevention and useful applications (W. F. Adler, ed). ASTM STP 664, 1979, P. 163-192.

70- G. P. Tilly
Erosion caused by air burne particles
Wear, Vol. 14, 1969, P. 63-79

71- G. P. Sheldon and I. Finnie
On the ductile behaviour of nominally brittle materials during erosive cutting
ASME Journal of Engineering for Industry, 1966, P. 387-392.

72- F. George and Jr. Schmitt
Liquid and solid particle impact erosion
Wear control handbook, ASME, 1980, P. 231-281

73- K. Wellinger and H. Uetz
Wear, 1 (1957-58), P. 225-231 (in German)

74- G. P. Tilly and Wendy Sage
The interaction of particle and material behaviour in erosion processes.
Wear, 16 (1970) pp 447-465.

75- G. L. Sheldon, I. Finnie
The mechanism of material removal in the erosive cutting of brittle materials.
ASME Journal of Engineering for industry. 1966, pp 393-400

76- S. Timoshenko and J. N. Goodier
Theory of Elasticity
2nd edition, McGraw Hill Book co. Inc. N.Y.

77- G. A. Evens, E. M. Gulden, E. G. Egyum, M. Rosenblatt
Impact damage in brittle materials in plastic response regime.
Report no. SC5023.9TR, Rockwell International Science Centre, Thousand oaks, California, 1976.

78- E. M. Gulden
Solid particle erosion of high technology ceramics (SiN_3, Glass-Bonded Al_2O_3, and MgF_2), Erosion ; prevension and useful applications, ASTM-STP-664, W. F. Alder, Ed., American Society for Testing and Materials, 1979, pp. 101-122.

79- R. P. Benedict
Fundamentals of pipe flow
John Wiley & Sons, Chapter 5, P. 178.

80- G. N. Abramovich
The theory of turbulent jets
MIT Press Cambridge, Mass. (1963).

81- L. Prandtl
Bericht Uber Untersuchungen zur ausgebildeten Turbulenz ZAMM, 5, 136, 1925.

82- K. Yanaida
Flow characteristics of water jets.
In. Proc. 2nd Int. Symp. on Jet cutting Technol. (Cambridge U.K, 1974),
Cranfield, U.K, BHRA Fluid Engng. ,1974 , Paper A2 ,P. A2-19.

83- R. K. Swanson, M. Kilman, S. Cerwin and W. Tarver
Study of particle velocities in water driven abrasive jet cutting.
Proc. 4th U.S. Water Jet Conference, 1987, P. 103.

84- G. Galecki and M. Mazurkiewicz
Hydroabrasive cutting head-energy transfer efficiency.
Proc. 4th U.S. Water Jet Conference, 1987, P. 109.

85- F. M. White
Fluid Mechanics
International Student Edition. McGraw Hill 1979

86- I. Finnie and M. C. Shaw
The friction process in metal cutting
Trans, ASME, 78 (1956) pp 1649.

87- A. F. Conn; G. D. Mehta and T. R. Sundaram.
Cavitating water jets; I- rview and applications
In: proc. Cavitation and Polyphase Flow Forum, (New Orleans, U.S.A: March 21-25, 1976), New York, U.S.A, ASME, 1976, Paper 5, p. 12-15.

88- A. F. Conn and V. E. Johnson
Further applications of the Cavijet method.
In. Proc. 2nd. Int. Symp. on Jet Cutting Technol., (Cambridge, U.K.: Apr. 2-4, 1974), Cranfield, U.K., BHRA Fluid Engng., 1974, p. D2,7-D2, 20.

89- W. Weibull
A statical theory of the strength of materials
Ingenior Vetenskaps Akademiens Handlinger, no. 151, 1939

Appendix III

Description of tests and some results

1- Specimen material (table 1)

Cutting tests are carried out on three types of materials, brittle (silceram), ductile (mild steel) as in most tests and very ductile (nickel).

Results of preliminary tests are used to find a suitable angle of attack for large and small volume removal rates hence the following angles are used:-

Silceram ≈ 90 and 40 degrees

Mild steel ≈ 90 and 20 degrees

Nickel ≈ 90 and 40 degrees

2- Tests on the cutting head (table 2)

Cutting head of conical mixing chamber, of 10 mm length, was used in all the cutting tests, as it gives fastest cutting speed.

Preliminary cutting trials were carried out to estimate the fastest time to cut the specimen by changing the number of passes. First, the specimen was cut in one pass then the number of passes was increased. It was found that fastest time of cut was reached when 3 to 5 passes were used to cut the specimen.

Focusing tubes from 4 different hard materials, of the variable lengths listed in Chapter 6, were used. The wear rate of these tubes is calculated in Tables 6.1, 6.2, 6.3, 6.4 and 6.5 in grams/kg of abrasive material/ mm length of the tube, since the tubes are not of the same length. In the same tables also, for the sake of comparison between the different materials wear rates, the wear rate is calculated in cubic centimetre (cc) to eliminate the effect of material density.

specimen material	angle of attack (degrees)	type of abrasive	material removal rate (cc/min)
Mild steel (ductile)	20	garnet	6
	90		1.44
Silceram (brittle)	40	garnet	2.4
	90		6.5
Nickel (very ductile)	40	garnet	1
	90		no cut (surface deformation)

Table 1 Conical cutting head performance

focusing tube material	type of abrasive	approximate tube operation life hours
tungsten carbide	flint	17.5 (no wear when bore = 4 mm)
	garnet	15
	white alumina	6.5
	type s alumina	9
zirconia	flint	16
	garnet	12
	white alumina	5.5
	type s alumina	7.5
silceram	all types	tube destroyed
alumina	all types	tube destroyed

Table 2 Focusing tube operation life (at bore = 4 mm life is considered to end)